Towards Low Complexity Matching Theory for Uplink Wireless Communication Systems

Abdulrahman Saeed Al Ayidh

Submitted in fulfilment of the requirements for the
Degree of Doctor of Philosophy

James Watt School of Engineering
College of Science and Engineering
University of Glasgow

August 2022

Abstract

Millimetre wave (mm-Wave) technology is considered a promising direction to achieve the high quality of services (QoSs) because it can provide high bandwidth, achieving a higher transmission rate due to its immunity to interference. However, there are several limitations to utilizing mm-Wave technology, such as more extraordinary precision hardware is manufactured at a higher cost because the size of its components is small. Consequently, mm-Wave technology is rarely applicable for long-distance applications due to its narrow beams width. Therefore, using cell-free massive multiple input multiple output (MIMO) with mm-Wave technology can solve these issues because this architecture of massive MIMO has better system performance, in terms of high achievable rate, high coverage, and handover-free, than conventional architectures, such as massive MIMO systems' co-located and distributed (small cells). This technology necessitates a significant amount of power because each distributed access point (AP) has several antennas. Each AP has a few radio frequency (RF) chains in hybrid beamforming. Therefore more APs mean a large number of total RF chains in the cell-free network, which increases power consumption. To solve this problem, deactivating some antennas or RF chains at each AP can be utilized. However, the size of the cell-free network yields these two options as computationally demanding. On the other hand, a large number of users in the cell-free network causes pilot contamination issue due to the small length of the uplink training phase. This issue has been solved in the literature based on two options: pilot assignment and pilot power control. Still, these two solutions are complex due to the cell-free network size.

Motivated by what was mentioned previously, this thesis proposes a novel technique with low computational complexity based on matching theory for antenna selection, RF chains activation, pilot assignment and pilot power control. The first part of this thesis provides an overview of matching theory and the conventional massive MIMO systems. Then, an overview of the cell-free massive MIMO systems and the related works of the signal processing techniques of the cell-free mm-Wave massive MIMO systems to maximize energy efficiency

(EE), are provided. Based on the limitations of these techniques, the second part of this thesis presents a hybrid beamforming architecture with constant phase shifters (CPSs) for the distributed uplink cell-free mm-Wave massive MIMO systems based on exploiting antenna selection to reduce power consumption. The proposed scheme uses a matching technique to obtain the number of selected antennas which can contribute more to the desired signal power than the interference power for each RF chain at each AP. Therefore, the third part of this thesis solves the issue of the huge complexity of activating RF chains by presenting a low-complexity matching approach to activate a set of RF chains based on the Hungarian method to maximize the total EE in the centralized uplink of the cell-free mm-Wave massive MIMO systems when it is proposed hybrid beamforming with fully connected phase shifters network.

The pilot contamination issue has been discussed in the last part of this thesis by utilizing matching theory in pilot assignment and pilot power control design for the uplink of cell-free massive MIMO systems to maximize SE. Firstly, an assignment optimization problem has been formulated to find the best possible pilot sequences to be inserted into a genetic algorithm (GA). Therefore, the GA will find the optimal solution. After that, a minimum-weighted assignment problem has been formulated regarding the power control design to assign pilot power control coefficients to the quality of the estimated channel. Then, the Hungarian method is utilized to solve this problem. The simulation results of the proposed matching theory for the mentioned issues reveal that the proposed matching approach is more energy-efficient and has lower computational complexity than state-of-the-art schemes for antenna selection and RF chain activation. In addition, the proposed matching schemes outperform the state-of-the-art techniques concerning the pilot assignment and the pilot power control design. This means that network scalability can be guaranteed with low computational complexity.

University of Glasgow

College of Science & Engineering

Statement of Originality

Name: Abdulrahman Saeed Al Ayidh
Registration Number:

I certify that the thesis presented here for examination for a PhD degree of the University of Glasgow is solely my own work other than where I have clearly indicated that it is the work of others (in which case the extent of any work carried out jointly by me and any other person is clearly identified in it) and that the thesis has not been edited by a third party beyond what is permitted by the University's PGR Code of Practice.

I declare that the thesis does not include work forming part of a thesis presented successfully for another degree.

I declare that this thesis has been produced in accordance with the University of Glasgow's Code of Good Practice in Research.

I acknowledge that if any issues are raised regarding good research practice based on review of the thesis, the examination may be postponed pending the outcome of any investigation of the issues.

Signature: ***Abdulrahman Saaed A. Al Ayidh***
Date: 04/08/2022

List of Publications

The following publications are the outcomes of the research done for this PhD.

- **A. Al Ayidh**, Y. Sambo, S. Olaosebikan, S. Ansari, and M. A. Imran, "Antenna Selection Based on Matching Theory for Uplink Cell-Free Millimetre Wave Massive Multiple Input Multiple Output Systems," *Telecom*, vol. 3, no. 3, pp. 448-466, 2022. [Online]. Available: https://www.mdpi.com/2673-4001/3/3/24.

- M. A. Imran, **A. Al Ayidh**, L. Li, G. Zhao, and Q. H. Abbasi, "URLLC massive MIMO link operation design for wireless networked control system." In: Tafazolli, R., Wang, C.-L. and Chatzimisios, P. (eds.) Wiley 5G Ref: The Essential 5G Reference Online. John Wiley sons Ltd. ISBN 9781119471509 (In Press) 2020.

- **A. Al Ayidh**, Y. Sambo, S. Ansari and M. A. Imran, "Hybrid Beamforming with Fixed Phase Shifters for Uplink Cell-Free Millimetre-Wave Massive MIMO Systems," 2021 Joint European Conference on Networks and Communications 6G Summit (EuCNC/6G Summit), 2021, pp. 19-24, doi: 10.1109/EuCNC/6GSummit51104.2021.9482579.

- **A. Al Ayidh**, Y. Sambo, S. Ansari, and M. A. Imran, "Low-complexity RF chains activation based on Hungarian algorithm for uplink cell-free millimetre-wave massive mimo systems," in 2022 IEEE 31st Annual International Symposium on Personal, Indoor and Mobile Radio Communications, vol. Accepted for publication, 2022.

- **A. Al Ayidh**, Y. Sambo, and M. A. Imran, "Mitigation pilot contamination based on matching technique for uplink cell-free massive mimo systems," Accepted with minor corrections for publication to Scientific Reports, 2022.

Contributions Outside This Thesis

The following publications have been completed throughout the PhD program but they are not included in the this thesis because they do not entirely correspond to its topic.

- **A. Al Ayidh**, J. B. Nadas, R. Ghannam, G. Zhao and M. A. Imran, "Communication and Control Co-Design Using MIMO Wireless Network," *2019 UK/ China Emerging Technologies (UCET)*, 2019, pp. 1-5, doi: 10.1109/UCET.2019.8881847.

- **A. Al Ayidh**, B. Chang, G. Zhao, R. Ghannam and M. A. Imran, "Energy-Efficient Power Allocation in URLLC Enabled Wireless Control for Factory Automation Applications," 2020 IEEE 31st Annual International Symposium on Personal, Indoor and Mobile Radio Communications, 2020, pp. 1-6, doi: 10.1109/PIMRC48278.2020.9217133.

Contents

List of Tables

List of Figures

List of Acronyms

Access Point	AP
Adaptive RF Chains Activation	ARFA
Analog-to-Digital Converter	ADC
AP Switch On/Off	ASO
Base Station	BS
Central Processing Unit	CPU
Constant Phase Shifters	CPSs
Channel Magnitude-Based with Dynamically Selected Antennas	CMDAS
Channel Magnitude-Based with Fixed Selected Antennas	CMFAS
Channel State Information	CSI
Cognitive Radio	CR
Coordinated Multi-Point	COMP
Decremental Search-Based Antenna Selection	DSAS
Digital-to-Analog Converter	DAC
Distributed Antenna System	DAS
Energy Efficiency	EE
Femtocell APs	FAPs
Fifth Generation	5G
Fixed CPSs	FCPSs

Frequency Division Duplexing	FDD
Frequency Range 2	FR2
Genetic Algorithm	GA
Internet of Things	IoTs
Key Performance Indicators	KPIs
Millimetre Wave	mm-Wave
Minimum Mean Squared Error	MMSE
Multiple Input Multiple Output	MIMO
Non-Orthogonal Multiple-Access	NOMA
Orthogonal Frequency Division Multiple Access	OFDMA
Partially-Matched Crossover	PMX
Primary User	PU
Physical Layer Security	PLS
Quality of Service	QoS
Radio Frequency Chain	RF Chain
Reconfigurable Intelligent Surfaces	RIS
Random Variables	RV
Secondary User	SU
Service Providers	SPs
Sixth Generation	6G
Spectral Efficiency	SE
Signal-to-Noise Ratio	SNR
Signal-to-Interference-plus-Noise Ratio	SINR
Time Division Duplexing	TDD
Unmanned Aerial Vehicle	UAV

User Equipment UE

Uniform Linear Array ULA

List of Symbols

M	Number of APs in the cell-free massive MIMO network.
K	Number of UEs.
N_r	Number of antenna at each AP.
N	Number of RF chains at each AP.
$\mathcal{Z}_{k,m}$	The network of switches for each RF chain at each AP.
N_Q	The CPSs at each AP.
τ_p	The length of uplink training phase.
Y_m	The received pilots at m_{th} AP from K UEs.
$h_{k,m}$	The channel between the m_{th} AP and k_{th} UE.
$\hat{h}_{k,m}$	The estimated channel between the m_{th} AP and k_{th} UE.
G_a	The antenna gain.
$\beta_{k,m}$	The pathloss between the m_{th} AP and k_{th} UE.
$P_{k,m}$	The number of propagation paths.
d_o	The reference distance.
λ	The wavelength.
$d_{k,m}$	The distance between the m_{th} AP and k_{th} UE.
ε	The average pathloss exponent over the distance.
$\chi_{k,m}$	The shadow fading component with zero mean and ς standard deviation.
$\alpha_{k,m}^{(p)}$	The complex small scale fading gain.

$\phi_{k,m}^{(p)}$	The azimuth angle of arrival (AoA) for each channel path.
$\mathrm{a}_r(\phi)$	The receive array response vector at the m_{th} AP.
$\hat{H}_m^e$	The effective channel to be used for hybrid beamforming technique.
d_s	The antenna spacing of half of a wavelength.
W_m	The analog combining for each AP.
r_m	The received signal at m_{th} AP.
$\Delta_{k,m}$	The switching network between the k_{th} RF chain and N_r at m_{th} AP.
ρ_p	The transmission power of each pilot symbol sent by k_{th} UE.
n_m^{noise}	The independent identically distributed (i.i.d.) received noise samples.
φ_k	The pilot sequence of k_{th} UE.
f	The carrier frequency.
B	The system bandwidth.
NF	The noise figure.
σ^2	The noise power.
x_k	The transmitted symbol by k_{th} UE.
$\tilde{q}$	The index of the selected CPSs.
S_m	The binary matrix with size $N_r \times K$.
SE_m	The uplink spectral efficiency.
$\mathrm{SINR}_{k,m}$	The effective instantaneous signal-to-interference-plus-noise ratio.
$\tilde{J}_m$	The antenna indices which are sorted in ascending order for each AP.
$\mathcal{R}$	Reward matrix of the proposed assignment problem in this chapter.
P_{FH_m}	The power consumed by m_{th} fronthaul link.
$P_{\mathrm{FH}_{max}}$	The maximum fronthaul power.
R_{FH_m}	The actual fronthaul rate between m_{th} AP and the CPU.
C_{FH_m}	The fronthaul capacity for m_{th} AP.

α_m	The number of quantization bits at m_{th} AP.
T_c	The coherence time in seconds.
η_k^{amp}	The power amplifier efficiency at k_{th} UE.
P_{RF}	The power consumed by the RF chain circuit at m_{th} AP.
P_{M}	The power consumed by the mixer.
P_{LO}	The power consumed by the local oscillator.
P_{LPF}	The power consumed by the low-pass filter.
P_{CP_k}	The amount of the required power to operate the circuit components.
P_{TX_k}	The transmit power of k_{th} UE.
P_{LNA}	The consumed power by low-noise amplifier.
P_{SP}	The consumed power by the splitter.
P_{SW}	The consumed power by the switch.
P_{CPS}	The consumed power by the CPS.
P_{C}	The consumed power by the combiner.
P_{ADC}	The consumed power by analog-to-digital converter.
P_{T}	The total power consumption.
n_m	The number of selected RF chains at m_{th} AP.
P_{HBF_m}	The power consumption of hybrid beamforming structure.
$\digamma$	The reward matrix of the proposed matching scheme in this chapter.
$u^{\star}_{m,N}$	The left singular value.
$M_s^{c_\ell}$	The sub square matrix, where $\ell = \{1, 2, ..., C\}$.
C	The number of sub square matrices.
$\mathcal{I}_{\mathcal{FS}}$	The total number of iterations for FS-ARFA scheme.
δ^{A}	The sets of active APs.
δ^{D}	The sets of inactive APs.

$g_{k,m}$	The channel coefficient vector for chapter 5 between k_{th} UE and m_{th} AP.
s_k	The k_{th} UE transmitted symbol.
DS_k	The desired signal.
BU_k	The beamforming gain uncertainty.
$\text{UI}_{kk'}$	The interference caused by k'_{th} UE.
Δ_ϕ	The pilot set includes $\{1, 2, ..., \tau\}$ orthogonal pilot sequences.
$\mathcal{J}_l$	The all possible cases of the pilot assignment.
$\text{PL}_{k,m}$	The pathloss model.
Γ	The number of iterations of the GA.

وَآخِرُ دَعْوَاهُمْ أَنِ الْحَمْدُ لِلَّهِ رَبِّ الْعَالَمِينَ

"The last of their call will be, Praise to Allah, Lord of the worlds" Quran, Yunus, Verse [10].

Acknowledgements

All credit is due to God, who gave me the wisdom to begin this journey and guided me every step of the way.

I would like to express my gratitude to my supervisors, Prof. Muhammad Ali Imran and Dr. Yusuf Sambo, for their considerable help and the way they have guided me and been patient with me over the years.

I would like to thank King Khalid University for providing me with a scholarship and for granting additional assistance for my travel expenses during this PhD course. The Saudi Arabian Cultural Bureau in London was also instrumental in my success.

I want to thank my CSI colleagues for their support. During my PhD, we had productive and enjoyable discussions that made the experience more pleasurable.

To my Saudi friends in Glasgow, I express my gratitude for their presence to alleviate the stress during my PhD course.

Finally, I want to express my gratitude to my family, particularly my mother, for her unending encouragement. My wife's unwavering love, understanding, and support during my PhD journey are greatly appreciated.

Chapter 1

Introduction

Mobile wireless communication development has been considered one of the most important research directions in recent decades to achieve high quality of service (QoS). Particularly, the sixth generation (6G) of wireless technology should be able to connect billions of wireless devices servicing billions of people [1], and is expected to support a wide range of new technologies which will affect our ways of life, such as artificial intelligence, terahertz communications, three dimensional (3D) networking and unmanned aerial vehicles (UAVs) [2–5]. Therefore, there is a massive demand for bandwidth, the primary resource of wireless communication. In addition, interference is unavoidable as the number of connected devices increases and the available bandwidth is limited [6]. Thus, it becomes a technical challenge to design wireless communication systems. Accordingly, experts are wondering whether the cellular network currently deployed is still relevant for supplying such different technologies with such demanding Key Performance Indicators (KPIs), such as ultra-high reliability, high spectral efficiency (SE), high energy efficiency (EE), high security and ubiquitous coverage. Previously, the main objective of the cellular network deployment has been to expand wireless coverage across a vast geographic area. A separate base station (BS) services each non-overlapping cell since a radio signal weakens as it is sent further away from the source. Different frequencies can be used for nearby cells to avoid interfering with each other. However, a lack of spectrum forces the cells to utilize the same frequency for preserving SE as their number of user equipments (UEs) and bandwidth-intensive applications rise. Because of this, the UE's performance might be substantially degraded by inter-cell interference, especially near the cell borders. As a result, the time to reassess its design has come due to the required demands to have a more flexible design without cells through using the tools and technologies that have recently developed. Therefore, the spectrum crunch can be solved by utilizing a large number of equipped antennas at the BS to serve

many users simultaneously on the same wireless resources [7, 8].

1.1 Motivation

1.1.1 Why cell-free massive MIMO network is required?

Cell-free massive multiple input multiple output (MIMO) [9, 10] is a recently-emerging concept for deploying massive MIMO systems without the restriction of cells. Therefore, the cell-free massive MIMO allows UEs to be served by all BSs simultaneously across a large coverage area instead of only one BS. In other words, a large number of BSs, also known as access points (APs), are connected to the Central Processing Unit (CPU) via fronthaul links to coordinate data transmission. In contrast, the coordination of the data transmission cannot be achieved in the conventional massive MIMO systems [11]. Additionally, at each coherence time, channel estimation and beamforming operations are performed at the APs in the cell-free network, while power allocation is performed at the CPU. In contrast, the conventional massive MIMO achieves beamforming and power allocation at the BS. Hence, the system performance can be enhanced in terms of better coverage and throughput per UE per area [10, 11].

On the other hand, the cell-free Massive MIMO systems and mm-Wave technology can be used to explore new wireless boundaries in future generations. This is because the availability of high bandwidth is a key factor in enabling such high data rates in future wireless generations. Thus, using mm-wave technology and high antenna gains can be considered a suitable solution to overcome the issue of large path loss [12]. This arrangement offers the most effective bandwidth use in cell-free mm-wave massive MIMO systems when different transmit-receive antenna pairs have independently fading channel coefficients. Notably, the cell fee mm-Wave massive MIMO system is also considered to solve the effects of blockage effect. However, there exists several challenges that should be taken into account when using mm-Wave technology with the cell-free massive MIMO systems. These challenges are:

- Hybrid beamforming is an efficient technique to overcome high power consumption due to higher hardware complexity and achieve near-optimal performance compared to digital beamforming [13]. However, due to many APs in the cell-free network, the hybrid beamforming design requires enormous computational complexity. For example, to minimize power consumption and hardware complexity, the antenna selection can be applied in the cell-free mm-Wave massive MIMO systems as the conventional mm-Wave

massive MIMO systems when only a single BS is in the coverage area. Therefore, it is noted that the cell free massive MIMO can enhance reliability by providing a large number of APs to serve the UEs coherently. The next chapter will discuss more details about the differences between these two structures. Still, this is an undesirable solution because of the loss of antenna gains, which indicates that signals transmitted or received by the antennas in a specific direction suffer from weakness [14]. Also, the computational complexity significantly increases as the number of antennas in the network increases. Therefore, it is necessary to propose an efficient method to address this issue in the cell-free mm-wave massive MIMO systems.

- Power consumption is proportional to both number of radio frequency (RF) chains and APs [15]. Turning off some RF chains at each AP will reduce the total power consumption of the cell-free mm-Wave massive MIMO system. However, the optimal number of active RF chains at each AP must be obtained to reduce the performance loss caused by switching off some RF chains. When dealing with a considerable number of APs, an exhaustive search approach achieves optimal results but with prohibitive computational complexity.

- The process of channel estimation is considered one of the essential operations in the cell-free massive MIMO systems, as it directly influences the computations of precoding and detection vectors utilized for the uplink and downlink data transmission [16, 17]. Regarding time division duplexing (TDD) communication mode, recent studies have developed pilot-based channel estimate algorithms in which UEs communicate τ-length pilot sequences to APs. The channel coherence time and the number of UEs are related to each other in the channel estimation process [12]. Furthermore, the pilot sequences assigned to UEs might be orthogonal or non-orthogonal; for instance, orthogonal pilot sequences can be allocated when there is a large τ_c coherence interval and a limited number of UEs. However, when τ_c is minimal, it is preferable to utilize non-orthogonal pilot sequences to reduce the resources required for channel estimation [17]. Therefore, the interference between the transmitted pilot signal from the desired UE and other transmitted pilot signals from other UEs at each AP leads to the degradation of the estimated channel accuracy, impacting system performance. The term for this issue is called pilot contamination.

1.1.2 Why matching theory?

New mathematical techniques for optimizing resource allocation in wireless systems have appeared. For instance, centralized optimization is an excellent example [18]. The algorithmic implementations of centralized optimization approaches, which can provide optimal solutions to resource allocation problems, have matured in recent years [18, 19]. As a result, they often demand a great deal of complexity. It is possible that centralized optimization might not be able to handle the complexities of dense and heterogeneous wireless environments [18]. Therefore, high performance, low complexity, and decentralized protocols have been developed by using matching theory which is a powerful tool to achieve dynamic and mutually advantageous relationships between rational and selfish agents [19]. Wireless networks are made up of a variety of self-interested and rational actors. All of them seek to maximize their profit from the network without regard for other agents. In this thesis, we focus on the application of one-to-one matching technique, also called an assignment problem, in the uplink cell-free massive MIMO systems due to high complexity of this kind of wireless networks. Thus, the main advantages of utilizing one-to-one matching technique in this thesis are:

- It can describe how different nodes, each of which has its type, goal, and information, interact with each other.
- Ability to specify "preferences" that can manage heterogeneous and complex aspects in wireless QoS.
- It is characterized by implementing its algorithms, such as Hungarian algorithm, in an efficient and low-complexity way.

1.2 Objectives

The objectives of this thesis are:

- To perform a hybrid beamforming scheme with constant phase shifters (CPSs) and antenna selection technique based on matching theory for the uplink cell-free mm-Wave massive MIMO systems to enhance EE, SE and low computational complexity compared to the state-of-the-art schemes.
- To maximize the EE by using matching theory to obtain the optimal number of active RF chains at each AP in the cell-free network coverage area while considering a hybrid beamforming scheme with fully connected phase

shifters. In addition, the proposed matching scheme will be compared with the state-of-the-art schemes.

- To solve the pilot contamination issue and maximize the channel estimation accuracy by proposing a matching theory for both pilot assignment and pilot power control. Then, to compare the results with the state-of-the-art schemes in terms of the system throughput and the complexity analysis.

1.3 Thesis Contributions

The main contributions of this thesis are demonstrated in Figure 1.1, and can be summarized as follows:

- The effects of antenna selection strategies on the system performance of the cell-free mm-Wave massive MIMO system are studied. Particular attention is given to the comprehensive analysis of the system performance concerning SE, EE, and power consumption with many distributed UE and APs. In addition, it has been discussed how to exploit the estimated channel quality implication to turn it into a positive outcome by the matching theory as a novel strategy for antenna selection. In particular, for all APs in the cell-free mm-Wave massive MIMO network, an assignment optimization problem has been formulated to accomplish one-to-one matching between RF chains and several sets of selected antennas based on channel conditions. Then, the Hungarian method has been proposed to solve the formulated optimization problem based on maximum-weight matching to maximize EE and achieve close to the optimal SE. In contrast to [14], instead of assuming that all RF chains in the AP have the same fixed active switches, the advantages of the matching theory based on the Hungarian algorithm have been exploited to assign each RF chain at each AP in the cell-free network to different number of activated switches depending on AP channel condition to maximize EE. The efficiency of the proposed matching scheme for the antenna selection technique is justified by the simulation results, with several scenarios of uplink cell-free mm-Wave massive MIMO systems, which show that the matching approach can attain around 20% EE improvement and 200% complexity reduction compared to the state-of-the-art schemes.

- A maximum-weighted assignment optimization problem has been formulated to obtain the optimal number of RF chains to activate at each AP to maximize the EE when hybrid beamforming with fully connected phase shifters is assumed for each AP in the cell-free massive MIMO network. The formulated problem has been considered as one-to-one matching and solved by proposing the Hungarian method. The power consumption of the proposed matching scheme has been investigated and compared with state-of-the-art methods of RF chain activation. Simulation results demonstrate that the proposed scheme achieves up to 13.5%, 20% and 58.7% EE improvement compared to state-of-the-art adaptive RF chains activation (ARFA), random access point activation and fixed activation scheme when all RF chains at each AP are switched on, respectively.

- Pilot assignment is used to mitigate the effect of pilot contamination. Therefore, an iterative Hungarian scheme is proposed to solve the formulated assignment optimization problem in order to obtain better-selected pilot sequences to reduce the complexity of the GA by using the selected pilot sequences instead of putting huge amount of possible combinations of the pilot sequences in the conventional GA, especially when there exists large number of UEs in the coverage area. This proposed model is used to find the optimal pilot sequences in the cell-free massive MIMO systems. Simulation results reveal that the proposed scheme can achieve higher throughput of the cell-free massive MIMO systems with different scenarios compared to the state-of-the-art schemes, and it can attain very close results to the exhaustive search method.

- A lower complexity pilot power control design with the proposed pilot assignment scheme in the previous contribution for the uplink cell-free massive MIMO systems based on matching theory has been proposed by formulating a minimum-weighted assignment optimization problem and using the Hungarian method in order to obtain the optimal assignment between the pilot power control coefficients and the minimum channel estimation error for all UEs. Comprehensive simulation results are provided to demonstrate the performance of the proposed pilot power control scheme using one-to-one matching under an extensive set of the cell-free massive MIMO scenarios. The proposed scheme can achieve 15% SE improvement with lower computational complexity compared to [17].

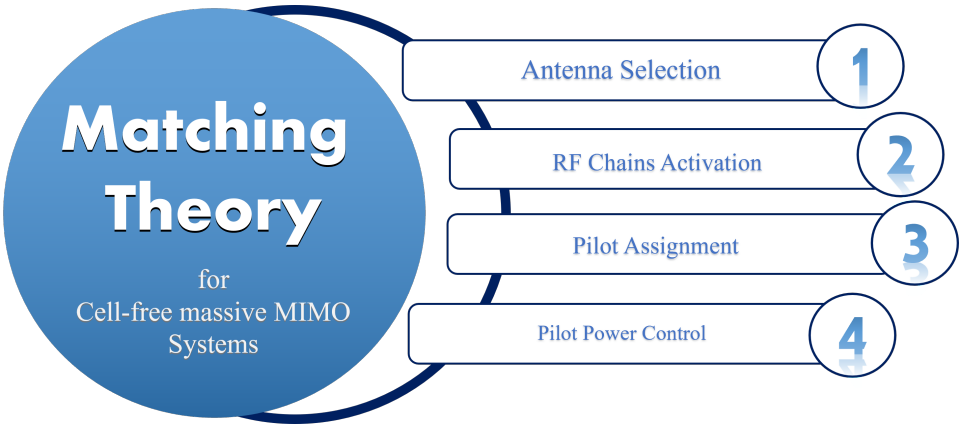

Figure 1.1: Thesis contributions based on applying matching theory in the cell-free massive MIMO systems.

1.4 Thesis Organization

The remainder of this thesis is structured as follows:

- **Chapter 2** presents the background and related works of using matching theory in the uplink cell-free massive MIMO systems. In particular, this chapter introduces an overview of matching theory and its applications in wireless networks. Then, an overview of massive MIMO systems are provided as well as mm-Wave technology, including its limitations and signal processing techniques with massive MIMO systems. Finally, an overview of the cell-free massive MIMO systems, including its communication protocols, channel estimation techniques, uplink data transmission, and the related works of the cell-free mm-Wave massive MIMO systems, are provided.

- **Chapter 3** presents the antenna selection technique based on matching theory for the uplink cell-free mm-Wave massive MIMO systems. This chapter introduces the system model, including the channel model, analog combining design, channel estimation, and uplink data transmission. Additionally, the power consumption and EE models are provided in this chapter. The methodology of applying the matching theory is presented as a novel technique to select the antennas for each AP that can contribute more to the desired signal power than the interference power. It has been formulated as an assignment problem to maximize the SE. Then, the Hungarian method is presented in detail to solve the formulated problem. Finally, comprehensive simulation results are provided in this chapter, including several scenarios of the cell-free mm-Wave massive MIMO systems. The complexity analysis of the proposed matching scheme is discussed in detail and compared to the state-of-the-art techniques.

- **Chapter 4** presents the RF chains activation based on matching theory for uplink cell-free mm-Wave massive MIMO systems. The system model for this chapter is introduced, including the channel model, the channel estimation, and the performance matrices of the work in this chapter in terms of the achievable rate and the EE. The methodology of the proposed matching theory of the RF chains activation for the uplink cell-free mm-Wave massive MIMO systems is provided, including the formulated assignment problem and how to function the Hungarian method to obtain the optimal RF chains at each AP in the cell-free coverage area. The complexity analysis of the proposed matching theory is discussed and compared to the state-of-the-art scheme. Finally, simulation results are provided concerning

the achievable rate, EE, and power consumption for different scenarios of the cell-free mm-Wave massive MIMO systems.

- **Chapter 5** proposes matching theory in the pilot assignment and pilot power control to mitigate the pilot contamination phenomenon, which degrades the channel estimation accuracy in the cell-free massive MIMO systems. The system model of this chapter which includes the channel model, channel estimation, uplink data transmission, and the SE performance metric, is presented. Then, the pilot assignment based on the integration between the Hungarian method and the GA is provided. Additionally, the pilot power control based on matching theory is provided by formulating an assignment problem between random pilot powers for each UE and their accuracy of the estimated channels to obtain the optimal pilot power for each UE with minimum channel estimation error. The complexity analysis of the proposed schemes and simulation results are given and compared to the state-of-the-art methods.

- **Chapter 6** gives the conclusion of the findings of the work in this thesis. Furthermore, this chapter explores future research directions. In particular, the ability of the proposed matching technique to be applied in different topics of wireless communications, such as proposing the same matching technique for RF chain activation in Chapter 4 with low-resolution analog-to-digital converters (ADCs) to further reduce the power consumption, and using the proposed matching scheme for both pilot assignment and pilot power control design to enhance the accuracy of the estimated channel in the cell-free mm-Wave massive MIMO systems in case of large number of UEs in the coverage area. In addition, integrating the matching theory and the GA minimizes the energy requirements. It is considered a promising solution to reduce the computational complexity in unmanned aerial vehicles (UAVs) technology, which is considered a viable option for providing backup connectivity in post-disaster scenarios due to the rising number of wireless networks being damaged due to natural disasters.

  The main sections of the chapters in this thesis are indicated in Figure 1.2.

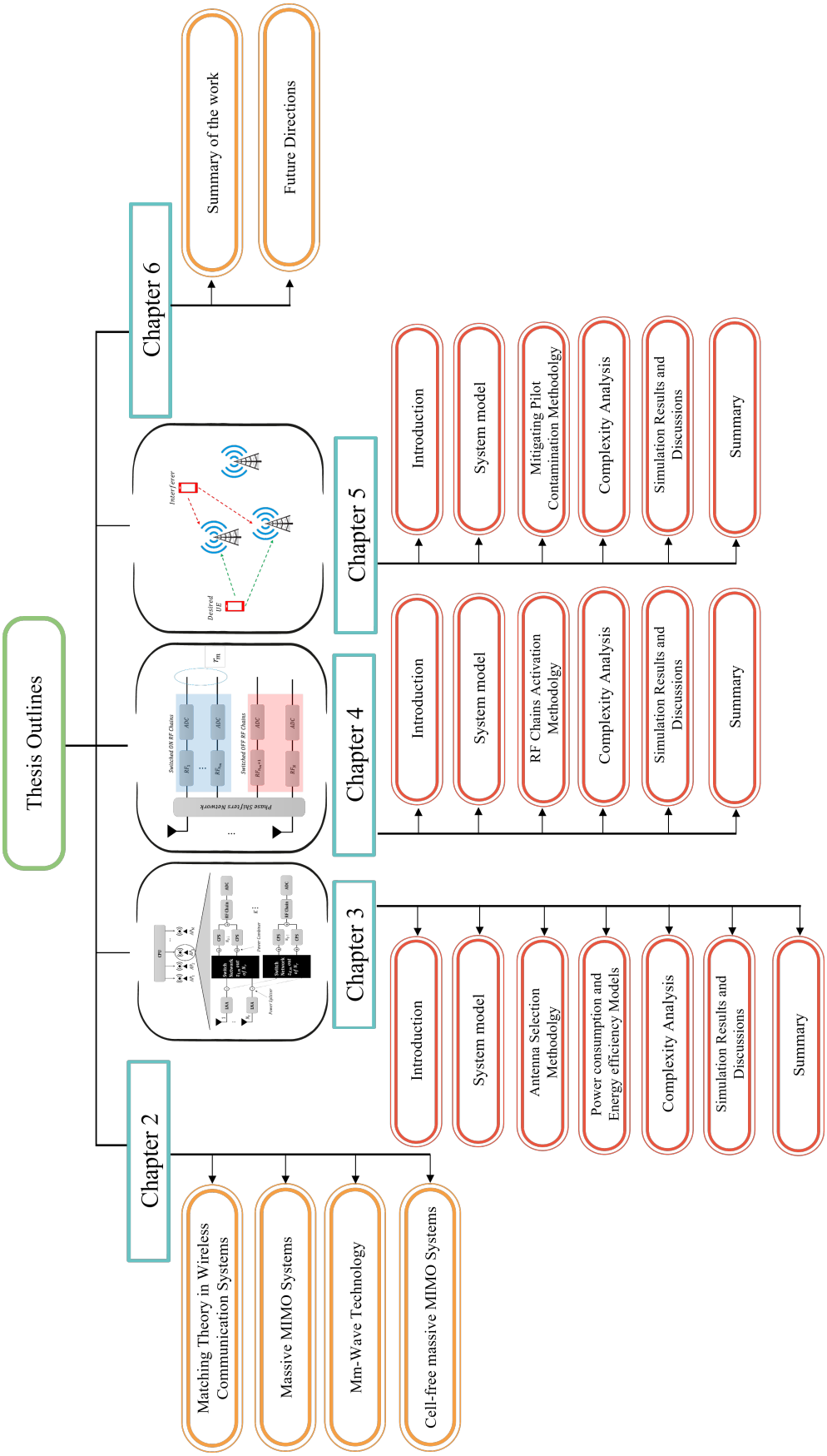

Figure 1.2: Thesis outline.

Chapter 2

Background and Related Works

This chapter provides a background on the matching theory and cell free massive MIMO. It starts with an overview of matching theory as well as its wireless network applications. Then, the main concept of massive MIMO wireless communication systems is presented and its integration with mm-Wave technology as well as the signal processing techniques in the mm-Wave massive MIMO systems. Finally, this chapter presents a background on the cell-free massive MIMO systems, including the transmission methods, channel estimation, uplink data transmission and the related works of the cell-free mm-Wave massive MIMO systems. Parts of the works in this chapter have been published in [20].

2.1 Matching Theory in Wireless Communication Systems

2.1.1 Overview

Resource management in wireless networks is defined as a match between available network resources and users [19]. There are a variety of abstraction layers for resources, which can represent base stations (BSs), time-frequency chunks, or power. Devices, stations, or smartphone applications can all be considered UEs for this framework's purposes [21]. Centralized optimization techniques can be utilized to provide optimal resource allocation for each UE [18, 19]. However, they require global network information and centralized control, causing high complexity. Therefore, channel allocation and user association are complicated combinatorial integer programming problems [21, 22]. The primary purpose of matching is to find the best possible match between resources and UEs based on their unique objectives and knowledge [22–24]. Preferences in general can be defined as choosing one thing better than others. Therefore, they provide the unique

perspective that each resource or UE has on the other set, based on information exclusive to that resource or UE. With this in mind, preference can be described as an objective utility function that measures how well a given resource-user match meets the UE's expectations. Even though utility functions can contain additional qualitative measurements gathered from the information accessible to UEs and resources, preferences are more general than utility functions [25, 26].

Matching can be defined as a collection of edges in the agent (x), as shown in Figure 2.1, that do not share any vertices. If a vertex is an incident to an edge that is not otherwise matched, it is referred to as being matched. There are three main types of matching, which are one-to-one, one-to-many and many-to-many. One-to-one matching each element in agent (x) should be matched to only on element in agent (y). The marriage problem is the simplest example of one-to-one matching, initially described by Gale and Shapley in [22]. The matching of men and women is discussed within an intriguing and highly applicable paradigm. Men have preferences over women in the marriage problem, while women have choices over men. The solution to the marriage problem must be a set of marriages in which no two individuals of opposing gender would prefer each other over their existing partners in order to achieve stable matching [22]. In addition to the one-to-one matching, one-to-many matching is to match one element from agent (x) to other elements of agent (y) [19]. For example, a group of students are matched to a college or users are assigned to the BS. Each college or BS can have more than one student or user in these cases. In this game of matching, the idea of group stability is used to ensure that a stable match is created. Finally, if there are no limits on the number of matches on either side of the matching, it turns into a many-to-many matching problem [27].

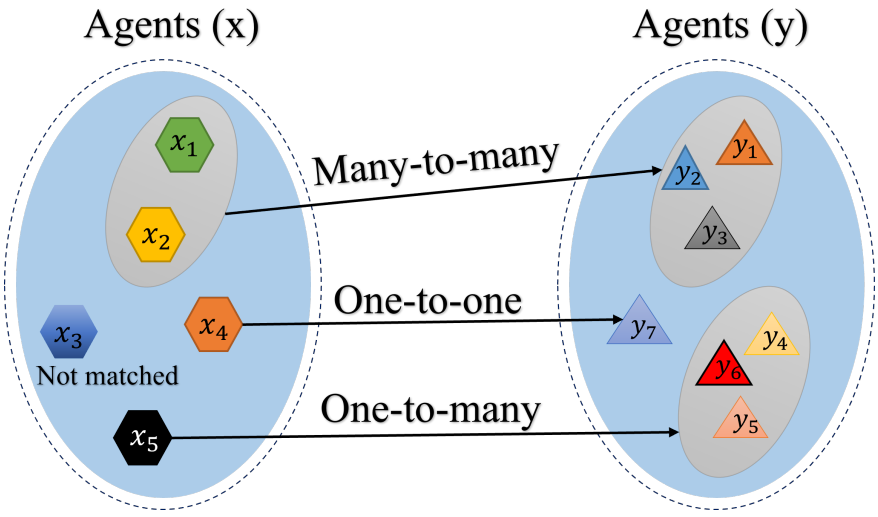

Figure 2.1: Overview of matching structures.

2.1.2 Weighted bipartite matching

A graph is considered bipartite if its vertices can be divided into two distinct sets, and each edge of the graph connects to precisely one of those sets [28]. Therefore, if each edge has a weight, the graph is termed a weighted bipartite graph as demonstrated in Figure 2.2. The maximum or minimum weighted bipartite matching means the maximum or minimum sum of edge weights after performing one-to-one matching between these two sets.

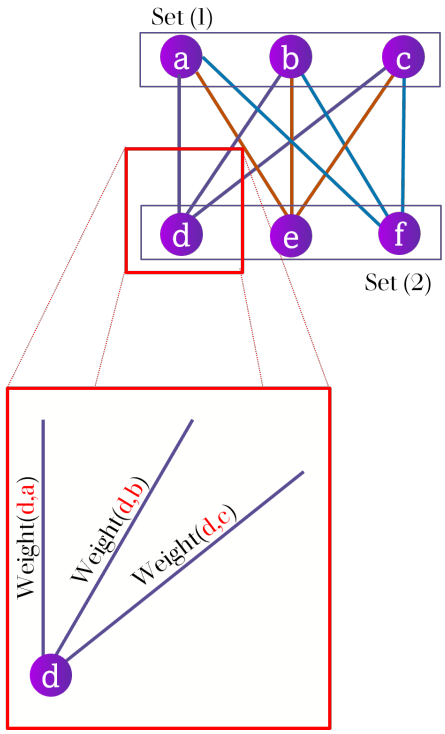

Figure 2.2: The structure of weighted bipartite matching.

2.1.3 Applications of matching theory in wireless communication systems

The matching theory has been used to solve resource allocation problems, such as those in cognitive radio (CR) and heterogeneous cellular networks, as well as in distributed orthogonal frequency-division multiple access (OFDMA) networks, routing and queuing systems in wireless networks [29–33]. The authors in [29] proposed matching theory in exchange for spectrum access and monetary compensation, the secondary user (SU) jointly delivers the primary user (PU) data in order to determine the priority of either PUs or SUs by altering control parameters when the data rate is more important than the monetary reward. Their results revealed that the proposed matching scheme can attain a result

similar to an optimal centralised solution, but with lower computational complexity. Furthermore, the authors in [31] examined the matching between the UE to the service providers (SPs) through low power APs, which are known as femtocell APs (FAPs), to enhance the system reliability and achieve high data rates. Therefore, the proposed approach encourages SPs and FAPs to collaborate the enhancement of the overall level of UE satisfaction. Then, the authors proposed a distributed subchannel allocation mechanism for uplink OFDMA networks. The authors in [31] proposed a distributed technique based on matching theory to protect numerous source-destination pairs from hostile eavesdroppers by using several friendly jammers to generate secure communications. To ensure that the final matching is stable and maximizes the sum of all source nodes' and friendly jammers' utilities, also known as the network social welfare, the matching algorithm in [31] determines the matched source node-friendly jammer pairs, and the precise amount of money transfer that encourages both source nodes and friendly jammers to cooperate. The proposed matching method converges to the competitive equilibrium under the framework of dynamic matching with the transfer. The results in [31] revealed that the proposed matching scheme can attain close results in terms of sum-secrecy rate in bits per seconds to the optimal centralized with lower computational complexity. The authors in [34] present a distributed resource allocation based on users and subcarrier preferences using the stable matching method of joint uplink and downlink for the OFDMA system to achieve QoS requirements. Their proposed approach provided better results compared to the conventional allocation approaches in terms of the average utility of the user leading to improvement in the fairness of subcarrier allocation [35].

2.2 Massive MIMO Systems

In a MIMO system, the fact that several antennas are available can be leveraged in various ways. For instance, the data rate can be maximized by taking advantage of the multiplexing gain, which occurs when numerous data streams are transmitted through several independent paths [6]. In addition, the reliability of the transmission can be increased by utilizing diversity in the form of sending the same data across various paths [6]. Antenna arrays at the BS and the network's numerous UEs can be viewed as a MIMO system in multi-user scenarios. Therefore, several UEs can be served at the same time, or each UE can be allocated to good propagation channels [36].

The multi-user MIMO system can also be constructed in massive MIMO form when the number of antennas that can provide service to a UE is the primary

characteristic that differentiates massive MIMO from standard multi-user MIMO. Massive MIMO is characterised by the fact that the total number of antennas employed is significantly more than the total number of UE antennas. When there are more antennas, the propagation channel experiences channel hardening, which implies that the singular value distribution of the propagation matrix becomes more deterministic [8]. This occurs because the number of antennas has a direct correlation to the channel hardening feature. Additionally, increasing the number of antennas at the BS for a few number of UEs makes the propagation more favourable since the channels tend to be nearly orthogonal [37]. This is because the number of antennas scales linearly with the number of UEs. Combining these advantages ultimately results in the practical benefits of massive MIMO, such as enhanced SE.

Co-located, distributed, and cell-free Massive MIMO systems have been studied extensively in recent years to see whether they can satisfy the varying demand fifth generation (5G), 5G-beyond and 6G networks to deliver a high quality of service (QoS).

2.2.1 Co-located massive MIMO systems

The classic implementation of massive MIMO networks is called co-located (centralized) massive MIMO, or generally massive MIMO. In these types of networks, macro BSs are equipped with an extremely high number of antennas to simultaneously serve a limited number of UEs, as shown in Figure 2.3, while using the same time and frequency resources [38]. It is worth noting that favourable propagation results from the broad system dimensions because the various UEs' channels are largely orthogonal [37]. Therefore, basic linear precoding and detection methods can be applied at the BS to transmit downlink data and detect uplink data, respectively [39]. It has come to light that implementing co-located massive MIMO can considerably provide high data rates and improve network reliability, coverage, and/or EE [40]. However, the system's performance deteriorates for UEs near the cell edge due to the decreased channel gain from the serving cell and the increased interference from nearby cells [12, 41].

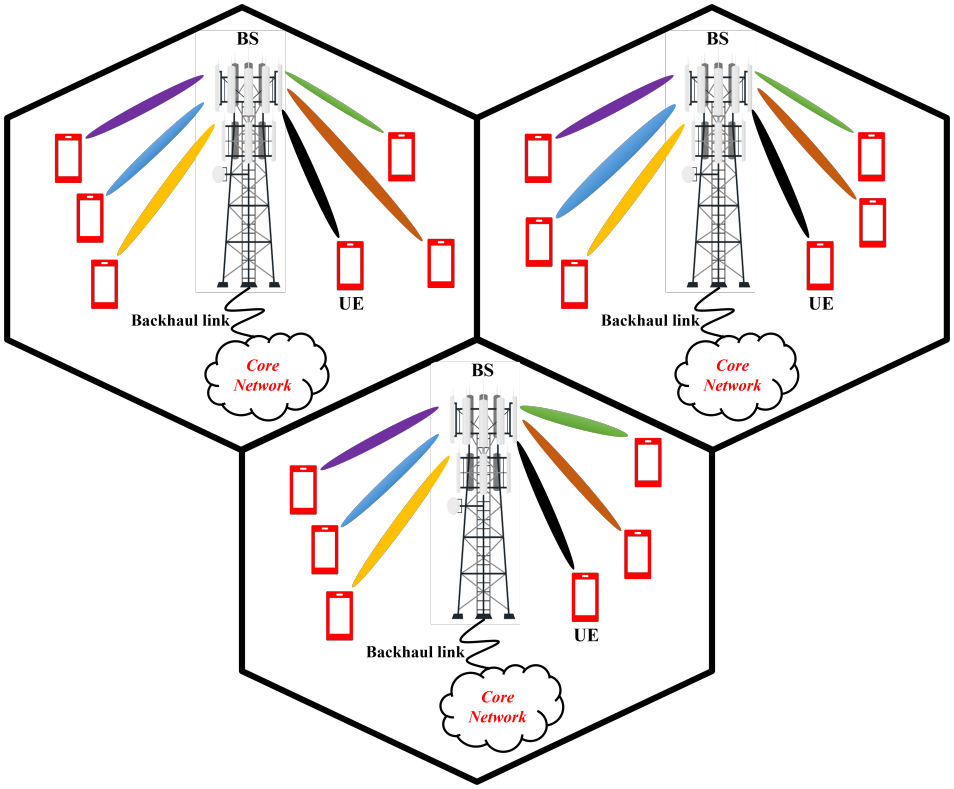

Figure 2.3: Co-located massive MIMO systems.

2.2.2 Distributed massive MIMO systems

Massive MIMO can be deployed distributed in small cells, which is distinguishable from co-located massive MIMO. This can be accomplished by deploying a large number of geographically dispersed APs, which are then linked to the CPU utilizing high-speed fibre or wireless backhaul/fronthaul links [42]. This system operates in a manner that is cooperatively similar to that of the Distributed Antenna System (DAS) setup [43] and Coordinated Multi-Point (COMP) with static disjoint cooperation clusters [44]. In both of these configurations, each cell is used to serve users who are located within its service area as shown in the Figure 2.4. The performance of distributed large MIMO systems with the performance of co-located systems has been evaluated in [45, 46]. According to the findings in [45, 46], distributed massive MIMO systems can enhance the data rate compared to co-located massive MIMO systems. This is feasible due to the significant diversity gain that is supplied to UEs as a result of the fact that each UE obtains different large-scale fading coefficients from other APs. In addition, the distributed system can deliver a high QoS to UEs on the cell edge due to the availability of many APs in each cell.

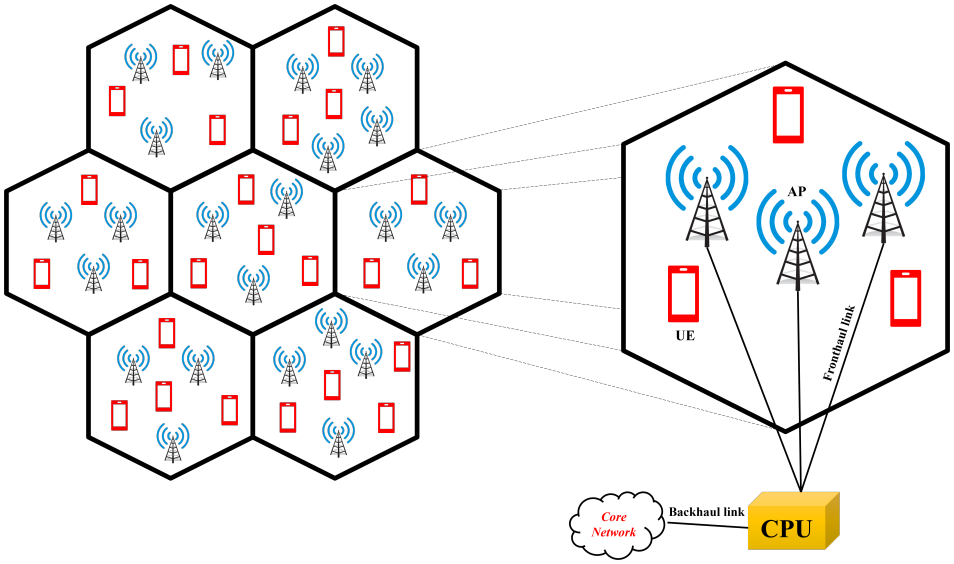

Figure 2.4: Distributed (small cell) massive MIMO systems.

2.3 Mm-Wave Technology

2.3.1 Overview

Over the last decade, rapid growth in mobile data demand has effectively congested the majority of conventional wireless frequency bands which is known as microwave technology, that spread between 300 MHz to 6 GHz, resulting in a seeming spectrum crunch and the necessity to seek other frequency bands to accommodate the future mobile generations and their promising services [36, 47]. Accordingly, 5G wireless communication can now operate in the mm-Wave frequency range 2 (FR2), which spans from 24 GHz to about 70 GHz [48] and will almost certainly play a vital role in the future generations such as 6G systems [49]. This is due to the large bandwidth available at these frequencies compared to the available bandwidth at sub-6GHz.

2.3.2 Limitations

The effectiveness of mm-wave communication technology suffers significantly due to propagation losses [47]. Huge path loss in the transmitted signal in the mm-Wave technology is caused by the high carrier frequency which affects on the cell coverage, the characteristics of air and molecular absorption and the attenuation caused by rain [50]. In addition, because mm-Wave signals do not have a strong ability to pass through obstructions, both static and dynamic impediments have the potential to obstruct the signals [51]. Devices under mm-Wave technology

need to transfer data over small distances or devices placed in locations free of obstacles due to the sensitivity of mm-Wave technology to lose its signal. Therefore, these characteristics of mm-Wave reduces the transmission range and signal processing techniques in massive MIMO systems are needed to compensate for the path loss, such as beamforming technique.

Table 1 presents a comparison between mm-Wave and microwave technologies in terms of frequency band, wavelength, bandwidth, antenna size, coverage, attenuation, and applications.

Table 1: Comparison Between Mm-Wave and Microwave Technologies [47].

Concept	**Mm-Wave Technology**	**Microwave Technology**
Bandwidth	High	Low
Wavelength	10 mm- 1 mm	1 m- 0.01 m
Antenna Size	Small	Large
Coverage	Short distances	Large distances
Attenuation	High	Low
Applications	Telecommunications, short-range radar, radio astronomy etc.	Cellular telephony, satellite, radio and television broadcasting etc.

2.3.3 Mm-Wave massive MIMO systems

A promising candidate technology for exploring new horizons for future wireless generations is the combination of mm-Wave technology with massive MIMO systems in order to use the large available bandwidth (in mm-Wave frequency ranges) and high antenna gains (achievable with the massive MIMO antenna arrays) [52]. Mm-Wave massive MIMO is allowed to surpass free of today's technological restrictions and face the challenges of rapidly increasing mobile data demand as mentioned previously. In addition, the integration between massive MIMO and mm-Wave technology increases reliability, compactness, and flexibility by opening up new scenarios for future applications due to its improved SE because proposing many antennas at the transmitter can lead to transmitting signals to a specific direction leading to reducing the interference. Each

antenna can consume a small amount of power, improving EE [53]. When various transmit-receive antenna pairs experience independently fading channel coefficients, mm-Wave massive MIMO systems can realise their highest potential advantages since this configuration allows for the most effective bandwidth, and this might be achieved if the distance between each element of the antenna is at least 0.5λ, where λ denotes the signal's wavelength [53]. Because the distance between antennas decreases as carrier frequency increases, it is possible to achieve a more significant number of elements in antenna arrays operating at the mm-Wave frequencies than at the sub-6GHz frequencies for arrays with the exact physical dimensions. In order to achieve this optimal performance, it is required to achieve high accuracy of the estimated channels [54–57]. In massive MIMO systems, transmission strategies such as beamforming, and/or spatial multiplexing are employed to enhance the performance of wireless networks [53]. Beamforming adjusts transmitted signals' phases and/or amplitudes based on the channel environment and application [58]. The references [59–66] provide a comprehensive review of beamforming types and architectures, while [58] and [67] provide a concise comparison of digital and hybrid beamforming with simulation-based link-level performance.

2.3.4 Signal Processing Techniques for mm-Wave Massive MIMO Systems

For mm-Wave massive MIMO cellular networks, fully digital, fully analog, and hybrid beamforming architectures, as demonstrated in Figure 2.5, are all models that have been developed over time [13]. In digital beamforming, each antenna is connected to RF chain; however, this is both prohibitively expensive and physically impossible owing to the limited available space. Still, the digital beamformer has optimal performance for conventional MIMO systems yet is practically infeasible for mm-Wave massive MIMO systems. On the other hand, analog beamforming consists of a single RF chain and many analog phase shifters in an entirely digital array. This beamforming design will reduce the hardware complexity. However, the system performance deteriorates since the antenna gain is minimal, and only the phases of the signals can be modified, not their amplitudes. According to recent research trends, massive hybrid beamforming consisting of many analog phase shifters and few RF chains are the most realistic and practical technique due to the ability of this structure to reduce the power consumption as well as the hardware complexity [68–70]. Therefore, the hybrid beamforming exhibits only minimal performance loss compared to the digital structure.

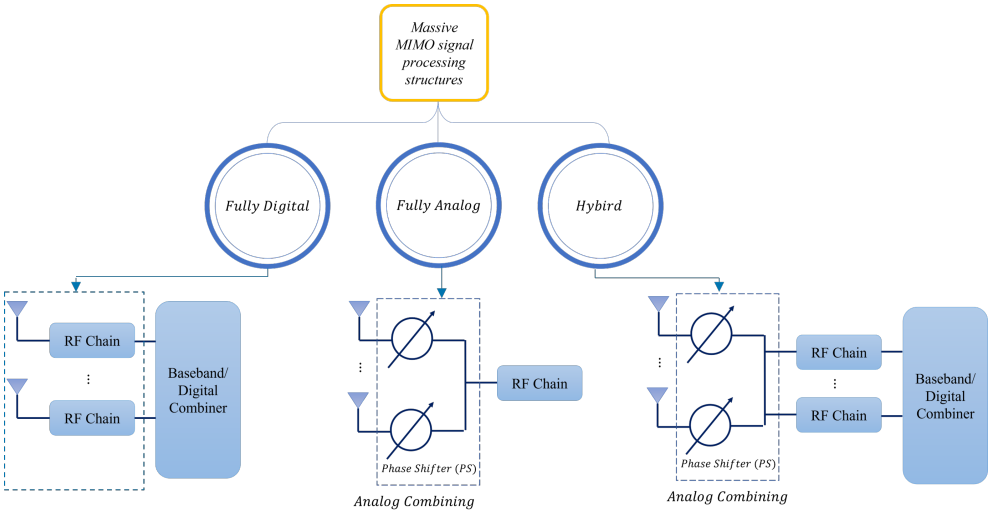

Figure 2.5: mm-Wave Massive MIMO signal processing structures.

Table 2 provides a comparison between analog and digital beamforming techniques in terms of components, complexity, inter-user interference, power consumption, and hardware cost.

Table 2: Analog and Digital Beamforming Comparison [13].

Beamforming Technique	**Components**	**Complexity and Inter-user Interference**	**Power Consumption and Hardware Cost**
Analog	Phase Shifters	Low/High	Low/Low
Digital	Analog-to-Digital (ADC) or Digital-to-analog (DAC) converter and Mixers	High/Low	High/High

Compared with digital beamforming, hybrid beamforming is a viable approach for the mm-Wave massive MIMO networks since it significantly reduces the number of required RF chains, the related power consumption and hardware cost [13]. Therefore, it achieves near-optimal performance compared to the digital beamforming [71]. This hybrid design is realised by employing two main steps [68, 71]. Firstly, it employs a small-size digital part with a small number of RF chains to cancel interference. Secondly, the analog part utilizes a large number of only phase shifters to increase the antenna array gain [68]. Furthermore, the hybrid

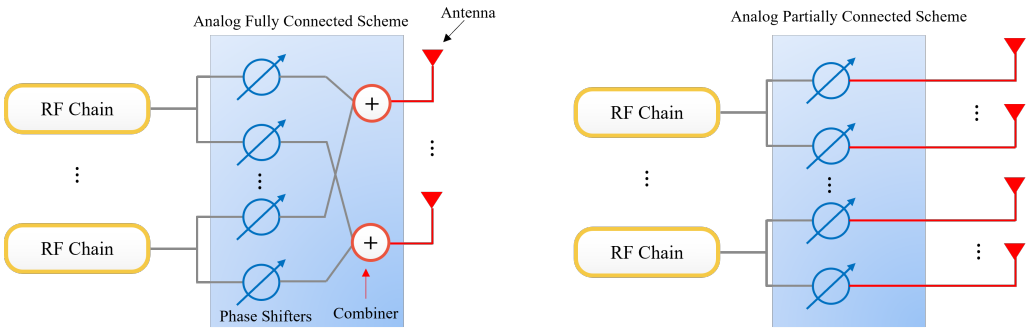

Figure 2.6: Analog precoding/combining structures in the hybrid beamforming technique.

beamforming can be divided into two main structural classes which are a fully and partially connected architectures. The fully connected architecture is defined as all BS (or AP) antennas being connected to each RF chain via phase shifters. In contrast, the partially connected architecture is a subset of BS (or AP) antennas connected to each RF chain [20], as illustrated in Figure 2.6. The main reason behind using partially connected phase shifters rather than fully connected phase shifter architecture is to reduce the size of the phase shifter network in order to reduce the power consumption of the hybrid beamforming scheme.

2.4 Cell-free massive MIMO systems

2.4.1 Overview

The cell-free massive MIMO network is a modified version of the distributed massive MIMO systems as illustrated in the Figure 2.7, in which all APs are positioned randomly over the coverage area without cell boundaries, and these APs are connected to the CPU to provide the service to all UEs at the same time-frequency resources [72]. This structure of massive MIMO systems can be considered as an important and promising new technology for wireless communication systems. In terms of uplink and downlink data achievable rates, the performance of the cell-free massive MIMO systems is compared to the small-cell massive MIMO systems in [10, 73, 74]. It has been discovered that the cell-free massive MIMO systems outperform the small-cell systems in terms of 95%-likely per-user throughput [10, 73–75]. Moreover, by utilizing max-min power control, the cell-free systems can provide uniformly good service to all UEs within the service area [10]. This structure also is presented as an exciting solution for next-generation indoor coverage applications, such as train stations, intelligent factories, small villages, shopping malls, hospitals, subways, universities' cam-

puses, and stadiums [76]. Several studies have shown that the cell-free massive MIMO network can outperform conventional cellular networks due to its higher achievable data rates, reliability, security, and connection density in high-velocity environments [10,73,75,77,78]. This new approach of massive MIMO is advocated for beyond-5G and 6G networks owing to its smooth mobility support without handover overhead by combining the cell-free massive MIMO network with non-orthogonal multiple-access (NOMA) [79–81], physical layer security (PLS) [82], reconfigurable intelligent surfaces (RIS) [83], radio stripes [84,85], and unmanned aerial vehicles (UAV) [86,87]. This will offer reliable QoS, which is contemplated as a challenge for vehicle technologies in the coming wireless networks [88]. Benefits comparison between co-located, distributed and cell-free massive MIMO systems are provided in Table 3.

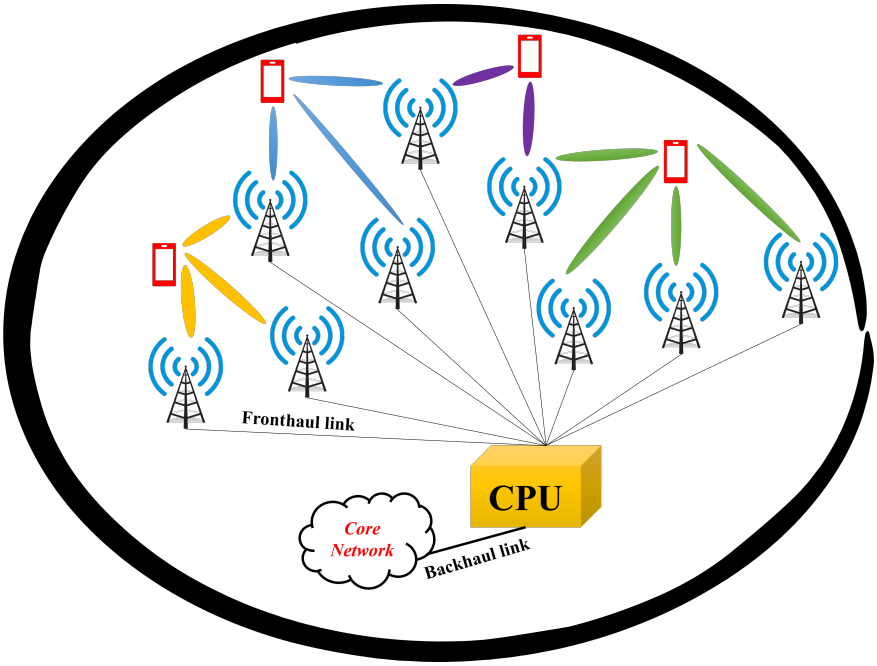

Figure 2.7: Cell-free massive MIMO systems.

Table 3: Comparison Between Co-located, Distributed and Cell-free Massive MIMO Systems [76].

Benefit	**Co-located**	**Distributed**	**Cell-free**
Antennas	Large	Moderate	Large
Deployment Cost	High	High	Low
Channel Hardening	Strong	Weak	Moderate
Favorable Propagation	Strong	Weak	Moderate
Coverage	Bad	Moderate	Good
EE	High	Low	Very High

2.4.2 Cell-free massive MIMO operations

Centralized and distributed manners are the operations of the cell-free massive MIMO systems. In centralized operation, the CPU is responsible for performing all signal processing operations, such as channel estimation, precoding, combining, encoding and decoding, based on channel reciprocity. In contrast, the distributed (decentralized) operation means most of the signal processing operations can be performed at the APs based on the local channel estimations [89] as shown in Figure 2.8. Therefore, the CPU sends only the downlink data signals to the APs in the distributed manner, while the APs in the centralized manner delegate the CPU to perform the encoding process of the downlink data. The centralized cell-free massive MIMO systems outperforms the distribute operation in terms of the computational complexity, but they can achieve close results in terms of the achievable rate [15]. Based on that, it has been proposed distributed operation for antenna selection and centralized for RF chain because the centralized operation for antenna selection requires enormous computational complexity due to a large number of both APs and antennas.

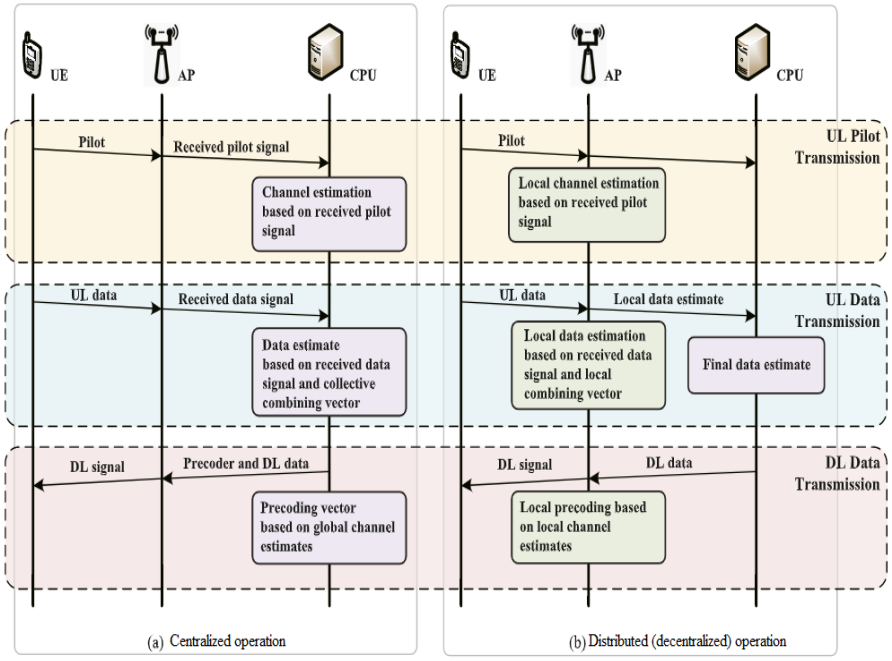

Figure 2.8: Cell-free massive MIMO operations [89].

2.4.3 Communication methods of the cell-free massive MIMO systems

The channel can be estimated using the received pilot sequences in the cell-free massive MIMO systems. The channel estimation might utilize the feedback sent from the receiver to the transmitter or employ both the feedback and the received pilot signals. This depends on the communication duplexing method adopted, either TDD or FDD, both of which are shown in Figure 2.9.

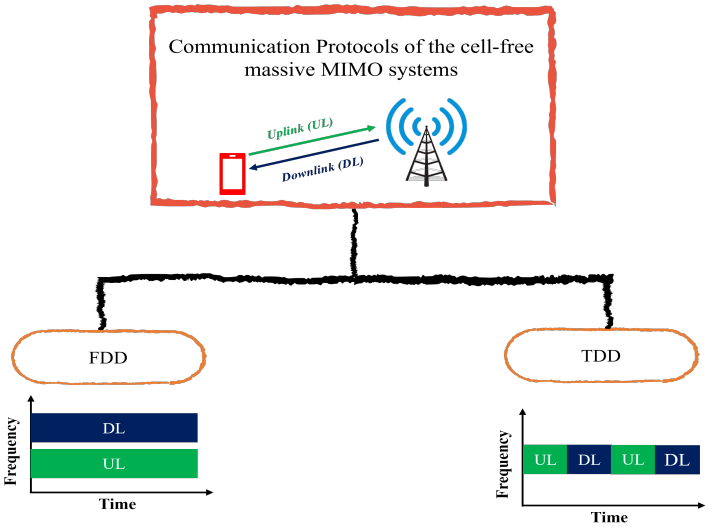

Figure 2.9: Communication protocols in the cell-free massive MIMO systems.

The uplink and downlink data transmissions occur at the same time in FDD systems across various frequency bands or in TDD systems in different time slots over the same frequency band. In FDD communication mode, the uplink and downlink channel coefficients do not reciprocally correspond to one another. Therefore, the APs are required to obtain the downlink channel coefficients to carry out the downlink precoding. Specifically, the channel coefficients can be obtained in the APs by operating through a downlink channel estimation phase, followed by CSI feedback [90,91]. The FDD, however, is impractical to be used in the cell free massive MIMO systems since the quantity of CSI acquisition and feedback increases linearly as the APs and antennas increase [90]. In addition, only the pilots in the feedback channels consume large amount of wireless resources. While TDD communication method utilizes the uplink estimated channel to perform the downlink data precoding without sending downlink pilot sequences due to the existence of the channel reciprocity property [12]. Table 4 provides a comparison between FDD and TDD in terms of spectrum usage, hardware complexity, coverage, wave propagation, control signalling and massive MIMO and beamforming technique.

Table 4: Comparison Between FDD and TDD methods [92].

Features	**FDD method**	**TDD method**
Spectrum usage	High	Low
Hardware complexity	High	Low
Coverage	Moderate	Good
Wave propagation	Different	Same
Control signaling	Difficult	Easy
Massive MIMO and beamforming technique	Complex	Simple

Based on what mentioned previously, the TDD method is suitable to be applied in the cell-free massive MIMO systems. Furthermore, the TDD communication frame consists of three main parts: uplink training, uplink data transmission, and downlink data transmission as shown in the Figure 2.10. To estimate the channel between UEs and the APs in the cell-free network, the UEs simultaneously send their pilot signals to the APs during the uplink training within, which τ_p denotes the length of the pilot sequences and τ_c is the length of coherence interval. The estimated channels by the APs can be used to perform precoding

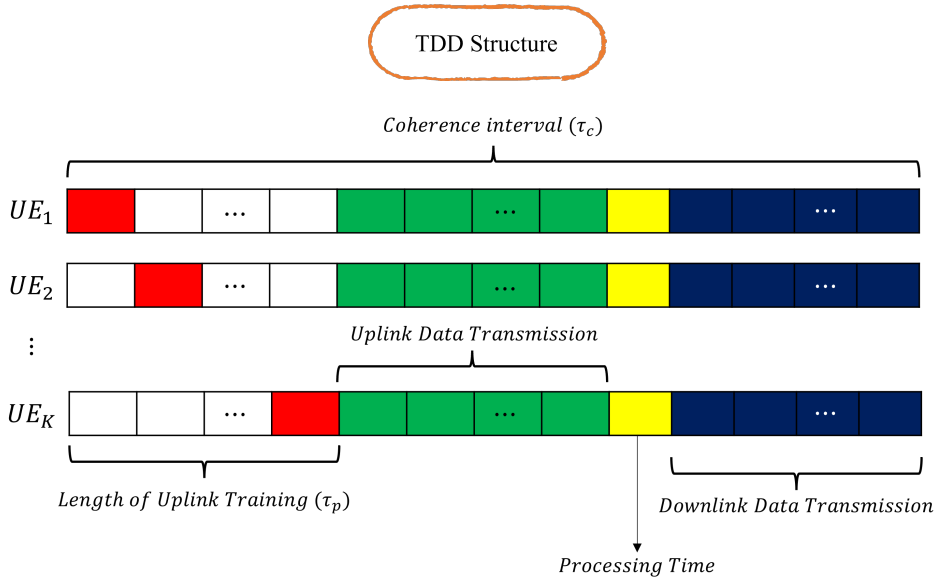

Figure 2.10: TDD communication protocol structure with orthogonal pilots.

and detection operations for the downlink and the uplink data transmissions, respectively. Let us consider where the communication between M APs and K single-antenna UEs, randomly distributed in the coverage area, is coordinated by a CPU. Each AP is equipped with N_r receive antennas. The pilot sequence for k_{th} UE is given by $\sqrt{\tau_p \eta_k}\phi_k \in \mathbb{C}^{\tau_p \times 1}$ where $||\phi_k||^2 = 1$ and η_k is the power control coefficient for k_{th} UE, where $0 < \eta_k \leq 1$. Then, m_{th} AP receives the $\tau_p \times 1$ pilot vector from all UEs to be used for the channel estimation and this vector is expressed as

$$Y_{p,m} = \sqrt{\tau_p \rho_p} \sum_{k=1}^{K} g_{k,m} \eta_k^{\frac{1}{2}} \phi_k^H + \mathbf{N}_{p,m}, \tag{2.1}$$

where $g_{k,m} \in \mathbb{C}^{N_r \times 1}$ denotes the channel coefficient vector between k_{th} UE and m_{th} AP and it is expressed as $g_{k,m} = \sqrt{\beta_{k,m}} h_{k,m}$, where $\beta_{k,m}$ represents the large scale fading and $h_{k,m} \in \mathbb{C}^{N_r \times 1}$ denotes the small scale fading vector. Each UE and AP is likely to have a various set of scatters due to the random distribution of APs and UEs over a wide service area. Furthermore, ρ_p denotes the normalized SNR of each pilot symbol (normalized by the noise power), where the noise power is $-174 \frac{\text{dBm}}{\text{Hz}} + 10 \log_{10}(B) +$ Noise Figure, where B is the system bandwidth. $\mathbf{N}_{p,m}$ gives the matrix of additive noise at m_{th} AP with size $N_r \times \tau$. Also, all entire elements of $\mathbf{N}_{p,m}$ are assumed to be independent identically distributed (i.i.d.) $\mathcal{CN}(0, 1)$ random variables (RVs). The performance of the cell-free massive MIMO systems in terms of the spectral and energy efficiencies is directly affected by the accuracy of the channel estimation [16]. The UEs simultaneously send pilot sequences at the length of τ_p to the APs. The pilot sequences assigned

to the UEs might be orthogonal or non-orthogonal depending on the number of UEs in the cell-free network, and the length of τ_p and τ_c. Moreover, orthogonal pilot sequences can be allocated to the UEs when there exists a large τ_c as well as the small number of UEs under low mobility scenarios, while non-orthogonal pilot sequences are allocated to the UEs under high mobility scenarios with large number of UEs and a small value of τ_c. The main reason behind using a small value of τ_c is to reduce the wireless resources during the channel estimation process [10, 12]. Furthermore, after receiving the pilot sequences at the APs, precoding and detection vectors are directly computed associated with the data symbol for each UE.

Most current research has focus on TDD with Rayleigh fading channels under the assumption that the large-scale fading coefficients are available between the UEs and the APs in the coverage area, such as [10,93–96]. This is owing to the fact that the large-scale fading coefficients slowly change during the channel coherence time [10]. As a result, minimum mean square error (MMSE) is preferable to be used as an estimator for the channels [93]. The estimated channel $g_{k,m}$ between k_{th} UE and m_{th} AP after performing projection the received pilot signal $Y_{p,m}$ onto ϕ_k is expressed as

$$\begin{aligned}\hat{y}_{p,k,m} &= \phi_k^H Y_{p,m} \\ &= \sqrt{\tau_p \rho_p} g_{k,m} \eta_k^{\frac{1}{2}} + \sqrt{\tau_p \rho_p} \sum_{k' \neq k}^{K} g_{m,k'} \eta_{k'}^{\frac{1}{2}} \phi_k^H \phi_{k'} + \phi_k^H \mathbf{N}_{p,m}.\end{aligned} \tag{2.2}$$

Thus, the MMSE can be used to estimate the channel between k_{th} UE and m_{th} AP as

$$\hat{g}_{k,m} = c_{k,m}(\sqrt{\tau_p \rho_p} g_{k,m} \eta_k^{\frac{1}{2}} + \sqrt{\tau_p \rho_p} \sum_{k' \neq k}^{K} g_{m,k'} \eta_{k'}^{\frac{1}{2}} \phi_k^H \phi_{k'} + \phi_k^H \mathbf{N}_{p,m}), \tag{2.3}$$

where $c_{k,m} = \frac{\sqrt{\tau_p \rho_p} \beta_{k,m} \eta_k^{\frac{1}{2}}}{\tau_p \rho_p \sum_{k'=1}^{K} \beta_{k',m} \eta_{k'} |\phi_k^H \phi_{k'}|^2 + 1}$. In addition, each AP in the coverage area individually estimates the channel and there is no cooperation among APs on the channel estimation process. On the other hand, several works proposed to use least square (LS) channel estimator when each UE has multiple antennas due to the absence of the large-scale fading coefficients [93–96]. The performance of the cell-free massive MIMO systems is studied based on using the MMSE and LS channel estimators and the results reveal that the MMSE can achieve higher data rates for both uplink and downlink [95, 96].

Another line of work has attempted to the enhance the channel estimation ac-

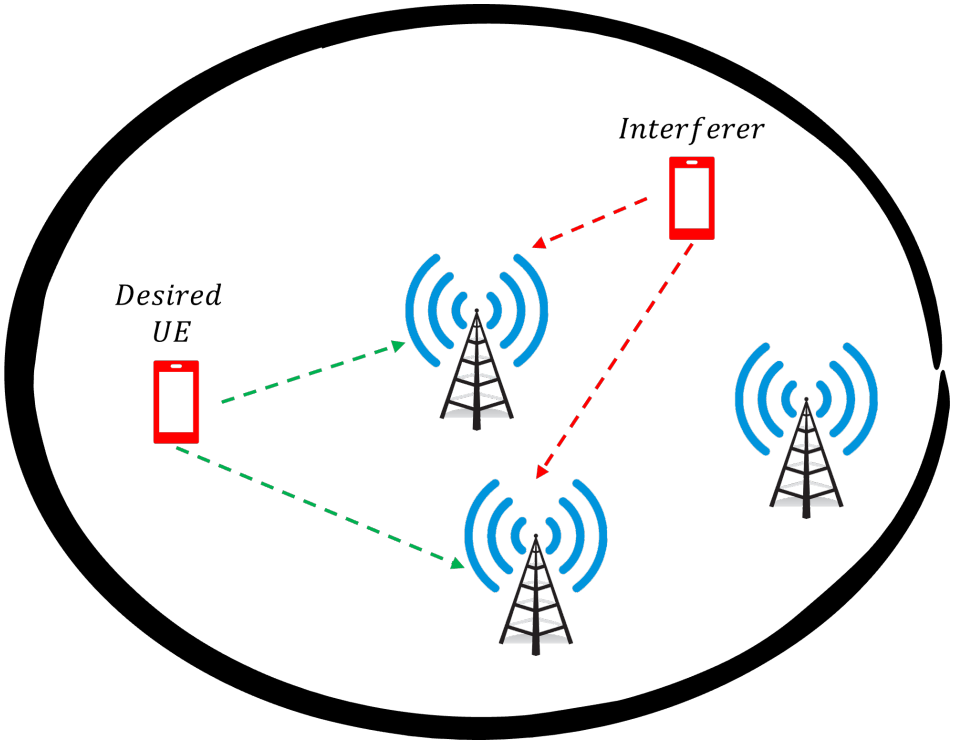

Figure 2.11: Pilot contamination phenomenon.

curacy based on pilot assignment techniques in order to mitigate the effect of the pilot contamination phenomenon [10, 97–99]. This phenomenon is defined as the interference between the transmitted pilot signal from the desired UE and other transmitted pilot signals from other UEs as shown in Figure 2.11. The authors in [10] proposed random and greedy pilot assignment schemes. Particularly, the random scheme is a simple algorithm that assigns available τ_p pilots to K UEs, then the reusable pilot sequences are assigned to the remaining $K - \tau_p$ UEs without considering the influence of the system performance. Whereas, the greedy scheme is proposed to maximize the UE with the worst data rate. Unfortunately, this scheme cannot provide the optimal pilot assignment since it is limited to the local optimum. The authors in [97] presents a Tabu-based approach to iteratively search for the sub optimal pilot assignment. This approach can attain 5% data rate improvement compared to the greedy approach in [10]. However, this scheme requires large number of iterations when there exists large number of K UEs and M APs in the cell-free network. The authors in [98] proposed Hungarian algorithm to solve the problem of the pilot assignment based on the large-scale fading coefficients between APs and UEs in the cell-free network, and this scheme can achieve better achievable data rate compared to the random and greedy schemes in [10]. Another direction of the pilot assignment based on graph theory is proposed in [100] in which a graph colouring-based and weighted graph-

based are presented where a limited number of neighbouring APs serve each UE. Consequently, depending on the APs selection algorithm, the large-scale fading coefficients are used to generate an interference graph. Therefore, the optimal pilot assignment is determined by modifying the interference graph. To increase the average downlink achievable rate, the authors in [99] proposed the GA to search for the sub optimal pilot sequences using its main operations which are selection, crossover and mutation. The GA approach outperforms other traditional schemes other traditional schemes, according to the numerical results. However, the GA lacks local search ability and is sensitive to 'rapid' convergence [101]. Table 5 presents a brief description of the applied techniques in the pilot assignment direction with their complexities analysis for cell-free massive MIMO systems to enhance the accuracy of the channel estimation.

Table 5: A brief description of the applied techniques in the pilot assignment direction for cell-free massive MIMO systems to enhance the accuracy of the channel estimation.

Applied Technique	**Description**	**Complexity Analysis**
Random [10]	It assigns available τ_p pilots to K UEs, then the reusable pilot sequences are assigned to the remaining $K - \tau_p$ UEs.	$\mathcal{O}(K)$
Greedy [10]	Starting from random assignment. Then, greedy algorithm is used to maximize the worst data rate for the UE.	$\mathcal{O}(KM)$, where M denotes the APs.

Continued on next page

Table 5: A brief description of the applied techniques in the pilot assignment direction for cell-free massive MIMO systems to enhance the accuracy of the channel estimation. (Continued)

Applied Technique	**Description**	**Complexity Analysis**
Tabu-Search [97]	Use Tabu-Search to avoid being trapped in in the local optimum. When using the assignment solution space, the *tabu list* is a matrix with size of $N_{tabu} \times K$ that is used to maintain track of previous pilot assignments in order to maximize the SE.	$\mathcal{O}(N_{tabu}K^2M)$.
Hungarian [98]	Based on the knowledge of the locations of APs in the coverage area, this algorithm can be optimized to maximize either the sum rate or the fairness among UEs.	$\mathcal{O}(K\tau^3)$.
Genetic algorithm (GA) [99]	It is used to search for the sub optimal pilot sequences based on its main operations are selection, crossover and mutation in order to maximize the total spectral efficiency for downlink cell-free massive MIMO systems.	$\mathcal{O}(\Gamma\mathcal{P}K)$, where $\mathcal{P}$ is the population size, which is τ^K [99, 101].

Regarding the pilot power control design, during the training phase, if all pilot signals are transmitted at full power, a UE with a weak channel might be highly contaminated by UEs with strong channels. As a result, the total system perfor-

mance deteriorates. In order to handle this issue, the authors in [17] proposed that pilot power coefficients be designed to increase the channel estimation accuracy during the training phase. They presented a min-max optimization problem which is expressed as

$$\begin{aligned} \min_{\eta_k} \quad & \max_{k=1,\ldots,K} \sum_{\mathrm{m}=1}^{\mathrm{M}} (1 - \sqrt{\tau_p \rho_p} \eta_k^{1/2} c_{k,m}) \\ \text{subject to} \quad & 0 \leq \eta_k \leq 1. \end{aligned} \tag{2.4}$$

The optimization problem in (2.4) aims to reduce the largest of all UEs' normalized mean-squared channel estimation errors, and this proposed optimization problem is non-convex. Then, they changed it to the second-order Taylor approximation. However, the proposed scheme in [17] has higher computational complexity in the real-time implementation when the cell-free network has large number of both APs and UEs.

2.4.4 Uplink Data Transmission

This section presents several uplink data detection techniques which are proposed for distributed and centralized transmission manners in the cell-free massive MIMO systems using TDD. The UEs data can be locally detected by implementing maximum ratio combining (MRC) at each AP based on the estimated channels [10]. Then, these detected signals are sent to the CPU, which averages the locally detected signals to obtain the UEs' signals. However, the authors in [74, 102] introduced three advanced techniques for the detection process: local detection, two-stage detection and fully centralized detection—the local detection approach based on MRC and MMSE is similar to [10]. In addition, two-stage detection employs local detection at the APs with MRC or MMSE, followed by large-scale fading detection at the CPU. Finally, the fully centralized approach, defined as the CPU, is responsible for detecting UE data when the received signals and the estimated channels are transmitted to the CPU via fronthaul links to perform detection.

According to [74, 102], using the MMSE detection strategy significantly outperforms the MRC one under various uplink detection techniques (local, two-stage, and centralized detection). The main reason is that the MMSE has better inter-user interference reduction than MRC. As a result of adopting the two-stage detection method, the uplink data rates are significantly improved by adding the large-scale fading-based detection step at the CPU level. While both local and two-stage data detection systems are superior in the uplink data rates, the central-

ized approach outperforms them. Since all UEs' channel conditions are available to the CPU during centralized network operation; as a result, the CPU can eliminate the interference caused by other UEs' data. According to [103], local and central partial-MMSE for fully distributed and fully centralized are proposed to maintain an extensible, scalable, cell-free massive MIMO system. Additionally, the proposed local and centralized partial MMSE for scalable system operation yields an equivalent uplink achievable rate to local and centralized MMSE detection.

2.4.5 Cell-free massive MIMO with mm-Wave Technology

This section seeks to provide the state-of-the-art schemes that utilize mm-Wave in the cell-free massive MIMO systems. The authors in [104] introduced the hybrid beamforming architecture for developing precoders and combiners in the cell-free mm-Wave massive MIMO systems under limited fronthaul capacity. They showed that it is possible to quantize the dominating eigenvectors of the channel covariance matrix which is known at the APs to obtain the phases of analog beamformers. A hybrid precoding approach employing antenna array response vectors is used for the distributed MIMO systems with partially connected hybrid beamforming architecture in [105]. The partially connected phase shifters network is proposed to reduce power consumption. However, its beamforming gain is lower than the fully connected phase shifters network, leading to a loss in the system performance in terms of the achievable rate [106]. An uplink multi-user estimation technique and low-complexity hybrid beamforming designs are introduced by Alonzo et al. in [107, 108]. Specifically, fully digital zero-forcing (ZF) precoding matrices are decomposed into baseband and analog precoders at each AP, employing the block-coordinate descent algorithm. Accordingly, the energy efficiency of the hybrid beamforming techniques specific to the cell-free mm-Wave massive MIMO systems is essential.

The literature exclusively includes a limited number of works that focus on optimizing the hybrid beamforming for the cell-free massive MIMO systems. To be more specific, in [104, 105, 107, 108], the analog beamformers are all separately generated at the APs based on the local CSI. The authors in [109] proposed the hybrid analog/digital structure by employing CPSs instead of using variable phase shifters (VPSs) due to huge power consumption and hardware complexity in the case of the fully connected scheme with a large number of antennas. They also utilized switches in the design of the analog beamforming. Thus, their proposed method achieved better energy efficiency and a slight loss in spectral efficiency due to using low-power CPSs. Additionally, the authors in [110] used the

same structure in [109] and maximized the signal-to-interference-plus-noise ratio (SINR) by presenting novel algorithms based on quasi-orthogonal combining. However, depending on the channel conditions, when signals received at many antennas are aggregated at the RF chain, a subset of antennas may contribute more to the interference than to the desired signal power, resulting in SINR loss.

The authors in [15] proposed adaptive RF chain activation (ARFA) schemes to reduce the power consumption in the uplink cell-free mm-Wave massive MIMO systems, where the fully connected hybrid analog/digital approach is individually created at each AP using known channel state information (CSI). However, the PSs in this technique are huge due to the vast number of antennas at each AP, resulting in high hardware implementation costs and power consumption. A hybrid beamforming technique with fixed phase shifters based on an alternating minimization algorithm for the uplink cell-free massive MIMO system was presented in [111]. They also employed fixed phase shifters with dynamic cascade switches at each AP to avoid the performance loss caused by erroneous fluctuation of the adaptive fixed number of phase shifters with channel conditions.

It is possible to use the antenna-selection techniques developed in [112,113] to the cell-free mm-Wave massive MIMO systems to lower power consumption. However, they have the potential to degrade performance, especially for the hybrid beamforming in the mm-Wave communication's highly correlated channels [114]. In addition, the power of the transmitted or received antennas is lower than that of hypothetical ideal antennas in a similar situation, as well as insufficient data rates [115]. Furthermore, because a massive MIMO system can use many receive antennas, the number of switches necessary to link the antennas to the RF chains is large, and these switches can consume a large amount of power. This problem is overcome in [14] by introducing a new hybrid beamforming architecture for conventional massive MIMO systems whereby each RF chain is connected to a subset of antennas that contributes more to the desired power rather than the interference power. Also, they introduced three low complexity algorithms compared with the exhaustive search approach to perform the selection process for the switches at the base station. However, the proposed work in [14] can be extended to the cell-free massive MIMO systems, but it is required to solve the issue of the huge computational complexity due to the large number of distributed APs. In addition, the proposed antenna selection techniques in [14] are suitable to be applied in the decentralized cell-free massive MIMO network because the subset of antennas at each AP can be switched off based on the estimated channel at this AP.

Low and/or variable resolution ADCs/DACs have been introduced to provide

a fair tradeoff between rate and power consumption in typical cellular (mm-Wave) massive MIMO systems [116]. Because of this tradeoff, the variable resolution ADCs can be applied in the cell-free mm-Wave massive MIMO systems. It is also possible to significantly reduce power consumption in the cell-free mm-Wave massive MIMO systems by using partially connected hybrid beamforming architectures [106, 117, 118]. These methods are comparable to the hybrid beamforming schemes for the small-cell or co-located mm-Wave massive MIMO systems, which are used when each AP in the cell-free mm-Wave massive MIMO network is considered a base station in the small-cell or co-located network.

2.5 Summary

This chapter presented the background and related works applying matching theory in wireless communications systems, massive MIMO systems, mm-Wave technology, and cell-free massive MIMO systems. In particular, this chapter provided the main concept of massive MIMO, its integration with mm-Wave technology and the signal processing techniques in mm-Wave massive MIMO systems. In addition, this chapter presented the background of the cell-free massive MIMO systems as well as the comparison between co-located and distributed massive MIMO systems in terms of several aspects, such as deployment cost, channel hardening, favorable propagation, coverage, and EE. Then, FDD and TDD communication methods, channel estimation enhancement techniques concerning the pilot assignment and pilot power control of the cell-free massive MIMO systems, and the uplink data transmission techniques were discussed. Finally, this chapter presented the related works of the cell-free massive MIMO with mm-Wave technology. Thus, it is noted that it is required to apply a low complexity method to enhance the system performance of the cell-free massive MIMO systems in terms of the SE, EE, and power consumption. The following three chapters propose a matching theory to achieve this aim.

Chapter 3

Antenna Selection Based on Matching Theory for Uplink Cell-Free Millimetre Wave Massive MIMO Systems

This chapter proposes a novel antenna selection technique based on the matching theory for the uplink cell-free mm-Wave massive MIMO systems assuming distributed operation when most signal processing operations are performed at the APs. The main reason for considering the distributed operation is to use the available CSI at each AP to switch off the subset of antennas that can contribute more to the interference power than the desired signal power. The proposed matching scheme in this chapter aims to maximize the EE while maintaining low computational complexity. In addition, the proposed matching scheme seeks to enhance the SE compared to the state-of-the-art techniques to mitigate the loss of the antenna gains due to switching some of them at the AP. The work in this chapter has been published in [119].

3.1 Introduction

This chapter presents a hybrid beamforming architecture with CPSs for uplink cell-free mm-Wave massive MIMO systems based on exploiting antenna selection to reduce power consumption. Current antenna selection techniques are applied for conventional massive MIMO, but have yet to be extended to the cell-free massive MIMO systems. Therefore, the significant computational complexity of these techniques to optimally select antennas for cell-free massive MIMO networks scales with the number of APs in the service area and the number of antennas.

The architecture proposed in this work solves this issue by employing a low-complexity matching technique to obtain the number of antennas, chosen based on channel magnitude and by switching off antennas that contribute more to interference power than to desired signal power for each RF chain at each AP, instead of assuming all RF chains at each AP have the same number of selected antennas.

This chapter investigates the flexibility of including or excluding the subset of antennas in the signal combining design by extending the proposed technique for selection antennas based on their contribution to the desired signal power compared to the interference signal power in in [14] from the conventional multi-user mm-Wave MIMO systems to the cell-free mm-Wave massive MIMO systems. Based on the assumption that there are a large number of APs, with each AP having a large number of antennas, a novel antenna selection strategy is proposed based on the matching technique in which each RF chain at the AP can be matched to the antennas that contribute more the desired power than the interference power. The proposed matching technique provides considerable power reduction while maintaining the system's SE. Furthermore, channel quality is utilized by each AP to assign each RF chain to its suitable set of selected antennas. Based on that, the proposed matching scheme can improve system performance and provide a tradeoff between SE, EE and computational complexity. In addition, to the best of our knowledge, no other works consider the Hungarian method [28] in the hybrid beamforming approach for cell-free massive MIMO systems.

The main contributions of this chapter are summarized as follows:

- Extension of the work in in [14], which has been proposed for conventional multi-user massive MIMO, to cell-free massive MIMO systems under the assumption of utilizing TDD communication mode to obtain the estimated channels between APs and UEs in the coverage area. The proposed algorithms in [14] have been adapted and applied in the cell-free massive MIMO systems to perform the antenna selection process at each AP.

- An assignment optimization problem has been proposed for all APs in the cell-free network to accomplish matching between RF chains and several sets of selected antennas based on channel magnitudes. Then, the Hungarian method is used to solve this optimization problem based on maximum weight matching in order to maximize EE. In contrast to [14], instead of assuming that all RF chains in the AP have the same fixed active switches, we exploit the advantages of the matching theory based on the Hungarian

algorithm to assign each RF chain at each AP in the cell-free network to the optimal number of activated switches depending on AP channel magnitude in order to maximize EE.

- Simulation results demonstrate the performance of the proposed antenna selection strategies under an extensive set of cell-free mm-Wave massive MIMO scenarios. In particular, the number of APs, the number of antennas, and the number of users in the network are analysed in terms of EE. In addition, computational complexity of the proposed algorithms is studied in this work.

Section 3.2 provides the system model of this work in this chapter, which includes the channel model, analog combining design, uplink channel estimation, uplink data transmission. In section 3.4, the proposed antenna selection scheme is introduced based on matching theory. The power consumption and EE models are presented in section 3.3. Section 3.6 presents the complexity analysis of the proposed antenna selection scheme based on matching theory in the uplink cell-free mm-Wave massive MIMO systems. Simulation results are provided in section 3.5. Section 3.7 concludes this chapter.

3.2 System Model

We consider the uplink of a cell-free mm-Wave massive MIMO system, where M APs and K single-antenna UEs are randomly distributed in the coverage area. Fronthaul links are utilized to connect the APs to the CPU, with each AP having N_r receive antennas and $N(\geq K)$ RF chains as shown in Figure 3.1. For simplicity, we assume that each AP utilizes exactly $K = N$ available RF chains to jointly serve K UEs, as in [109, 120]. The received signal at the m_{th} AP is distributed to multiple RF chains via a power splitter. In addition, the networks of switches and CPSs are denoted by $\mathcal{Z}_{k,m}$ and N_Q CPSs, respectively. N_Q can be used to connect k_{th} RF chain to $\mathcal{Z}_{k,m}$ out of N_r antennas at m_{th} AP. A power combiner before the RF chain combines the signals of $\mathcal{Z}_{k,m}$. Each antenna can be connected to the N_Q CPSs when the switch is activated.

The CPU coordinates communication between the M APs and the K UEs utilizing TDD communication method in which each frame is divided into three main phases: uplink training, uplink data transmission, and downlink data transmission. In this work, we focus on the uplink cell-free mm-Wave massive MIMO system, and whereby all UEs transmit their pilot signals to the APs in the cov-

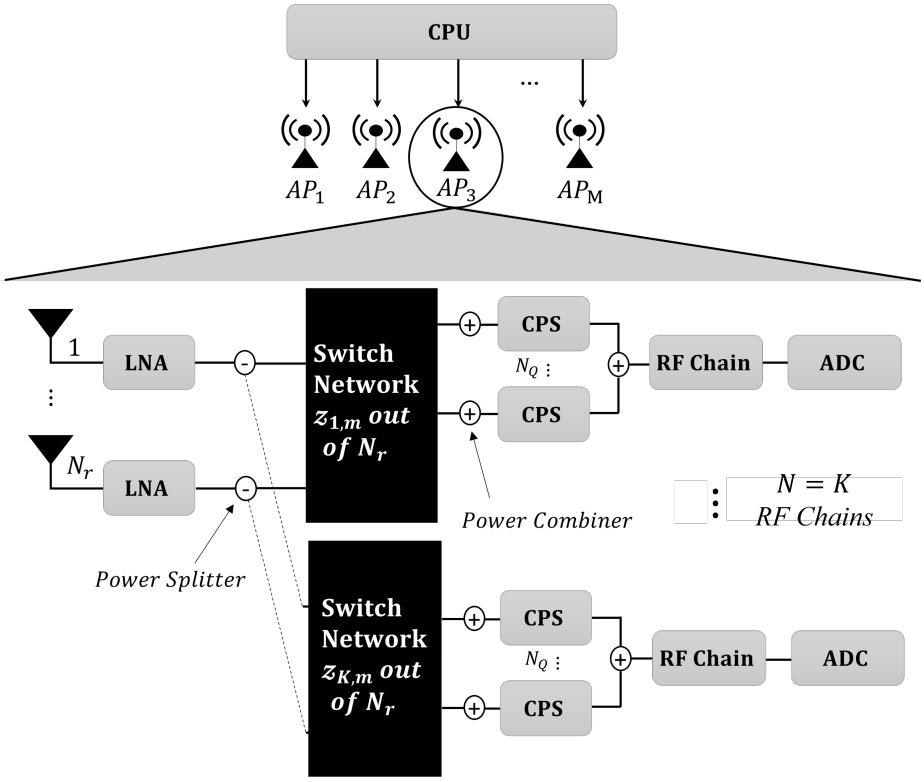

Figure 3.1: Hybrid beamforming structure for each AP in uplink cell-free massive MIMO systems with CPSs connected to RF chains via switch network.

erage area during the uplink training phase, allowing the APs to estimate the channels to each UE. The signals transmitted by the UEs in the uplink data transmission phase are subsequently detected based on channel estimates. The length of the uplink training, represented by τ_p, should not exceed the channel's coherence time/bandwidth interval, denoted by τ_c.

3.2.1 Channel Model

A narrowband block-fading channel model is adopted as the propagation environment between transmitters and receivers [66, 121–123], which is known as geometric Saleh–Valenzuela channel model. The channel between the m_{th} AP and k_{th} UE is expressed as

$$h_{k,m} = \sqrt{\frac{G_a N_r}{\beta_{k,m} P_{k,m}}} \sum_{p=1}^{P_{k,m}} \alpha_{k,m}^{(p)} \mathrm{a}_r(\phi_{k,m}^{(p)}), \tag{3.1}$$

where G_a denotes antenna gain, and $\beta_{k,m}$ represents the pathloss between the m_{th} AP and k_{th} UE, which can be expressed from [15, 124, 125] as

$$\beta_{k,m}[dB] = 10 \log_{10}(\frac{4\pi d_o}{\lambda})^2 + 10\ \varepsilon \log_{10}(\frac{d_{km}}{d_o}) + \chi_{k,m}, \tag{3.2}$$

where d_o is the reference distance, which is equal to one, λ is the wavelength, $d_{k,m}$ represents the distance between the m_{th} AP and k_{th} UE, the average pathloss exponent over the distance is represented by ε, and $\chi_{k,m} \sim \mathcal{N}(0, \varsigma^2)$ gives the shadow fading component with zero mean Gaussian random variable and ς standard deviation. Moreover, $P_{k,m}$ represents the number of propagation paths, the complex small scale fading gain is denoted by $\alpha_{k,m}^{(p)} \sim \mathcal{CN}(0,1)$ for all the APs and UEs in the service area, and $\phi_{k,m}^{(p)} \in [0, 2\pi]$ is known as the azimuth angle of arrival (AoA) for each channel path. Each AP is assumed to be equipped with a uniform linear array (ULA), and this structure of the antenna array is utilized to obtain the receive array response vector at the m_{th} AP, where a_r is given by

$$\mathrm{a}_r(\phi) = \frac{1}{\sqrt{N_r}}[1, e^{j\frac{2\pi}{\lambda}d_s \sin\phi}, \ldots, e^{j(N_r-1)\frac{2\pi}{\lambda}d_s \sin\phi}]^T, \tag{3.3}$$

where d_s denotes antenna spacing of half of a wavelength [122]. Finally, let us consider $\mathcal{A}_{k,m} = [\mathrm{a}_r(\phi_{k,m}^{(1)}), \ldots, \mathrm{a}_r(\phi_{k,m}^{(P_{k,m})})] \in \mathbb{C}^{N_r \times P_{k,m}}$ and $\Upsilon_{k,m} = [\alpha_{k,m}^{(1)}, \ldots, \alpha_{k,m}^{(P_{k,m})}] \in \mathbb{C}^{P_{k,m} \times 1}$. Then, $h_{k,m}$ can be expressed as [15]

$$h_{k,m} = \sqrt{\frac{G_a N_r}{\beta_{k,m} P_{k,m}}} \mathcal{A}_{k,m} \Upsilon_{k,m}. \tag{3.4}$$

Thus, $h_{k,m} \sim \mathcal{CN}(0, \sqrt{\frac{G_a N_r}{\beta_{k,m} P_{k,m}}} \mathbb{E}\{\mathcal{A}_{k,m} \mathcal{A}_{k,m}^H\})$. In addition, the channel matrix between K UEs and the m_{th} AP is given by $H_m = [h_{1,m}, \ldots, h_{K,m}] \in \mathbb{C}^{N_r \times K}$, and the total channel between K UEs and all APs in the coverage area is defined as $H = [H_1, \ldots, H_M]^T \in \mathbb{C}^{MN_r \times K}$.

3.2.2 Analog Combining Design

The analog combining W_m for each AP is based on N_Q CPSs and $\mathcal{Z}_{k,m}$ switches. Therefore, W_m is given as

$$W_m = [\Delta_{1,m}\omega_m, \Delta_{2,m}\omega_m, \ldots, \Delta_{K,m}\omega_m], \forall m, \tag{3.5}$$

where $\omega_m = [1, e^{j\frac{2\pi}{N_Q}}, \ldots, e^{j\frac{2\pi(N_Q-1)}{N_Q}}]^T$ denotes an array of N_Q CPSs for m_{th} AP, while $\Delta_{k,m} \in \mathcal{B}^{N_r \times N_Q}$ represents the switching network between the k_{th} RF chain and N_r at m_{th} AP. Thus, the switching matrix for all K RF chains can be expressed as $\Delta_m = [\Delta_{1,m}, \Delta_{2,m}, \ldots, \Delta_{K,m}] \in \mathcal{B}^{N_r \times KN_Q}$. The first constraint of the switching network that should be satisfied for k_{th} RF chain inside m_{th} AP [14] is expressed as $[\Delta_{k,m}]_{n,i} \in \{0,1\}$, where $n = \{1, 2, \ldots, N_r\}$ symbolizes the receive antenna index at each AP, while $i = \{1, \ldots, N_Q\}$ CPSs index. The second con-

straint restricts each antenna on each RF chain to be connected at most to one CPS. Therefore, this restriction can be presented as $\sum_{i=1}^{N_Q}[\Delta_{k,m}]_{n,i} \in \{0,1\}$. Thus, the main objective of using the previous constraints in the design of W_m is to easily exclude the antennas that contribute more to interference than to desired signal power, and their corresponding entries in W_m become zeros. Furthermore, the $\mathcal{Z}_{k,m}$ for each RF chain in m_{th} AP is shown as

$$\mathcal{Z}_{k,m} = \sum_{i=1}^{N_Q}\sum_{n=1}^{N_r}[\Delta_{k,m}]_{n,i}, 1 \leq \mathcal{Z}_{k,m} \leq N_r. \tag{3.6}$$

3.2.3 Uplink Channel Estimation

The channels can be estimated at the APs when K UEs simultaneously start to transmit their pilot sequences of τ_p. The received pilot sequence at m_{th} AP from K UEs, is expressed by

$$Y_m = \sqrt{\tau_p \rho_p}\sum_{k=1}^{K} h_{k,m}\varphi_k^H + n_m^{\text{noise}}, \tag{3.7}$$

where φ_k is the pilot sequence of k_{th} UE. ρ_p denotes the transmission power of each pilot symbol sent by k_{th} UE, $\sqrt{\tau_p}\varphi_k$ gives $\tau_p \times 1$ pilot assigned to k_{th} UE with $||\varphi_k||^2 = 1$, and $n_m^{\text{noise}} \in \mathbb{C}^{N_r \times \tau_p}$ is known as a matrix of independent identically distributed (i.i.d.) received noise samples, with each entry distributed as $\mathcal{CN}(0,\sigma^2)$, in which σ^2 is the noise power that can be computed as $\sigma^2 = -174\frac{\text{dBm}}{\text{Hz}} + 10\log_{10}(B) + NF$, where B is the system bandwidth, and NF is the noise figure. It is worth noting that the vast majority of practical scenarios hold $K > \tau_p$; hence, several UEs are allocated to a given pilot sequence, which leads to the pilot contamination phenomenon [16,126]. Therefore, this work focuses on the case of $K \leq \tau_p$. The pilot contamination issue will be discussed in chapter 5 when the number of UEs is larger than τ_p. Based on Y_m, the m_{th} AP can estimate the channel $h_{k,m}$. Denote $y_{k,m}$ as the projection of Y_m onto φ_k, which is given as

$$y_{k,m} \triangleq Y_m\varphi_k = \sqrt{\tau_p\rho_p}(h_{k,m} + \sum_{\hat{k}\neq k}^{K} h_{\hat{k},m}\varphi_{\hat{k}}^H\varphi_k) + n_m^{\text{noise}}\varphi_k. \tag{3.8}$$

Thus, the minimum mean square error (MMSE) is utilized to obtain the estimated channel $\hat{h}_{k,m}$ under the assumption of the knowledge of $\mathbb{E}\{\mathcal{A}_{k,m}\mathcal{A}_{k,m}^H\}$, which is the correlation matrix for all UEs is available at m_{th} AP [74]. For the MMSE estimation technique, we assume that the signals received at all of the AP's antennas are available. As a result, the low-complexity MMSE estimator

can be used to estimate the full channel state information (CSI) associated with all N_r antennas. There is also a compressed sensing-based technique, as given in [122], that can be used to extract the entire CSI in the situation of sparse channels and very slow fading; however, this approach is highly complex, especially in cell-free massive MIMO systems. Thus, $\hat{h}_{k,m}$ can be derived as [127]

$$\hat{h}_{k,m} = \mathbb{E}\{h_{k,m} y_{k,m}^H\}(\mathbb{E}\{y_{k,m} y_{k,m}^H\})^{-1} y_{k,m} \tag{3.9}$$

$$= \sqrt{\tau_p \rho_p}\left(\frac{G_a N_r}{\beta_{k,m} P_{k,m}}\right)\mathbb{E}\{\mathcal{A}_{k,m}\mathcal{A}_{k,m}^H\}$$

$$\left(\tau_p \rho_p \sum_{\hat{k}=1}^{K} \frac{G_a N_r}{\beta_{\hat{k},m} P_{\hat{k},m}} \mathbb{E}\{\mathcal{A}_{\hat{k},m}\mathcal{A}_{\hat{k},m}^H\}|\varphi_{\hat{k}}^H \varphi_k|^2 + \sigma^2 I_{N_r}\right)^{-1} y_{k,m}.$$

As a consequence, the total estimated channels between APs and K UEs is given as $\hat{H}_m = \left[\hat{h}_{1,m}, \hat{h}_{2,m}, \ldots, \hat{h}_{K,m}\right] \in \mathbb{C}^{N_r \times K}$ and $\hat{H} = \left[\hat{H}_1, \hat{H}_1, \ldots, \hat{H}_M\right]^T \in \mathbb{C}^{MN_r \times K}$. The next section explains how to employ the estimated channels $\hat{H}$ and $\hat{H}_m$ for the hybrid combining design in uplink data transmission.

3.2.4 Uplink Data Transmission

The symbol sent from the k_{th} UE to all APs is denoted by x_k, and it can be detected by applying hybrid beamforming to the received signal at m_{th} AP. Then, the received signal is expressed as

$$r_m = \sqrt{\rho} {W_{\text{HBF}}}_m^H \hat{h}_{k,m} x_k + \sqrt{\rho} {W_{\text{HBF}}}_m^H \sum_{\hat{k} \neq k}^{K} \hat{h}_{\hat{k},m} x_{\hat{k}} + {W_{\text{HBF}}}_m^H n_m^{\text{noise}}, \tag{3.10}$$

where ρ is the average transmit power from all UEs, and x_k represents the transmitted symbol by k_{th} UE, and thus $x = [x_1, \ldots, x_K]^T$ with $\mathbb{E}\{xx^H\} = I_K$. In addition, $n_m^{\text{noise}} \sim \mathcal{CN}(0, \sigma^2)$ is a vector of the noise, while the hybrid combining is ${W_{\text{HBF}}}_m^H = W_m w_{BB,k,m}$, where $w_{BB,k} \in \mathbb{C}^{K \times 1}$ denotes the digital combining vector for x_k at m_{th} AP, and $W_m \in \mathbb{C}^{N_r \times K}$ is the analog combining matrix at m_{th} AP. Note that the first term in (3.10) represents the received desired signal at m_{th} AP, the second term describes the interference, and the last term is the additive noise. In addition, the sum of the second and third terms is considered to be the interference plus noise, which is also known as effective noise. Furthermore, the received signal at each AP is forwarded to the CPU, and it is simultaneously processed using $w_{BB,k,m}$. $w_{BB,k,m}$ can be obtained by the MMSE beamforming scheme, which uses the effective channel $\hat{H}_m^e = W_m \hat{H}_m$ [14, 128]. Specifically, the

$w_{BB,k,m}$ is expressed as

$$w_{BB,k,m} = (1 + \frac{\rho}{\sigma^2}(\hat{H}_m^e \hat{H}_m^{e^H}))^{-1} \hat{h}_{k,m,e}^H,\ k = 1, 2, \ldots, K \tag{3.11}$$

where $\hat{h}_{k,m,e}^H$ is the k_{th} column of $\hat{H}_m^e$. There are two main stages to obtain W_m, as mentioned in [14]. The first stage is to consider all switches in the active state, and the switching matrices corresponding to Δ_m and $\Delta_{k,m}$ are symbolized by $\hat{\Delta}_m$ and $\hat{\Delta}_{k,m}$, respectively, with the same matrix sizes. As a consequence, the previously mentioned constraints are modified for each AP as $\sum_{i=1}^{N_Q}[\hat{\Delta}_{k,m}]_{n,i} = 1$, and $\sum_{i=1}^{N_Q}\sum_{n=1}^{N_r}[\hat{\Delta}_{k,m}]_{n,i} = N_r$. Thus, $\hat{W}_m \in \mathbb{C}^{N_r \times K}$ denotes the analog combiner that has non-zero elements due to the active states for all switches at m_{th} AP. Euclidean distance is adopted to design the switching matrix $\hat{\Delta}_m \in \mathcal{B}^{N_r N_Q \times K}$. We also utilize QR decomposition to express $\hat{H}_m = \tilde{H}_m Q_m$ in which $\tilde{H}_m \in \mathbb{C}^{N_r \times K}$ and $Q_m \in \mathbb{C}^{K \times K}$ are orthogonal and right-triangular matrices, respectively. In addition, CPSs with their phase of the channel coefficient of n_{th} antenna in each AP $\tilde{\theta}_{k,m_n}$ from ω_m corresponding to $[\tilde{h}_{k,m}]_n$ can be selected by the antenna's switch in $\hat{\Delta}_{k,m}$ based on the shortest Euclidean distance. Thus, $\tilde{\theta}_{k,m_n}$ can be obtained by

$$\tilde{\theta}_{k,m_n} = \frac{2\pi(\tilde{q} - 1)}{N_Q}, \tag{3.12}$$

where $\tilde{q}$ is the index of the selected CPSs, which is given by

$$\tilde{q} = \arg\min_{q \in \{1,\ldots,N_Q\}} \mid \theta_{k,m} - \frac{2\pi(q-1)}{N_Q} \mid, \tag{3.13}$$

where $\theta_{k,m} = [\tilde{h}_{k,m}]_n$. Thus, the n_{th} antenna switch that corresponds to $\tilde{q}$ is in an active state. The next stage considers a strategy to convert $\hat{\Delta}_m$ to Δ_m which describes the selected antennas for each RF chain in each AP. Therefore, we consider $S_m = [s_{1,m}, \ldots, s_{K,m}]$, which is a binary matrix with size $N_r \times K$. The main aim for considering this matrix is to describe the state for each antenna at m_{th} AP depending on if it is connected to k_{th} RF chain or not, whereas ones denote the selected antennas, while deactivated antennas are depicted as zeroes in S_m. Additionally, if n_{th} antenna at m_{th} AP is not connected to k_{th} RF chain, that does not mean this antenna will not be connected for other RF chains. Thus, Δ_m is generated by element-wise multiplication of each column vector of S_m by each column $\hat{\Delta}_m$, where $\hat{\Delta}_m = [\Omega_{1,m}, \Omega_{2,m}, \ldots, \Omega_{N_{Q_m}}]$ as expressed below

$$\mathcal{Z}_m = S_m \odot \hat{\Delta}_m. \tag{3.14}$$

Consequently, $\hat{W}_m$ is converted to W_m as follows

$$W_m = S_m \odot (\hat{\Delta}_m \omega_m). \tag{3.15}$$

Thus, $w_{BB,k,m}$ can be obtained with the help of the obtained optimal W_m [129].

The uplink SE can be obtained based on similar analysis techniques, such as [10, 14, 73, 104, 126]. The fast fading random variables in complex numbers are independent, and they characterize the propagation model between UEs and APs. Cell-free massive MIMO systems with perfect CSI have a known capacity in some cases [130], while the ergodic capacity is unknown in the case of imperfect CSI. However, the SE can be analysed by using standard-capacity lower bounds in this system [74, 127]. Thus, the uplink SE for m_{th} AP (SE_m), which is measured in bits per second per Hertz, is obtained as follows

$$\mathrm{SE}_m = \sum_{k=1}^{K} \mathrm{SE}_{k,m} = \frac{\tau_c - \tau_p}{\tau_c} \sum_{k=1}^{K} \log_2(1 + \mathrm{SINR}_{k,m}), \tag{3.16}$$

where $\mathrm{SINR}_{k,m}$ denotes the effective instantaneous signal-to-interference-plus-noise ratio between k_{th} UE and m_{th} AP, which can be given as [14, 128]

$$\mathrm{SINR}_{k,m} = \frac{\rho |w_{BB,k,m}^H W_m^H \hat{h}_{k,m}|^2}{\rho \sum_{\hat{k} \neq k}^{K} |w_{BB,k,m}^H W_m^H \hat{h}_{\hat{k},m}|^2 + \sigma^2 \|w_{BB,k,m}^H W_m^H\|^2}. \tag{3.17}$$

Therefore, the total uplink SE for all APs is expressed as

$$\mathrm{SE} = \sum_{m=1}^{M} \mathrm{SE}_m. \tag{3.18}$$

The problem formulated to obtain the optimal number of selected antennas for each RF chain is NP-hard [14, 109]. Therefore, when there are a large number of APs in the cell-free network, and each AP is equipped with a large number of N_r, this will lead to remarkably high computational complexity to determine the optimally selected antennas using an exhaustive search method across $2^{N_r K}$. Additionally, the findings in [14] indicate that using channel quality to switch on antennas that have a large channel magnitude can overcome the quasi-coherent combining algorithm for fixed CPSs (FCPSs) [110] when the selected number of antennas for each RF chain is 75% of N_r antennas; further, similar performance compared with [110] is achieved when 50% of the selected antennas are utilized. Based on these findings, it is reasonable to conclude that excluding a particular number of antennas from W_m can enhance SE_m, implying that these antennas

contribute more to interference signal power than the desired signal power. In addition, these results motivated us to put forth the following question: How can we an assignment problem to find the optimal number of selected antennas for each RF chain at each AP to enhance EE without a significant loss in SE based on the channel quality utilizing a low-computational complexity approach in an uplink cell-free mm-Wave MIMO network?

3.3 Power Consumption and Energy Efficiency Models

Total power consumption model similar to that applied in, for example, [14, 115, 131–135], is used in the considered uplink cell-free massive MIMO systems. Therefore, the power consumed by m_{th} AP fronthaul link to the CPU depends on the amount of traffic on the link that should be transferred. Thus, the power consumed by m_{th} fronthaul link is given as

$$P_{\mathrm{FH}_m} = \frac{P_{\mathrm{FH}_{max}} R_{\mathrm{FH}_m}}{C_{\mathrm{FH}_m}}, \tag{3.19}$$

where $P_{\mathrm{FH}_{max}}$ is the maximum fronthaul power, C_{FH_m} denotes the fronthaul capacity for m_{th} AP, and R_{FH_m} gives the actual fronthaul rate between m_{th} AP and the CPU and is expressed as

$$R_{\mathrm{FH}_m} = \frac{2K(\tau_c - \tau_p)\alpha_m}{T_c}, \tag{3.20}$$

where α_m and T_c represent the number of quantization bits at m_{th} AP and the coherence time (in seconds), respectively. For simplicity, we assume that all APs have the same value of $P_{\mathrm{FH}_m}, \alpha_m$, and C_{FH_m}. In addition, the power consumed by the RF chain circuit at m_{th} AP is expressed as

$$P_{\mathrm{RF}} = P_{\mathrm{M}} + P_{\mathrm{LO}} + P_{\mathrm{LPF}}, \tag{3.21}$$

where $P_{\mathrm{M}}, P_{\mathrm{LO}},$ and P_{LPF} are the power consumed by the mixer, local oscillator, and low-pass filter, respectively. The total circuit power consumption for all APs in the considered uplink cell-free mm-Wave massive MIMO systems is expressed as

$$P_{\mathrm{T}} = \sum_{k=1}^{K} P_{\mathrm{CP}_k} + P_{\mathrm{TX}_k} + \sum_{m=1}^{M} P_m^{\mathrm{FH}} + MN_r(P_{\mathrm{LNA}} + P_{\mathrm{SP}}) + +M(\sum_{k=1}^{K} \mathcal{Z}_{k,m} P_{\mathrm{SW}}$$

$$+K(N_Q P_{\mathrm{CPS}} + P_{\mathrm{C}}(N_Q + 1) + P_{\mathrm{RF}} + P_{\mathrm{ADC}})), \tag{3.22}$$

where P_{TX_k} and P_{CP_k} are the transmit power of k_{th} UE and the amount of power required to operate the circuit components, respectively. P_{TX_k} is shown as $P_{\mathrm{TX}_k} = \rho\sigma^2 \sum_{k=1}^{K} \frac{\mathbb{E}\{|x_k|^2\}}{\eta_k^{\mathrm{amp}}}$, where η_k^{amp} denotes the power amplifier efficiency at k_{th} UE. In addition, all UEs have the same value of both η_k^{amp} and P_{CP_k}. Furthermore, $P_{\mathrm{LNA}}, P_{\mathrm{SP}}, P_{\mathrm{SW}}, P_{\mathrm{CPS}}, P_C$, and P_{ADC} are the power consumed by the low-noise amplifier, splitter, switch, CPSs, combiner, and analog-to-digital converter, respectively. Thus, the total uplink EE, which is measured in bits per Joule, is given as

$$\mathrm{EE} = \frac{B.\mathrm{SE}}{P_{\mathrm{T}}}. \tag{3.23}$$

3.4 Antenna Selection Methodology

3.4.1 Problem Formulation

To answer the aforementioned question, we propose the matching theory, which is matching in weighted bipartite graphs seeking to maximize the total weight of the matching operation, to assign each RF chain at AP to its suitable number of selected antennas to maximize the EE by choosing the optimal predefined value of each RF instead of assuming a single predefined value of active antennas as mentioned in [14]. Furthermore, we consider half of the RF chains at each AP have selected antennas exceeding 50% of the total number of antennas based on channel condition. On the other hand, each of the remaining RF chains might be connected to 50% or less of the total number of N_r at m_{th} AP based on channel condition, as mentioned in [14]. Thus, this will be considered a compromise between maximum EE and avoiding significant SE loss. To achieve this aim, we formulate an assignment optimization problem to match each RF chain at m_{th} AP to its suitable predefined value of the selected antennas, as shown in Figure 3.2. The proposed linear assignment optimization problem to compute the optimal

match between K RF chains and $\mathcal{Z}_m$ in this chapter can be formulated as

$$\begin{aligned} \max_{x_{u,b}\in\{0,1\}} \quad & \sum_{u=1}^{K}\sum_{b=1}^{\mathcal{Z}_{K,m}} \mathrm{R}_{k,m}^{(\mathcal{Z}_{k,m})} x_{u,b} \\ \text{s.t.} \quad & \sum_{u=1}^{K} x_{u,b} = 1, \text{for } u = 1,\ldots,K, \\ & \sum_{b=1}^{K} x_{u,b} = 1, \text{for } b = \mathcal{Z}_{1,m},\ldots,\mathcal{Z}_{K,m}. \end{aligned} \tag{3.24}$$

where $R_{k,m}^{(\mathcal{Z}_{k,m})} = \log_2(1 + \mathrm{SINR}_{k,m})$ is the reward function of the above linear program, ${x_{u,b}}^{K\times K}$ gives the binary matrix, where $x_{u,b} = 1$ if and only if u_{th} RF chain is assigned to b_{th} $\mathcal{Z}_{k,m}$ switches. In addition, $\mathcal{Z}_{k,m} = N_r - \varkappa\kappa$, where $\kappa = \frac{N_r}{K}$ and $0 \leq \varkappa \leq K$. Thus, $\mathcal{Z}_m = [N_r^{(1)}, N_r - \kappa^{(2)}, N_r - 2\kappa^{(3)}, \ldots, N_r - \varkappa\kappa^{(K)}]$ based on the number of RF chains at each AP.

3.4.2 Problem Solution

We utilize the Hungarian method, which is a combinatorial optimization algorithm, to solve the proposed bipartite graph assignment problems in this work with K RF chains at each AP and $\mathcal{Z}_m = [\mathcal{Z}_{1,m}, \mathcal{Z}_{2,m}, \ldots, \mathcal{Z}_{K,m}]$. The reason behind assuming the length of $\mathcal{Z}_m$ equals to the number of RF chains at each AP is to obtain a square matrix for the reward matrix $\mathcal{R}$ in order to make the assignment operation less complicated for the proposed Hungarian algorithm.

Algorithm 1 summarises the whole procedure of the proposed antenna selection matching strategy for maximizing the EE for uplink cell-free mm-Wave massive MIMO systems. The first three steps are utilized to generate $\tilde{W}_m$ based on Equation (3.13) for each AP. Then, all connections between N_r and the RF chains are in the inactive state, and antenna indices are sorted in ascending order based on the smallest channel magnitude for each AP, and symbolized as $\tilde{J}_m = [\tilde{j}_{1,m}, \tilde{j}_{2,m}, \ldots, \tilde{j}_{K,m}]$. Thus, each RF chain has several values of SE_m based on $\mathcal{Z}_m$. Therefore, reward matrix $\mathcal{R}$ describes the problem formulated in (3.24), and it can be solved based on the steps of the Hungarian algorithm mentioned in Algorithm 1. The Hungarian algorithm is used to arrange the reward matrix $\mathcal{R}$ in order to maximize weight matching. Moreover, as shown in Figure 3.2, the suggested algorithm's high-level diagram begins by assigning to each RF chain randomly a $\mathcal{Z}_{k,m}$ from the set $\mathcal{Z}_m$. Then, the Hungarian algorithm starts by reducing each row in the input reward matrix, which consists of the computed $R_{k,m}$ with all elements of the set $\mathcal{Z}_m$, by subtracting the minimum item in each row

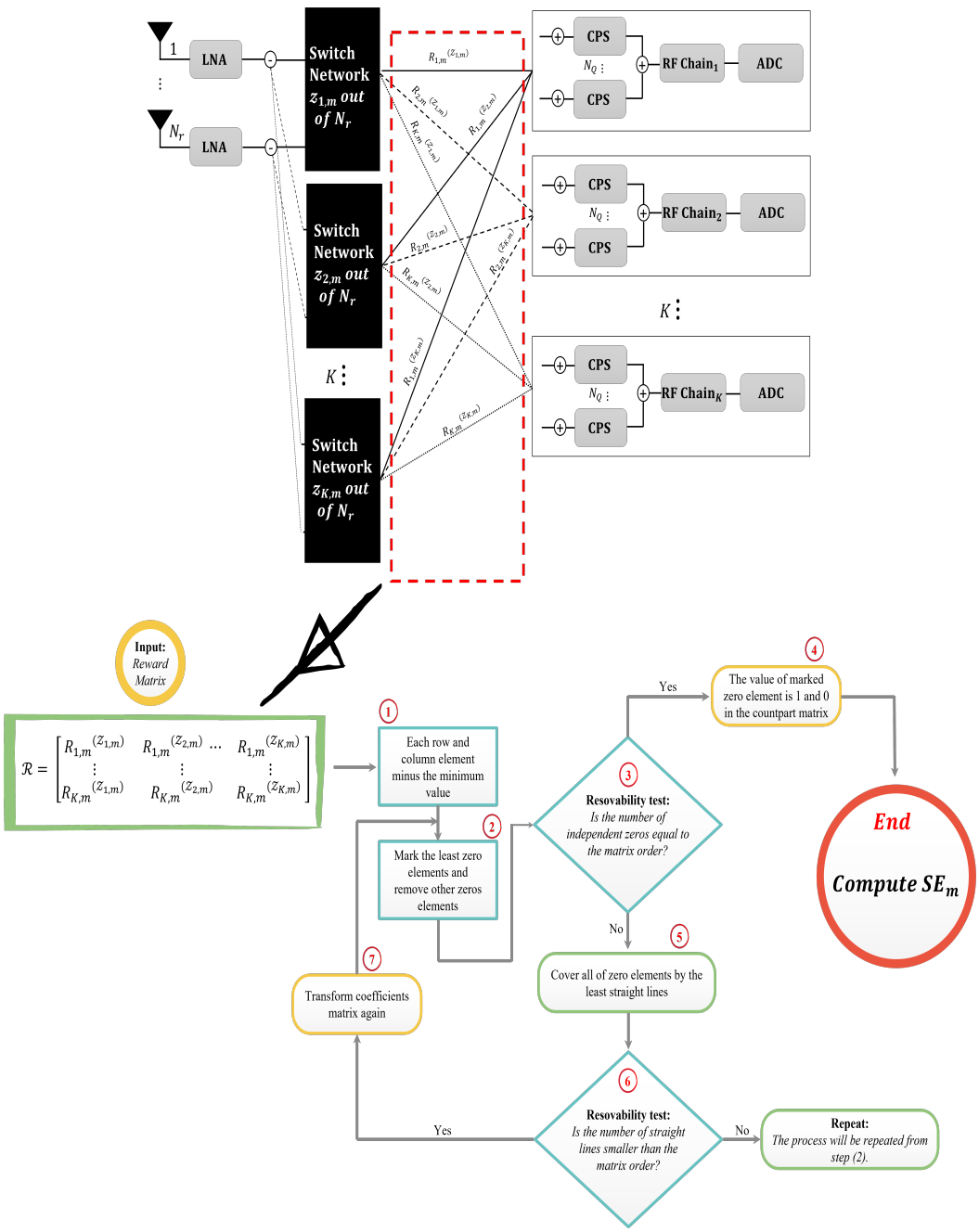

Figure 3.2: Proposed matching strategy for RF chain-subset selected antennas for each AP diagram with flowchart of the Hungarian algorithm.

from all other items in the same row, and repeating the process for each column. Accordingly, we look for the convenient $\mathcal{Z}_{k,m}$ switches for each RF chain. If k_{th} RF chain is already assigned to $\mathcal{Z}_{k,m}$ switches, it is better to be assigned with another $\mathcal{Z}_{k,m}$; we prime the alternative before moving on to the next $\mathcal{Z}_{k,m}$ candidate switches; however, if that is the only $\mathcal{Z}_{k,m}$ switches for which k_{th} RF chain is qualified, we would like to reassign any other RF chain to those $\mathcal{Z}_{k,m}$ switches. We reassign RF chains to their alternate selected antennas to guarantee the assignment can provide the maximum SE for each AP, which is the resolvability test. As a result, we can be confident that we progress toward our goal of identifying the best assignment with each iteration. Finally, because our proposed algorithm does not require a high number of iterations to reach the maximum total SE, especially when there exists a large number of both APs and/or N_r equipped for each AP, this proposed technique employing a matching strategy has much lower complexity compared to the state-of-the-are schemes, as presented in Section 3.6.

3.5 Simulation Results and Discussions

This section includes a comprehensive collection of simulation results that investigate the performance of our proposed matching scheme in terms of total power consumption and EE in the uplink cell-free mm-Wave massive MIMO. In order to emphasize the importance of our results through matching between several fixed values of activated antennas based on the channel quality and RF chains at each AP, our proposed scheme is compared with the methods from conventional mm-Wave multi-users MIMO in [14] expanded to cell-free mm-Wave massive MIMO systems, which are decremental search-based antenna selection (DSAS), channel magnitude-based with dynamically selected antennas (CMDAS), and channel magnitude-based with fixed selected antennas (CMFAS). Furthermore, DSAS scheme uses descending search method to find the optimal switching network, which maximizes the SE for each AP. The first step in this scheme is to assume that all antennas for m_{th} AP are connected to all RF chains and, based on that, the initial SE for m_{th} AP is computed. Then, an antenna in each RF chain at m_{th}AP is turned off at each iteration to find the maximum SE increment compared to the initial one computed in the first step. Therefore, once the maximum SE increment for that RF chain is obtained, its antenna is switched off. CMDAS scheme is proposed to lower the computational complexity by minimizing the number of searching iterations compared to the DSAS scheme, especially when the number of APs rises. Assuming all antennas for m_{th} AP are connected to the

Algorithm 1: Matching strategy for RF chain-subset selected antennas based on the Hungarian algorithm.

Input: N_Q, ρ, $\hat{H}_m$, σ^2

for $m = 1 \rightarrow M$ **do**
  for $k = 1 \rightarrow K$ **do**
    - Use QR decomposition to obtain $\tilde{H}_m$ based on $\hat{H}_m$.
    - Quantize the phase $\theta_{k,m}$ of each element of $\tilde{H}_m$ to $\hat{\theta}_{k,m}$ based on (3.13).
    - Generate the analog combining $\tilde{W}_m$ based on (3.15).
  end
  - Initialize $S_m = [s_{1,m}, s_{2,m}, \ldots, s_{K,m}]$ as $0_{N_r \times K}$.
  - Then, $J_m = [j_{1,m}, \ldots, j_{K,m}]$ where $j_{k,m} = [1, \ldots, N_r]^T$.
  for $k = 1 \rightarrow K$ **do**
    - Sort the elements of $j_{k,m}$ in ascending order of $|[\tilde{H}_m]_{n,k}|$ to find $\tilde{j}_{k,m}$, where $n = 1, \ldots, N_r$.
  end
  - Initialize $\mathcal{Z}_m = \{\mathcal{Z}_{1,m}, \mathcal{Z}_{2,m}, \ldots, \mathcal{Z}_{K,m}\}$.
    - Then, S_m is generated corresponding to $\mathcal{Z}_m$ by converting $\mathcal{Z}_{k,m}$ zero entries in each column of $s_{k,m}$ to ones.
  - Compute $R_{k,m}$ corresponding to S_m, where $R_{k,m}$ represents the reward of the assignment of k_{th} RF chain to k_{th} selected antennas, i.e., $\mathcal{Z}_{k,m}$.
    - Prepare the reward matrix $\mathcal{R} = \sum_{u=1}^{K} \sum_{b=1}^{K} R_{k,m}$.
    - Generate the Hungarian algorithm [28] to solve (3.24) as demonstrated in Figure 3.2.
  - Compute SE_m based on (3.16).
end
Finally, compute SE based on (3.18).

k_{th} RF chain, we calculate the initial SE. Then, we consider the antenna indices for each AP as $J_m = [j_{1,m}, j_{2,m}, ..., j_{K,m}]$ where $j_{k,m} = [1, 2, ..., N_r]^T$. Also, it is required to construct a matrix $\tilde{J}_m$ which consists of the columns of the antenna indices as $\tilde{J}_m = [\tilde{j}_{1,m}, \tilde{j}_{2,m}, ..., \tilde{j}_{K,m}]$. These columns are sorted in ascending order based on $|\tilde{H}_m|$. Thus, we have K connections to each antenna. In addition, the number of iterations is equal to the number of receive antennas at m_{th} AP. Then, in each iteration, K connections are converted to zeros because their channel magnitudes are small. The SE is then computed and compared to the initial SE in the first step, a similar procedure to the DSAS scheme. Finally, if the obtained SE after removing the K connections is larger than the SE for the initial state, when all antennas are connected at m_{th} AP, the switching matrix is updated. Finally, the same steps are repeated until MN_r maximum iteration for all APs in the cell-free network. CMFAS scheme varies considerably with the channel magnitude-based with dynamic switches for each RF chains scheme at m_{th} AP by using a predefined value of switches which is used for all RF chains at m_{th} AP whereas $\mathcal{Z}_m = \mathcal{Z}_{k,m}$ for all K RF chains. The steps for this scheme do not need any iterations, and its process is repeated for all APs. Therefore, the complete procedure to obtain the optimal network switch for each AP in the coverage area by utilizing a predefined value for the selected antennas for all APs based on the channel condition.

Similar to what has been done in the literature on cell-free massive MIMO, and to improve the modelling of network performance by removing boundary effects, M APs are randomly distributed in a $D \times D$ square service area, where $D = 1000$ m [10, 15], and boundaries are wrapped around. In addition, due to the limited scattering in mm-Wave channels, the effective channel paths between k_{th} UE and m_{th} AP is assumed as $P_{k,m} = 20$ $\forall k, m$ [120, 122]. Based on (3.2), the large scale fading coefficients can be determined by setting $\varepsilon = 4.1$ and $\varsigma = 7.6$ [15, 124]. Table 1 contains the parameters used in all simulations in this section.

Table 1: Simulation parameters.

Parameter	**Value**
Carrier frequency (f)	28 GHz [123]
Bandwidth (B)	500 MHz [123]
Antenna gain (G_a)	15 dBi [15, 124]
Noise figure (NF)	9 dB [10, 15]

Continued on next page

Table 1: Simulation parameters. (Continued)

Parameter	**Value**
Coherence interval length (τ_c)	200 samples
Length of pilot sequence (τ_p)	20 samples
Pilot transmit power (ρ_p)	100 mW
Quantization bits (α_m)	2 bits [133]
Fronthaul capacity (C_{FH})	100 Mbps [37]
Amplifier efficiency (η_k^{amp})	0.3 [131]
Coherence time (T_c)	2 ms [37]
Power components:	$P_m^{\text{FH,fix}} = 5$ W, $P_{\text{FH}max} = 50$ W, $P_{\text{CP}} = 1$ W, $P_{\text{RFC}} = 40$ mW, $P_{\text{LNA}} = 20$ mW, $P_{\text{SP}} = 19.5$ mW, $P_{\text{SW}} = 5$ mW, $P_{\text{CPS}} = 5$ mW, $P_{\text{C}} = 19.5$ mW, and $P_{\text{ADC}} = 200$ mW.

Figure 3.3 show the impact of the number of N_r receive antennas on the SE when $M = 80$, $K = 8$ UEs, $N_Q = 8$ and $\rho = 23$ dBm. As it can be observed, increasing the number of antennas,N_r, at each AP results in an increasing in the SE as shown in Figure 3.3. The SE when $N_r = 48$ is improved compared to FCPSs scheme by 13.65%, 9.67%, 7.92%, 7.1% and 0.015% for the DSAS, the proposed matching scheme, CMFAS with 75% and with 50% selected antennas out of N_r schemes, respectively. It is noted that the proposed matching scheme outperforms CMFAS with both 75% and 50% selected antennas out of N_r, and FCPSs scheme because each half of RF chains is assigned to more than 50% of the antennas at each AP while each of the remaining RF chains is matched to 50% or lower of antennas. It is noted that the DSAS scheme can achieve higher SE compared to all schemes. In contrast, the proposed matching scheme can achieve close results to the DSAS. This is reasonable because half of RF chains at each AP can guarantee improvement of the sum rate and the remaining RF chains can use minimum amount of selected antennas in order to maximize the EE.

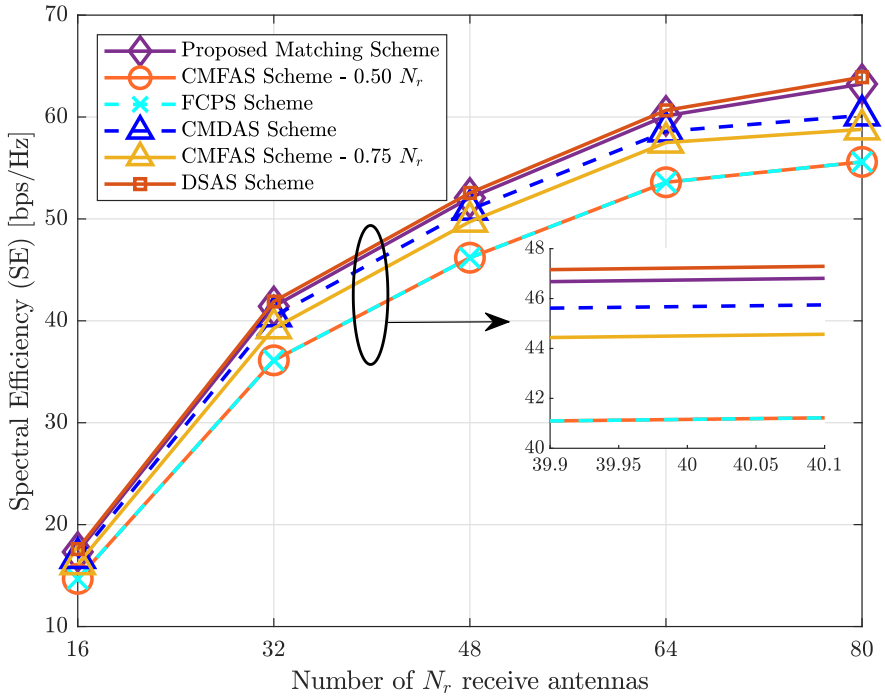

Figure 3.3: SE versus number N_r of antennas, where $M = 80$ APs, $N_Q = 8$, $\rho = 23$ dBm, and $K = 8$ UEs.

Figures 3.4 and 3.5 show the impact of the number of N_r on both EE and total power consumption when $M = 80$, $K = 8$, $N_Q = 8$, and the transmit power $\rho = 23$ dBm. It is observed from Figure 3.4 that the EE for all schemes decrease when N_r increases, which is obvious because the additional N_r come with a resultant increase in power consumption. The proposed matching scheme for antenna selection in uplink cell-free mm-Wave massive MIMO systems is advantageous in terms of EE in both cases when the APs have fewer antennas and more antennas. In the case of the APs having fewer antennas, the channel quality worsens, leading to degradation in system performance in terms of the SE. However, the proposed scheme can mitigate this issue by offering each half of the RF chains be assigned to more than 50% of the N_r at each AP, while each of the remaining RF chains is matched to 50% or less of N_r. Therefore, half of the RF chains assigned to more than 50% of the selected antennas at each AP can guarantee improvement of the sum rate, and the remaining RF chains set to 50% or less can maximize EE. For example, when $N_r = 16$ antennas are equipped for each AP, the proposed antenna matching selection strategy can achieve 12.5171%, 18.33%, 21.384%, 21.6%, and 40.387% compared to the CMFAS scheme with both 50% and 75% of the selected antennas fixed, and CMDAS, DSAS, and FCPSs in [110], respectively.

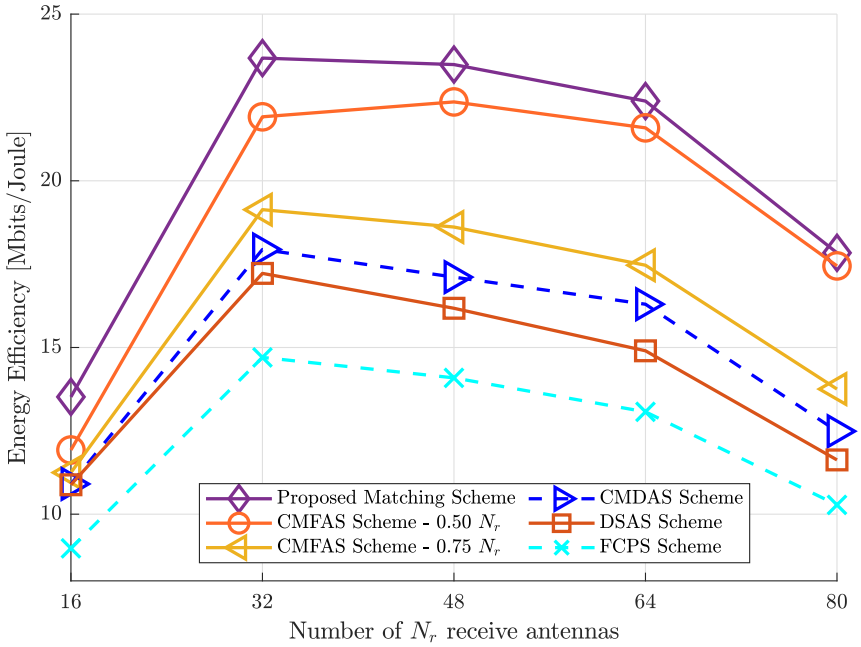

Figure 3.4: EE versus number N_r of antennas, where $M = 80$ APs, $N_Q = 8$, $\rho = 23$ dBm, and $K = 8$ UEs.

On the other hand, Figure 3.5 shows total power consumption increases when N_r increases. It is obvious that CMFAS with 50% of the selected antennas fixed has the lowest total power consumption. Then, the proposed matching scheme comes in second place and then CMDAS, DSAS, and FCPSs, in which DSAS and FCPSs attain similar total power consumption. Therefore, it can be seen that the proposed matching based on the Hungarian algorithm can outperform CMDAS, DSAS, and FCPSs. For example, when $N_r = 48$, the proposed matching scheme uses 1108.48 W, while CMFAS with 50% of the selected antennas fixed uses 1023.63 W. In addition, CMDAS, DSAS, and FCPSs use 1487.67 W, 1627.09 W, and 1639.39 W, respectively.

In Figure 3.6, we show the SE of the considered schemes versus various numbers of APs. It can be seen that the proposed matching scheme outperforms the FCPSs, CMDAS, CMFAS with both 75% and 50% of the selected antennas scheme with respect to the SE. This is because half number of RF chains at each AP in the cell-free massive MIMO network are connected to large number of selected antennas for each of the mentioned half RF chains. Therefore, this can guarantee and keep higher sum rate for each AP from the channel conditions.

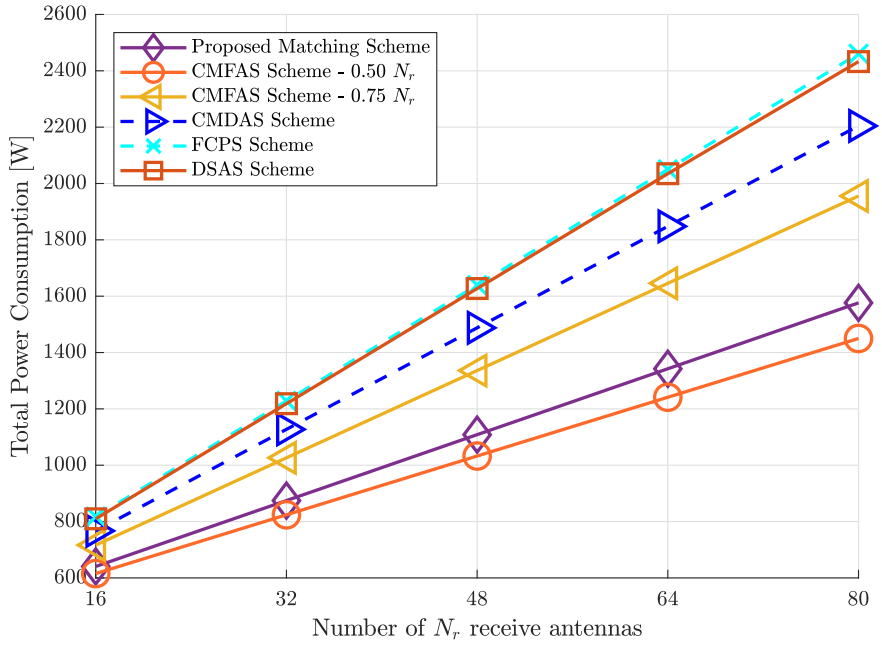

Figure 3.5: Total power consumption versus number N_r of antennas, where $M = 80$ APs, $N_Q = 8$, $\rho = 23$ dBm, and $K = 8$ UEs.

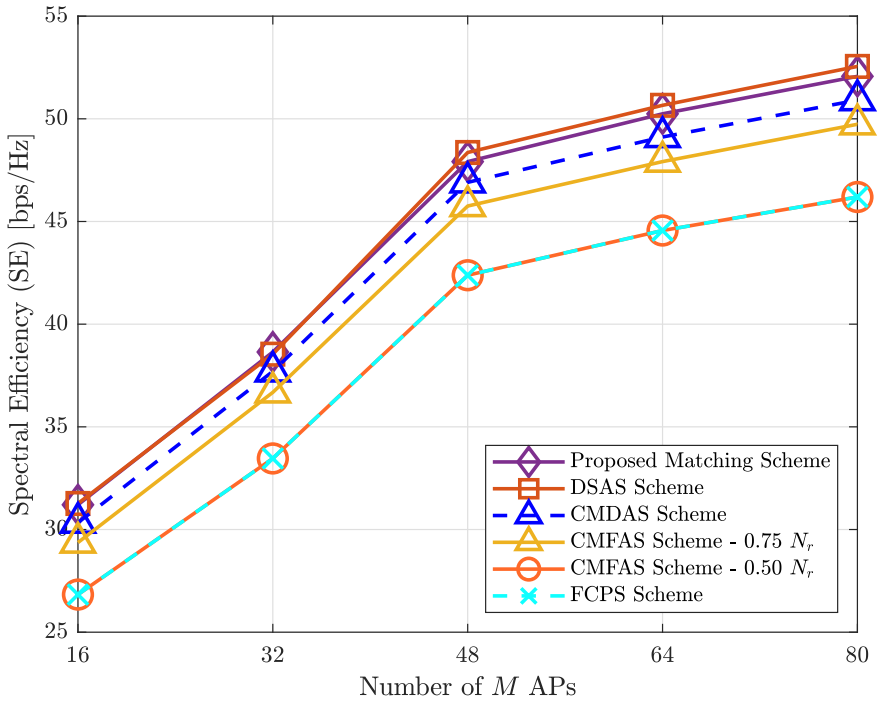

Figure 3.6: SE versus number of APs, where $N_r = 48$ APs, $N_Q = 8$, $\rho = 23$ dBm, and $K = 8$ UEs.

Figure 3.7 shows EE performance against increasing number M of APs for $K = 8$, $N_r = 48$, $N_Q = 8$, and $\rho = 23$ dBm. As the number of APs increases, we observe that the EE of all schemes decreases. This is because the power consumption of each AP rises as well, owing to the inclusion of massive hardware components such as RF chains, CPSs, analog-to-digital converters, and so on. This can lead to a decrease in the EE. However, the proposed matching scheme can achieve satisfactory performance concerning the EE over all the schemes mentioned in this chapter. However, DSAS lowers EE compared to all other techniques. This is appropriate since the design of W_m for each RF chain excludes a small number of antennas, and these antennas are switched OFF because of their considerable contribution to the interference signals at each AP.

Figure 3.8 presents that total power consumption increases when M increases. It can be seen that CMFAS with 50% of the selected antennas has the lowest total power consumption. Then, the proposed matching strategy comes after CMFAS with 50% of the selected antennas. This is because the number of selected antennas for each RF chain at each AP plays an important role in minimising total power consumption. Furthermore, it is noted that the number of selected antennas for each RF chain at each AP is no more than 50% in CMFAS, which can lead to lower total power consumption. Therefore, activating a large number of antennas at all the APs causes extremely high power consumption for the uplink cell-free mm-Wave massive MIMO system, as illustrated in the state-of-the-art schemes, motivating the proposed matching scheme in this work to maintain lower power consumption by matching half of the RF chains at each AP to a large number of active antennas to mitigate a significant loss in the SE, while the rest of the RF chains are assigned to fewer selected antennas to maximize the EE. Thus, it can be noted that the proposed matching scheme can overcome DSAS, CMFAS with 75% of the selected antennas, CMDAS, and FCPSs.

Figure 3.9 demonstrates the impact of K UEs on the EE of the uplink cell-free mm-Wave massive MIMO network when $M = 80$, $N_r = 48$, and $\rho = 23$ dBm. It is obvious that the EE increases as K increases. This is because inter-user interference cannot affect the SE of the uplink systems. In particular, it indicates that large K UEs in the proposed matching perform better than other schemes in terms of SE. This is because with more data streams received, the chance that the optimal large number of antennas are activated for the half of RF chains at each AP increases. This will enhance the preservation of the system from significant loss in SE. In contrast, the rest of the RF chains are responsible for maintaining EE by choosing fewer antennas. Compared with the extended

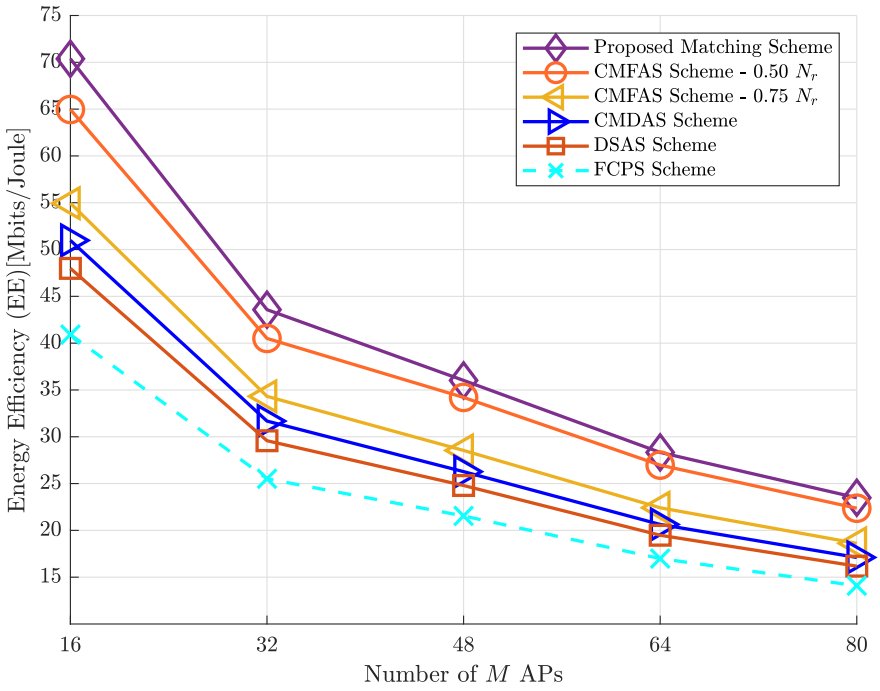

Figure 3.7: EE versus number of APs, where $N_r = 48$ APs, $N_Q = 8$, $\rho = 23$ dBm, and $K = 8$ UEs.

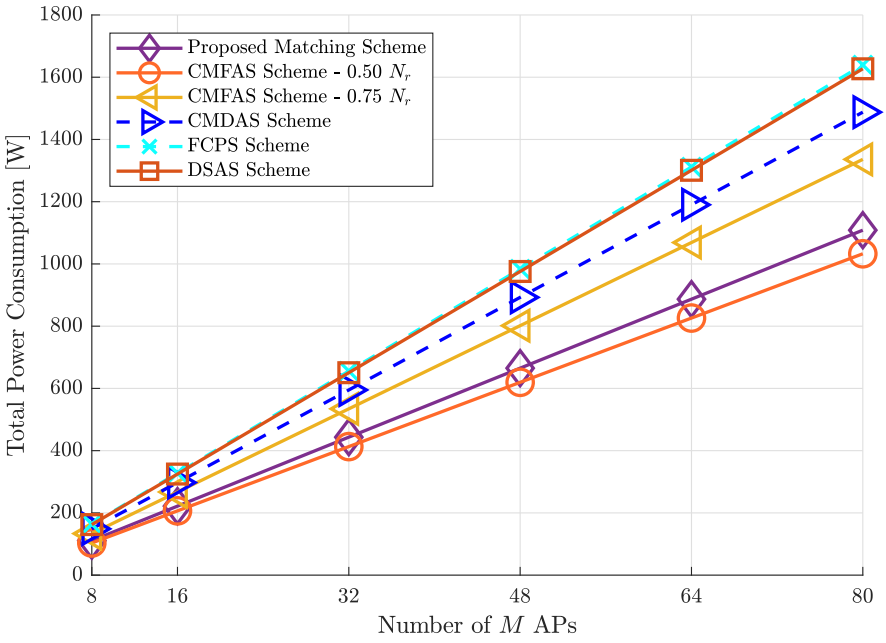

Figure 3.8: Total power consumption versus number of APs, where $N_r = 48$ APs, $N_Q = 8$, $\rho = 23$ dBm, and $K = 8$ UEs.

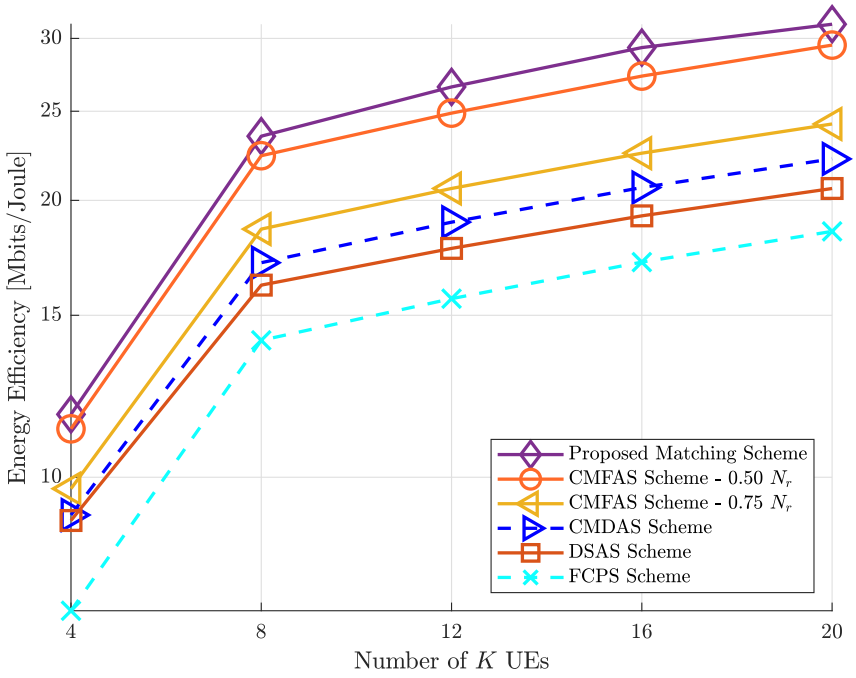

Figure 3.9: EE versus number of UEs, where $M = 80$ APs, $N_Q = 8$, $\rho = 23$ dBm, and $N_r = 48$.

schemes and FCPSs, the proposed matching technique provides much-enhanced EE, as anticipated. For example, when $K = 12$ UEs, the proposed matching scheme can attain approximately 6.55%, 25.3%, 33.53%, 39.9%, and 52% EE improvement compared to CMFAS with 50% and 75% of the selected antennas, CMDAS, DSAS, and FCPSs. We also observe that the proposed matching scheme can optimize SE and EE. In contrast, other schemes, namely, DSAS and CMDAS, seek to optimize only the SE without taking into consideration the total power consumption, especially when the cell-free network has a large number of M APs, N_r antennas, and K UEs.

Figure 3.10 presents clear gains in the total power consumption obtained by the extended and proposed schemes in this chapter. Figure 3.10 also demonstrates that when K increases, so does the total power consumption. For example, the proposed matching scheme uses 1615.2 W, while CMFAS with 50% of the selected antennas fixed uses 1539.38 W with $K = 12$, $N_r = 48$, $N_Q = 8$, $M = 80$, and $\rho = 23$ dBm. In addition, the proposed matching scheme achieves lower total power consumption compared to DSAS, CMDAS, CMFAS with 75% of the selected antennas fixed, and FCPSs by 40.53%, 31.62%, 21.01% and 41.046%, respectively.

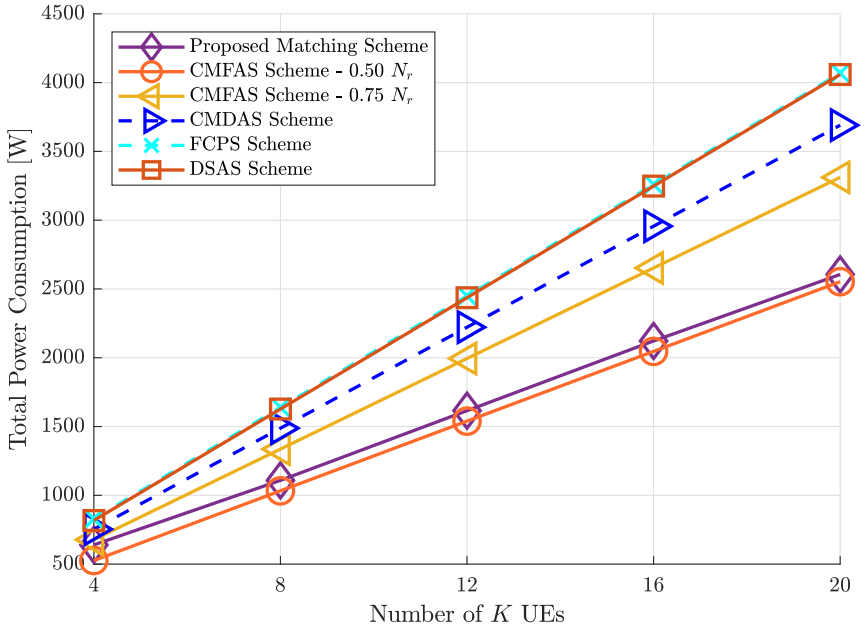

Figure 3.10: Total power consumption versus the number of UEs, where $M = 80$ APs, $N_Q = 8$, $\rho = 23$ dBm, and $N_r = 48$.

Finally, in uplink cell-free mm-Wave massive MIMO systems, there is a tradeoff between EE, SE, and the number of FLOPs used as a complexity analysis in this chapter. Figure 3.11 illustrates this tradeoff. The solid curves in this figure show the proposed matching scheme's energy efficiency, spectral efficiency, and FLOPs tradeoff when $M = \{16, 32, 48, 64, 80\}$, $K = 8$, $\rho = 23$ dBm, $N_Q = 8$ CPSs, and $N_r = 48$. In addition, the dashed curves demonstrate the EE, SE, and the FLOPs tradeoff when $N_r = 80$. The EE decreases when both M APs and N_r increase while the SE increases. The FLOPs present a reverse trend when compared with the EE and SE tradeoff, i.e., FLOPs increase when both M APs and N_r increase.

Analysis of the simulation results provides clear insight into antenna selection techniques for uplink cell-free mm-Wave massive MIMO systems when different scenarios of M APs, K UEs, and N_r are considered. Overall, the results confirm that the proposed matching strategy based on the Hungarian method can provide better EE and lower complexity compared to the other schemes. Moreover, the proposed matching scheme for antenna selection can achieve a tradeoff between SE, EE, total power consumption, and computational complexity.

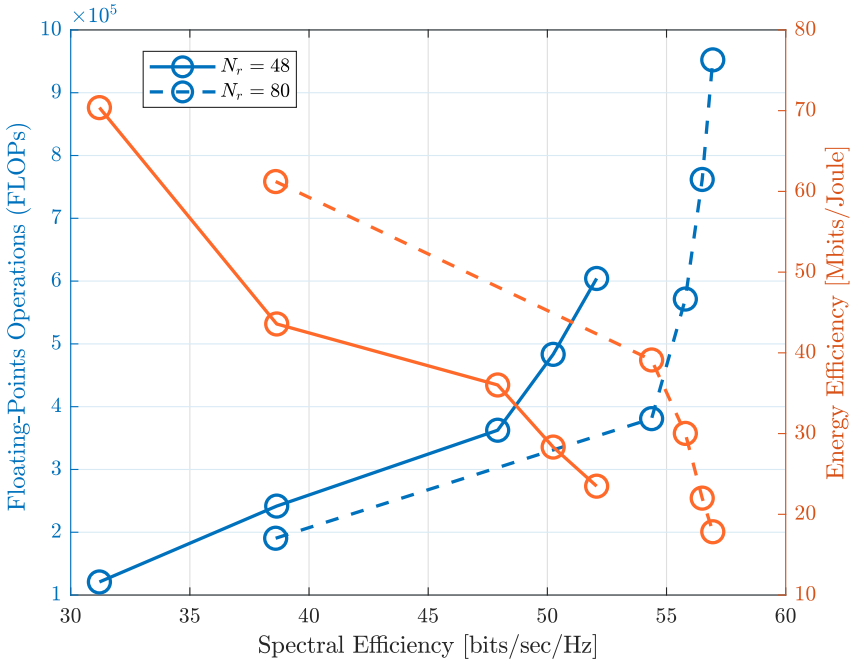

Figure 3.11: EE and SE and the complexity tradeoff as a function of M of APs when $M = \{16, 32, 48, 64, 80\}$, $\rho = 23$ dBm, $K = N_Q = 8$, and $N_r = \{48, 80\}$ for the proposed matching scheme.

3.6 Complexity Analysis

The computational complexity analysis is the last intriguing result worth highlighting. Floating-points operations (FLOPs) [136] are used to assess the complexity of the algorithms proposed in this chapter. Figure 3.12 compares the FLOPs versus the number of APs, the number of N_r, and the number of UEs for the uplink cell-free mm-Wave massive MIMO system. Because DSAS executes more iterations to acquire the antenna subset selection solution, it has higher complexity than CMDAS and CMFASs. In contrast, the proposed matching scheme overcomes DSAS and CMDAS and attains an approximate number of FLOPs. Figure 3.12a shows the FLOPs versus the number of APs, and it is obvious that the proposed matching scheme can overcome DSAS and CMDAS by achieving 193.51% and 199.177% complexity reduction ratio compared to CMDAS and DSAS, respectively. Figure 3.12b,c also present the FLOPs against the number N_r of antennas and the number K of UEs in the cell-free network, respectively. It can be seen that the proposed matching scheme achieves lower computational complexity concerning the number of FLOPs versus both N_r and K compared to CMDAS and DSAS. It is also noteworthy that although our proposed matching scheme based on the Hungarian algorithm has a slightly higher complexity compared to the CMFAS, it is evident that the proposed matching

scheme has better EE with all investigated scenarios of uplink cell-free mm-Wave massive MIMO systems.

Moreover, the computational complexities of the proposed schemes can be affected by the number of required iterations to obtain the optimal number of selected antennas for each RF chain at each AP, which results in obtaining the maximum SE_m, and the number of iterations is affected by the number N_r of antennas and the number of APs in the coverage area. Furthermore, the number of iterations is given by $\imath = \sum_{m=1}^{M} \sum_{i=K+1}^{N_r K} (i)_m$ for DSAS, $\imath = \sum_{m=1}^{M} (N_r)_m$ for CMDAS, and $\imath = M$ for both the matching strategy for antenna selection based on the Hungarian algorithm and CMFAS. Thus, the computational complexity to obtain the total SE for all APs in the cell-free systems based on (3.17) is $\mathcal{O}(\imath N_r K^2)$. It is noticeable that DSAS requires many iterations, especially when the M APs and the N_r equipped for each AP is vast. For example, if $N_r = 64$, $M = 32$ APs, and $K = 8$ UEs, the required total number of iterations to obtain the maximum total SE is around 16,380 for all APs. While CMDAS needs 2048 iterations to reach the maximum total SE. In addition, the channel magnitude with the predefined value of selected antennas for each AP based on the channel condition strategy has the lowest number of iterations, which is equal to the number of APs inside the coverage area. Regarding the proposed matching algorithm based on the Hungarian method strategy, if $N_r K^2 > K^3$ (i.e., $N_r \geq K$), then its computational complexity is $\mathcal{O}(\imath(N_r K^2 + N_r K + K^3)) = \mathcal{O}(\imath(N_r K^2))$, and the required number of iterations to obtain the maximum total SE is also equal to the number of APs, which is considered to be similar to the channel magnitude with predefined value of the selected antennas based on the channel condition scheme. In addition, if $N_r K^2 < K^3$ (i.e., $N_r < K$), then the computational complexity of the proposed matching algorithm based on the Hungarian method strategy is $\mathcal{O}(\imath(K^3))$ [137], which is similar to the Hungarian algorithm complexity analysis multiplied by $\imath$, which is equal to the number of APs in the cell-free network, and in this case, the proposed matching scheme for antenna selection has higher complexity than the channel magnitude with the predefined value of the selected antennas based on the channel condition scheme. The computational complexities of the proposed matching scheme compared to the benchmark schemes to obtain the total SE based on (3.17) are summarized in Table 2. Therefore, when comparing the proposed matching scheme for antenna selection for each RF chain at each AP to DSAS and CMDAS, the proposed matching strategy can yield a computational complexity reduction of around 200%.

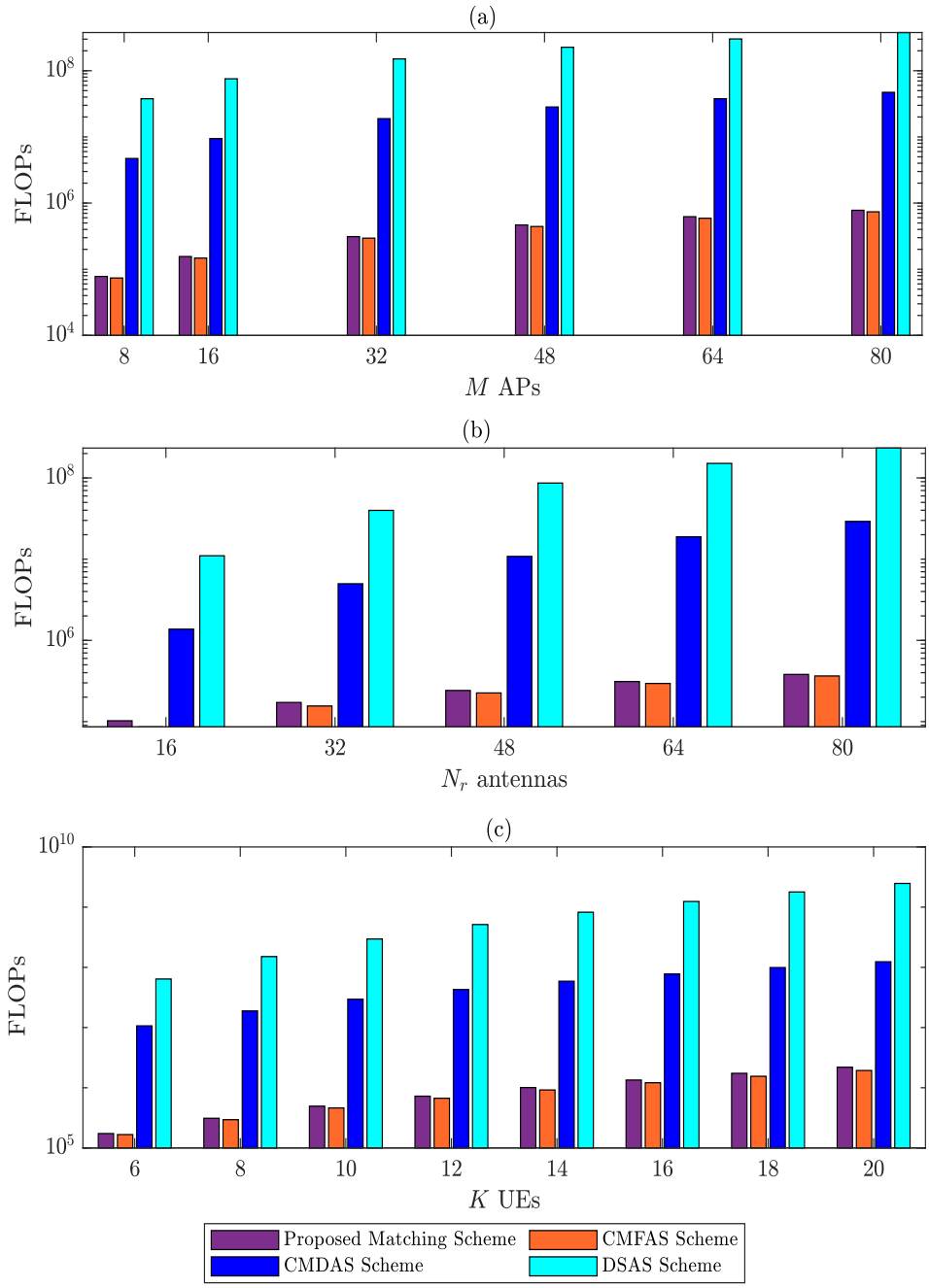

Figure 3.12: Complexity analysis based on floating-points operations (FLOPs) with different scenarios of uplink cell-free mm-Wave massive MIMO systems. (**a**) FLOPs versus M APs for a system with $N_r = 48$, $K = 8$, $\rho = 23$ dBm, and $N_Q = 8$ CPSs. (**b**) FLOPs versus N_r antennas with $M = 80$, $K = 8$, $\rho = 23$ dBm, and $N_Q = 8$ CPSs. (**c**) FLOPs versus the number of K UEs with, $M = 80$, $N_r = 48$, $\rho = 23$ dBm, and $N_Q = 8$ CPSs.

Table 2: Comparison of Computational Complexities.

Schemes	**Complexities**
DSAS	$\mathcal{O}(\sum_{m=1}^{M}\sum_{i=K+1}^{N_rK}(i)_m(N_rK^2))$
CMDAS	$\mathcal{O}(\sum_{m=1}^{M}(N_r)_m(N_rK^2))$
CMFAS	$\mathcal{O}(M(N_rK^2))$
Proposed Matching	If $N_rK^2 > K^3$, $\mathcal{O}(M(N_rK^2))$. If $N_rK^2 < K^3$, $\mathcal{O}(M(K^3))$

3.7 Summary

In this chapter, we investigate a hybrid beamforming scheme with CPSs and antenna selection technique based on matching theory for uplink cell-free mm-Wave massive MIMO systems to achieve two objectives: enhancement of the EE while maintaining high SE and low computational complexity. These objectives have been addressed by introducing a novel matching scheme based on the Hungarian method for maximum weight matching. Firstly, the assignment problem is formulated to match the RF chains at each AP and several sets of activated antennas based on the channel magnitude. Secondly, the Hungarian method is proposed to solve the formulated problem due to its lower computational complexity. The efficiency of the proposed matching scheme for the antenna selection technique is justified by the simulation results, with several scenarios of uplink cell-free mm-Wave massive MIMO systems, which show that the matching approach can attain around 20% EE improvement and 200% complexity reduction compared to the state-of-the-art schemes. By utilizing the matching theory, half of the RF chains at each AP are connected to a minimum number of selected antennas in the proposed matching method. In contrast, each of the remaining RF chains is connected to a large number of selected antennas. The tradeoff between SE, total power consumption, and computational complexity can be guaranteed.

Chapter 4

RF Chains Activation Based on Matching Theory for Uplink Cell-Free mm-Wave Massive MIMO Systems

This chapter proposes a novel RF chains activation technique based on the matching theory for the uplink cell-free mm-Wave massive MIMO systems under the assumption of considering the centralized operation when all signal processing operations are executed at the CPU. Therefore, the CPU can utilize the global CSI to obtain all analog combining for all APs. Then, the proposed matching scheme will activate and deactivate the RF chains based on the total analog combining, aiming to achieve maximum EE while maintaining low computational complexity compared to the state-of-the-art techniques and a significant loss in the achievable rate. The work in this chapter has been published in [138].

4.1 Introduction

The increasing demand for throughput, ultra-low latency, ultra-high reliability, and ubiquitous coverage have made researchers explore several novel solutions to set the basis for future generations of wireless communications. These demands, however, will consume a significant amount of resources, particularly in the case of cell-free mm-Wave massive MIMO systems, which is the promising approach for future wireless generations. Optimization of hybrid beamformers for the cell-free mm-Wave massive MIMO system is vital in improving system performance. Therefore, the flexibility of activating or deactivating the RF chains in the signal combining design is essential due to the computational complexity of the algo-

rithms to perform this task, mainly when there exist a large number of APs inside the coverage area. This motivates us to design novel schemes for RF chains activation based on matching theory for hybrid beamforming for mm-Wave massive MIMO cell-free network. In addition, to the best of our knowledge, no other works consider the matching approach in designing RF chains activation for the hybrid beamforming for the cell-free massive MIMO systems.

In this chapter, to allocate each AP to different sets of RF chains, it has been proposed an efficient low-complexity algorithm based on matching theory in order to maximize the total EE for the cell-free network. The following are the chapter's most significant contributions.

- The total power consumption in the cell-free mm-Wave massive MIMO systems depends on two essential things: the M APs in the coverage area and N RF chains at each AP. Because of large M APs in the cell-free massive MIMO systems, which leads to a large number of N RF chains, the total power consumption is steadily increasing whenever the APs and the RF chains increase. To tackle this challenge, it has been proposed a novel scheme based on matching theory for activating RF chains at each AP depending on the channel state information (CSI) to reduce total power consumption while maintaining the total achievable rate from a significant loss due to the deactivated RF chains. It has been formulated maximum-weighted assignment optimization problem to assign each AP to its number of active RF chains.

- It has been proposed the Hungarian algorithm to solve the formulated optimization problem and obtain the maximum total EE.

- Simulation results demonstrate the performance of the proposed scheme under an extensive set of cell-free mm-wave massive MIMO scenarios. In particular, the number of APs, the number of antennas, and the number of UEs in the network have been analyzed in terms of the achievable rate and the EE. In addition, the computational complexity analysis for the proposed scheme is studied compared to the state-of-the-art schemes in this chapter.

Section 4.2 provides the system model of this work in this chapter. In section 4.3, the proposed RF chain activation scheme is introduced based on matching theory. Section 4.4 provides the complexity analysis of the proposed scheme against the state-of-the-art schemes. Simulation results are provided in section 4.5. Section 4.6 concludes this chapter.

4.2 System Model

Consider the uplink of cell-free mm-Wave massive MIMO system, where M APs and K single-antenna UEs are distributed in the coverage area. Also, fronthaul links are used to connect the APs to the CPU, in which each AP is equipped with N_r receive antennas and $N(\leq N_r)$ RF chains as presented in [66]. Furthermore, each AP has a fully connected analog combining architecture and a narrowband-block fading channel model is applied as the propagation environment between M APs and K UEs as mentioned previously in Section (3.2.1). Additionally, the estimated channel can be obtained by similar procedures as mentioned in Section (3.2.3).

4.2.1 Uplink Data Transmission

The symbol sent from the k_{th} UE to all APs is symbolized by x_k, such that $\mathbb{E}\{|x_k|^2\} = 1$ and it can be detected by applying hybrid beamforming to the received signal at m_{th} AP. The received signal at m_{th} AP is presented as

$$r_m = \sqrt{\rho}\sum_{k=1}^{K} F_m^H W_m^H h_{k,m} x_k + F_m^H W_m^H Z_m, \tag{4.1}$$

where ρ represents the maximum transmit power at k_{th} UE. Z_m is $\sim \mathcal{CN}(0, \sigma^2)$ is a vector of the noise with i.i.d. random variables (RVs); while W_m; such that $W_m \in \mathbb{C}^{N_r \times N}$ is the analog combining matrix at m_{th} AP in which its n_{th} column is given as $w_{m,n} = [w_{m,n}^{(1)}, ..., w_{m,n}^{(N_r)}]^T$ corresponding to n_{th} RF chain while i_{th} element of $w_{m,n}$ is obtained by $w_{m,n}^{(i)} = \frac{1}{\sqrt{N_r}} e^{j\theta_{m,n}^{(i)}}$. $F_m \in \mathbb{C}^{N \times K}$ denotes the digital combining matrix at m_{th} AP. Then, r_m is sent to the CPU by m_{th} AP via fronthaul link to be detected. In addition, the information is sent between the APs and the CPU via a simple centralized decoding technique. As a result, at the CPU, the final decoded signal is the average of local estimations $\frac{1}{M}\sum_{m=1}^{M} r_m$ [74]. Therefore, the CPU's composite received signal is represented as

$$\begin{bmatrix} r_1 \\ r_2 \\ . \\ . \\ r_M \end{bmatrix} = \sqrt{\rho}\sum_{k=1}^{K} \begin{bmatrix} F_1^H W_1^H h_{k,1} \\ F_2^H W_2^H h_{k,2} \\ . \\ . \\ F_M^H W_M^H h_{k,m} \end{bmatrix} x_k + \begin{bmatrix} F_1^H W_1^H Z_1 \\ F_1^H W_1^H Z_2 \\ . \\ . \\ F_M^H W_M^H Z_M \end{bmatrix}. \tag{4.2}$$

The analog and digital combining for all APs in the coverage area of the cell-

free mm-Wave massive MIMO network are denoted as $W = \text{blkdiag}\{W_1, W_2, ..., W_M\} \in \mathbb{C}^{MN_r \times MN}$ and $F = \text{blkdiag}\{F_1, F_2, ..., F_M\} \in \mathbb{C}^{MN \times MK}$, respectively.

4.2.2 Achievable Rate

The differences between this chapter and the previous chapter are the ways to perform the signal processing operations, and the analog combining design. The previous chapter discusses the decentralized cell-free massive MIMO systems. In contrast, this chapter utilizes the centralized cell-free massive MIMO. It also focuses more on minimizing power consumption by reducing the size of the analog phase shifters network based on the activation/deactivation of RF chains. Therefore, we assume that all analog and digital combiners for all APs are computed at the CPU based on the estimated channel $\hat{H}$ which is considered as CSI in order to obtain $\{W_1, ..., W_M\}$. Therefore, (4.2) can be rewritten as

$$r = \sqrt{\rho} W^H F^H \hat{H} x + W^H F^H Z, \tag{4.3}$$

where $x = [x_1, ..., x_K]^T \in \mathbb{C}^{K \times 1}$. Thus, the total achievable rate is given as [121]

$$R = \upsilon \log_2 \det |I_{M,K} + \rho \delta^{-1} W^H F^H \hat{H} \hat{H}^H F W|, \tag{4.4}$$

where $\upsilon = \frac{\tau_c - \tau_p}{\tau_c}$, and $\delta = \sigma^2 F^H W^H F W$. This work seeks to propose a novel design of hybrid combining for the uplink cell-free mm-Wave massive MIMO systems based on the matching theory. Then, the first step is to design the analog combining W and the digital combining F can be obtained by using the designed W. Therefore, the total achievable rate R for the cell-free massive MIMO network is expressed as [15]

$$R = \sum_{m=1}^{M} R_m, \tag{4.5}$$

where $R_m = \upsilon \log_2 \det(I_N + \frac{\rho}{\sigma^2} W_m^H \hat{H}_m \mu_{m-1}^{-1} \hat{H_m}^H W_m)$ with $\mu_o = I_K$ and $\mu_{m-1} = \mu_{m-2} + \frac{\rho}{\sigma^2} \hat{H}_{m-1}^H W_{m-1} W_{m-1}^H \hat{H}_{m-1}$. The proof about how to obtain the total achievable rate R for the centralized uplink cell-free mm-Wave massive MIMO is available in [15].

4.2.3 Power Consumption and Energy Efficiency Models

The uplink cell-free mm-Wave massive MIMO systems' total power consumption is expressed as [121, 133]

$$P_{\text{Total}} = \sum_{k=1}^{K} P_{\text{TX}_k} + P_{\text{CP}_k} + \sum_{m=1}^{M} (P_{\text{fix}_m} + P_{\text{HBF}_m} + P_{\text{FH}_m}), \tag{4.6}$$

where P_{TX_k} and P_{CP_k} represent the transmit power and the amount of power required to operate the circuit components for each UE in the coverage area, respectively. Furthermore, P_{TX_k} is expressed as [139]

$$P_{\text{TX}_k} = \rho\sigma^2 \sum_{k=1}^{K} \frac{\mathbb{E}\{|x_k|^2\}}{\eta_k^{\text{amp}}}, \tag{4.7}$$

where η_k^{amp} denotes the power amplifier efficiency at k_{th} UE, and $\sigma^2 = -174\frac{\text{dBm}}{\text{Hz}} + 10\log_{10}(B) + NF$, where B is the system bandwidth, and NF is the noise figure. Furthermore, $P_{\text{fix}_m}, P_{\text{HBF}_m}$, and P_{FH_m} are fixed power consumption, power consumption related to the hybrid beamforming architecture, and the consumed power of the fronthaul link for m_{th} AP, respectively.

Regarding the hybrid beamforming structure, each antenna at m_{th} AP is connected to a low-noise amplifier (LNA) and two mixers while each RF chain requires one analog-to-digital converter (ADC) and $N_r N$ phase shifters (PSs) network. Therefore, P_{HBF_m} can be expressed as

$$P_{\text{HBF}_m} = N_r(P_{\text{LNA}} + 2P_{\text{mixer}}) + n_m(N_r P_{\text{PS}} + P_{\text{RF}} + P_{\text{ADC}}), \tag{4.8}$$

where $P_{\text{LNA}}, P_{\text{mixer}}, P_{\text{PS}}, P_{\text{RF}}$ and P_{ADC} present the consumed power by LNA, mixer, PSs, RF chains and ADC, respectively. n_m is the number of selected RF chains at m_{th} AP. Furthermore, the required maximum power for the fronthaul traffic at full capacity C_{FH_m} is denoted by P_{FH_m} and expressed as [133]

$$P_{\text{FH}_m} = \frac{P_{\text{FH}_{max}} R_{\text{FH}_m}}{C_{\text{FH}_m}}, \tag{4.9}$$

where R_{FH_m} gives the actual fronthaul rate between m_{th} AP and the CPU and is expressed as

$$R_{\text{FH}_m} = \frac{2K(\tau_c - \tau_p)\alpha_m}{T_c}, \tag{4.10}$$

where α_m and T_c represent the number of quantization bits at m_{th} AP, and the coherence time (in seconds), respectively.

For simplicity, we assume that all APs have the same value of $P_{\mathrm{FH}_m}, \alpha_m, C_{\mathrm{FH}_m}$ and P_{fix_m}. In addition, all UEs have the value of both η_k^{amp} and P_{CP_k}. Thus, P_{Total} can be rewritten as

$$P_{\mathrm{Total}} = \frac{K\rho}{\eta} + KP_{\mathrm{CP}} + MP_{\mathrm{fix}} + MP_{\mathrm{FH}} + \sum_{m=1}^{M} P_{\mathrm{HBF}_m}. \tag{4.11}$$

It is noted that the power consumption related to the hybrid beamforming architecture of this chapter is completely different compared to the previous chapter because the hybrid beamforming design in the previous chapter includes switching network and CPSs. Thus, the EE in $[\frac{\mathrm{bit}}{\mathrm{Joule}}]$ of the cell-free mm-Wave massive MIMO systems can be expressed as

$$\mathrm{EE} = \frac{\sum_{m=1}^{M} BR_m}{P_{\mathrm{Total}}}. \tag{4.12}$$

4.3 RF Chains Activation Based on Matching Theory Methodology

The achievable rates $\{R_1, R_2, ..., R_M\}$ are determined by the analog combiners that correspond to the APs $\{1, ..., M\}$ in the cell-free network. As a result of the APs' random distribution throughout the coverage area, variable pathloss and shadowing effects exist on the communication channels. The analog combiners' contributions to achievable rates at various APs are then varied. Different contributions to R_m can be obtained by combining vectors of $W_m = \{w_{m,1}, ..., w_{m,N}\}$.

When the subset of the analog combining vectors $\{w_{1,1}, ..., w_{M,N}\}$ is omitted from W, it is unlikely to cause significant performance loss. As a consequence, the analog combining of each AP in the cell-free massive MIMO network demonstrates the impact of the $N_r N$ PSs possible connections to the RF chains and followed by ADC. Insignificant analog combining vectors can be excluded from signal combining by switching off their RF chains, ADC and PSs, which reduces total power consumption as shown in Figure (4.1a). This motivates us to propose a novel design of activation RF chains based on matching theory to maximize the energy efficiency of the uplink cell-free mm-Wave massive MIMO systems. Let us consider $n = \{n_1, ..., n_M\}$, in which n_m presents the number of selected RF chains at m_{th} AP and is constrained to $0 \leq n_m \leq N$ as demonstrated in Figure (4.1b). All RF chains at m_{th} AP are turned off when $n_m = 0$. Therefore, this AP does not consume any power to perform the process of the signal combining.

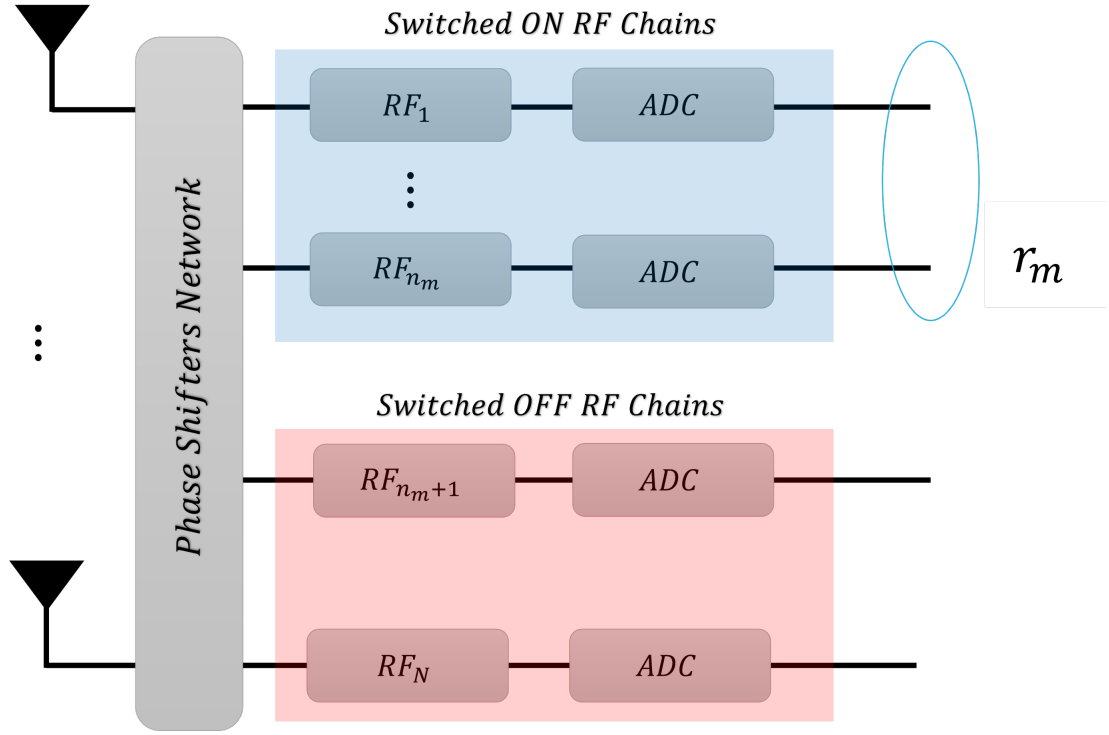

(a) Hybrid beamforming structure for each AP after utilizing RF chains activation based on Figure (4.1b).

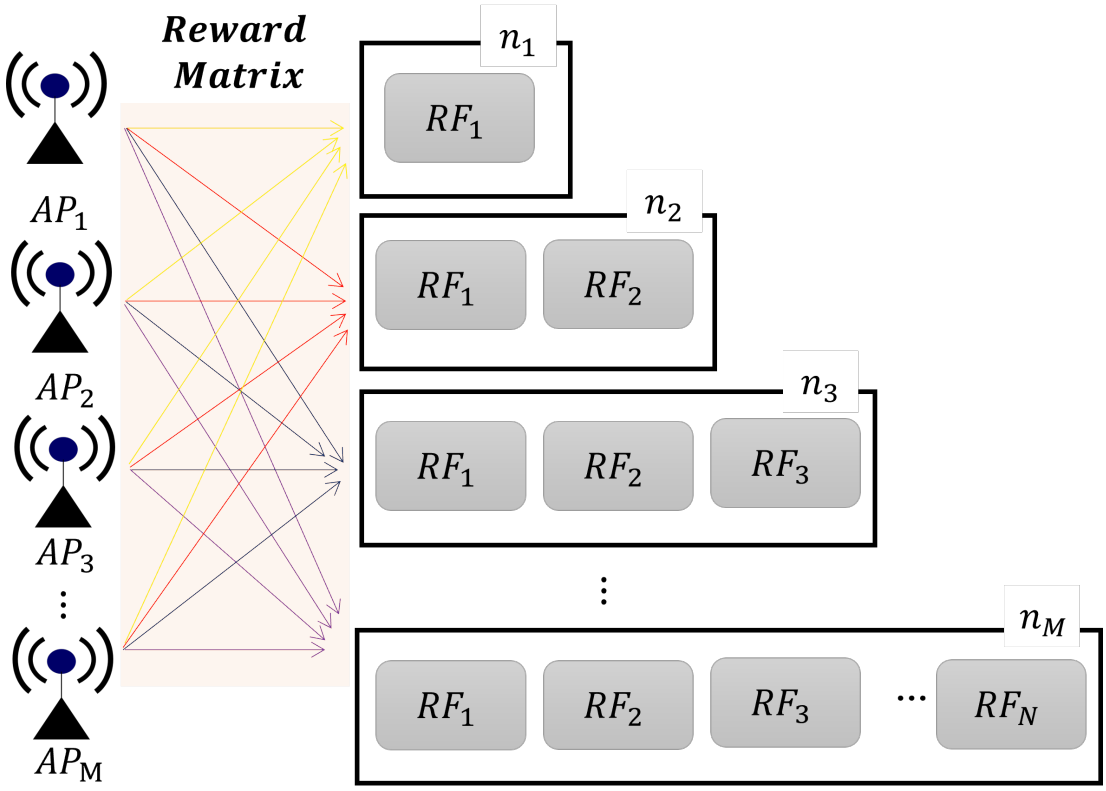

(b) Bipartite graph construction for RF chains activation scheme for each AP.

Figure 4.1: The illustration of matching scheme for RF chains activation in the uplink cell-free mm-Wave massive MIMO systems.

4.3.1 Problem Formulation

It is essential to formulate an assignment problem, which is a fundamental combinatorial optimization problem, in order to determine the optimum assignment of n_m to m_{th} AP, that can maximize the EE of the cell-free mm-Wave massive MIMO network as illustrated in Figure (4.1b). Thus, the proposed assignment problem is formulated as

$$\begin{aligned} \max_{x_{n_m,m}} \quad & \frac{B\sum_{m=1}^{M}\sum_{n_m=0}^{N-1} R_m^{(n_m)} x_{n_m,m}}{P_{\text{Total}}} \\ \text{s.t.} \quad & x_{n_m,m} \in [0,1], \\ & 0 \leq n_m \leq N, \end{aligned} \tag{4.13}$$

where $x_{n_m,m}$ shows that each AP is assigned to just one n_m out of N. Moreover, $x_{n_m,m}$ equals 1 if m_{th} AP is assigned to n_m RF chains and vice versa. In this work, we formulate a reward matrix to make the assignment between M APs and n_m RF chains as shown in Figure (4.1b). The reward matrix might be non-square due to $M > N$. Thus, the obtained reward matrix coming with size $M \times N$ where the element in the i_{th} row and j_{th} column represents $\text{EE}_{m,n}$ between m_{th} AP and n_m RF chains. The sum of $\text{EE}_{m,n}$ is the maximum EE of the cell-free network. For simplicity, the reward matrix ($\digamma$) in this work is divided into sub matrices and each one of them, the number of APs equals N RF chains. The total number of sub square matrices is expressed as $C = \frac{M}{N}$, and each sub square matrix is denoted by $M_s^{c_\ell}$, where $\ell = \{1, 2, ..., C\}$. For example, if $M = 16$ APs and $N = 8$ RF chains, $\digamma$ is with size (16×8) and $C = 2$ sub square matrices and each one of them is with size 8×8, such that $M_s^{c_1}$ and $M_s^{c_2}$ have 8 APs out of M APs. It is noted that $M_s^{c_1} \cap M_s^{c_2} = \varnothing$ and $M_s^{c_1} \cup M_s^{c_2} = \{1, ..., M\}$.

4.3.2 Proposed Solution

$\digamma$ that can be used for matching is obtained by Algorithm 2. The first two steps are used to find the analog combining for each AP. Then, the next two steps give the total achievable rate R and EE_m, respectively. Then, digital combining for m_{th} AP is computed based on $W^\star$. $\digamma$ is obtained and its elements are $EE_m^{n_m}$ between each AP and n_m RF chains. Therefore, $\digamma$ is the input of the proposed Hungarian algorithm as illustrated in Algorithm 3, and $\digamma$ is divided into sub square matrices when $M > N$. Thus, the Hungarian algorithm is applied at each $M_s^{c_\ell} \times N$ matrix to obtain the maximum weighted matching. This algorithm is one of the most well-known and often used combinatorial methods for solving the maximum weighted matching problem in a bipartite network. In Algorithm 3,

we provide the details of the proposed fast and efficient implementation of James Munkres' Hungarian algorithm [28].

Algorithm 2: Hybrid beamforming design [15] to obtain the reward matrix $\mathcal{F}$

for $m = 1 \rightarrow M$ **do**
  for $n = 1 \rightarrow N$ **do**
    - Compute the Singular value decomposition (SVD) for $\hat{H}_m \mu_{m-1}^{-1} \hat{H}_m^H$;
    - The left singular vector $W_m^\star = \{u_{m,1}^\star, u_{m,2}^\star, ..., u_{m,N}^\star\}$.
    - Compute R_m corresponding to n_m using (4.5).
  end
  $Q_m = \hat{H}_m^H W_m^\star W_m^{\star\, H} \hat{H}_m$
  $\mu_m = \mu_{m-1} + \frac{\rho}{\sigma^2} Q_m$
  Compute digital combining for m_{th} AP as
  $F_m^\star = \frac{W_m^\star \hat{H}_m}{W_m^{\star\, H} \hat{H}_m \hat{H}_m{}^H W_m^\star} + \frac{\sigma^2 W_m^\star W_m^{\star\, H}}{\rho}$.
  - Compute P_{Total} and EE_m from (4.11) and (4.12), respectively.
end
- $\mathcal{F}$ with size $M \times N$ is obtained, whose (m, n_m)-entries are $\text{EE}_m^{n_m}$,
where $n_m = \{0, 1, 2, ..., N\}$.

Algorithm 3: The Hungarian algorithm [28] to solve (4.13).

if $M > N$ **then**
- $\digamma$ from Algorithm 1 is divided into ℓ sub matrices and
  each one of them is with size $M_s^{c_\ell} \times N$.
- Find Δ^+ which is maximum element in $\digamma$
- Then, $\bar{\digamma} = \Delta^+ 1_{M_s^{c_\ell} \times N} - \digamma$.
- Find the lowest element in each row of $\bar{\digamma}$ and
  subtract it from all other elements in the row.
- In each column, repeat the process of previous step.
- Cover all zeros with a few horizontal and vertical lines.
- χ = the total number of lines.

  if $\chi = M_s^{c_\ell}$ **then**
  Among the zeros, optimal assignment is achieved.
  Break.
  else
  repeat
  - Let $\bar{\Delta}^*$ is the smallest uncovered element,
    by a line and subtract it from all
    uncovered elements, then add it to all elements
    that are covered twice.
  - Cover all zeros with a few horizontal
    and vertical lines as possible.

  until $\chi = M_s^{c_\ell}$
  end
  Among the zeros, optimal assignment is achieved.

end
- Repeat until $\sum_{\ell=1}^{C} M_s^{c_\ell} = M$,

end
-Then, $\mathrm{EE}^\star = \sum_{\ell=1}^{C} \mathrm{EE}_\ell^\star$.

4.4 complexity Analysis

The computational complexities are affected by the number of N RF chains and M APs in the coverage area to obtain the optimal number of the activated RF chains at each AP, which results in obtaining the total EE. Thus, the total computational complexity to obtain the total achievable rate for all APs in the cell-free systems by utilizing FS-ARFA scheme [15] is $(\mathcal{I}_{\mathcal{FS}}+1)\mathcal{O}(K^3+2K^2N_r+NN_r^2+NKN_r+2NK^2+(N^2+1)K)+2K^2N_r$ where $\mathcal{I}_{\mathcal{FS}}$ denotes the number of iterations. Regarding our proposed matching scheme, its total computational complexity is $\mathcal{O}(K^3+2K^2N_r+NN_r^2+NKN_r+2NK^2+(N^2+1)K+2K^2N_r+C(M_s^{c_\ell})^3)$. It is obvious that the proposed matching scheme overcomes the FS-ARFA scheme because our proposed scheme does not require large number of iterations to obtain the optimal number of active RF chains at each AP. Another way to analyse the computational complexity of our proposed scheme compared to the FS-ARFA scheme is to count how many number of examined candidates of the total number of active RF chains for all APs in the cell-free network. For example, when $M = 48$, $N = 8$ and $K = 8$, the required number of examined candidates is 105 for the FS-ARFA, whereas our proposed scheme requires only 8 candidates, based on the number of sets of RF chains from 0 to N, to perform matching between these sets and APs to obtain the maximum total EE. Thus, the complexity-reduction ratio is 189.6%

4.5 Simulation Results and Discussions

This section includes the simulation results that evaluate the performance of our proposed scheme in terms of total power consumption, total EE and total achievable rate. In this chapter, we employed Monte Carlo simulation, whereby new APs positions are randomly distributed over a square area of 1000×1000 m. Furthermore, we assume $f = 28$ GHz, and $B = 500$ MHz [123]. To obtain the path loss coefficients between the APs and the UEs based on (3.2), we assume $\varepsilon = 4.1$, and $\varsigma = 7.6$. Table 1 contains the utilized parameters in all simulations in this section.

Table 1: Simulation parameters.

Parameter	**Value**
τ_c, and τ_p	200, and 20 samples
Propagation paths ($P_{k,m}$)	3 $\forall$ k, m [15]
Pilot sequence transmit power (ρ_p)	100 mW
T_c and α_m	2 ms, 2 bits [37, 133]
Noise Figure (NF)	9 dB
Amplifier efficiency (η_k^{amp})	0.3 [131]
Fronthaul capacity (C_{FH})	500 Mbps
Fronthaul maximum power (P_{FH})	50 W
Power components:	$P_{\text{LNA}} = 20$ mW, $P_{\text{ADC}} = 200$ mW, $P_{\text{RF}} = 40$ mW, $P_{\text{PS}} = 30$ mW, $P_{\text{mixer}} = 0.3$ mW, $P_{\text{CP}} = 1$ W, $P_{\text{fix}} = 0.825$ W, $\rho = 23$ dBm.

Figure 4.2 shows that the total achievable rate versus different numbers of APs in the coverage area for $N = K = 8$, and $N_r = 64$. It is obvious that the maximum of the total achievable rate can be achieved when all RF chains are in active state at all APs in the coverage area. In addition, switching off some RF chains can affect on the total achievable rate. Therefore, it can be seen that our proposed matching scheme outperforms the fixed activation scheme when $N = n_m = 4$ for all AP and the random AP activation scheme when all RF chains are turned on at each AP. This is reasonable because a fixed activation scheme with 50% active RF chains for each AP is unable to achieve maximum achievable rate, whereas our proposed matching scheme can exploit the advantages of matching theory to assign each AP to a set of RF chains, restricted to $0 \leq n_m \leq N$ RF chains, in order to maximize the achievable rate. Regarding the random AP activation scheme, we choose $\bar{n} = 4$ which is the average number of active RF chains for all APs, and the number of selected APs is equal $\frac{M*\bar{n}}{N}$ in order to make a fair comparison as mentioned in [15]. The random AP activation technique is outperformed by our proposed scheme because it turns off the APs without considering the impact on system performance in terms of the overall achievable rate. Furthermore, when all RF chains are turned on, FS-ARFA achieves 10.8% close to the fixed

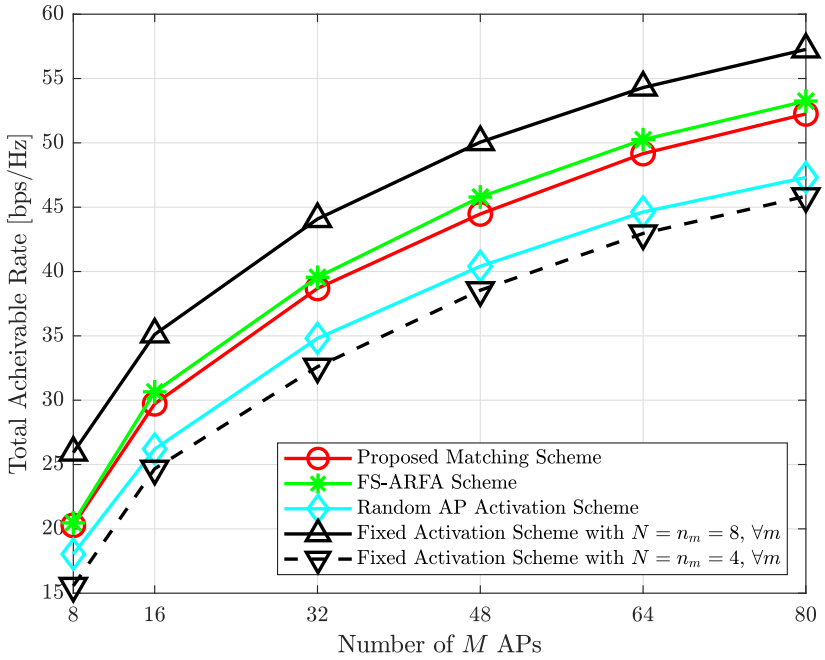

Figure 4.2: The total achievable rate versus M APs, in which the proposed matching scheme is compared to ARFA schemes in [15], random APs activation scheme [140] when each AP has $N = 8$ RF chains, and fixed RF chain activation schemes when $K = 8$, $N_r = 64$, and $N = 8$.

activation scheme, whereas our proposed scheme performs within 12.9% of the fixed activation scheme. The FS-ARFA system, on the other hand, has a very high computational complexity to obtain optimal results, whereas our suggested scheme has the lowest computational complexity, as explained earlier.

Figure 4.5 shows the total power consumption against increasing number of APs for $N = K = 8$ and $N_r = 64$. It is evident that our proposed scheme based on the Hungarian algorithm consumes less power when $M = 80$ compared to the fixed activation schemes both with $N = 8$ or $N = n_m = 4$, FS-ARFA scheme and random AP activation by 71.80%, 16.74%, 13.87% and 10.45%, respectively. Furthermore, the obtained results revealed that our proposed matching scheme can achieve lower power consumption and computational complexity compared to the state-of-the-art schemes without a significant performance loss in terms of the total achievable rate.

Figure 4.4 shows the total EE performance against increasing number of APs for $N = K = 8$ and $N_r = 64$. It is observed that the total energy efficiency for all schemes decrease when M increases, which is obvious because the additional APs come with resultant increase in power consumption as seen in Figure 4.5. Our proposed matching technique outperforms existing schemes by matching each AP

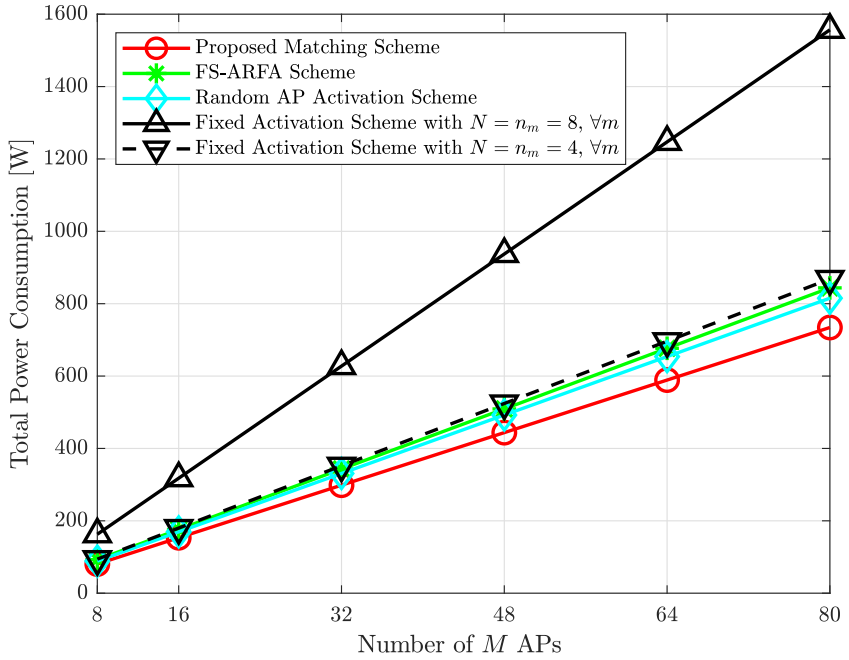

Figure 4.3: The power consumption versus M APs with same simulation parameters as well as same comparable schemes as mentioned in Figure 4.2.

to the appropriate active RF chains to maximize energy efficiency. Our proposed scheme can attain 13.5%, 20%, 32.56% and 58.7% EE improvement compared to FS-ARFA, random AP activation scheme, fixed activation with partially RF chains activated ($N = n_m = 4$), and with fully RF chains activation scheme, respectively.

Figure 4.5 depicts the effect of the number of N_r receive antennas on the EE and the total power consumption when $M = 32$, $N = 8$, and $K = 8$, respectively. The EE decreases as the number of N_r increases this is because increasing the number of antennas leads to increasing the size of the phase shifters network at each AP, which in turns an increasing in the total power consumption, as seen in Figure 4.6. In comparison to the mentioned schemes in this work, the proposed matching scheme achieves the highest EE. For example, the proposed matching strategy can achieve when $N_r = 32$ antennas equipped for each AP, 13.978%, 20.431%, 32.87% and 55.92% compared to the FS-ARFA scheme, the random AP activation scheme, fixed activation schemes when $N = n_m = 4$ and $N = n_m = 8$ for all APs in the cell-free network, respectively. This is reasonable because the proposed matching scheme exploits the the benefits of the matching theory to assign each AP to the active number of RF chains, this will reduce the consumed power by the phase shifters network between antennas and the active RF chains. While the other schemes focused on how to maximize the total

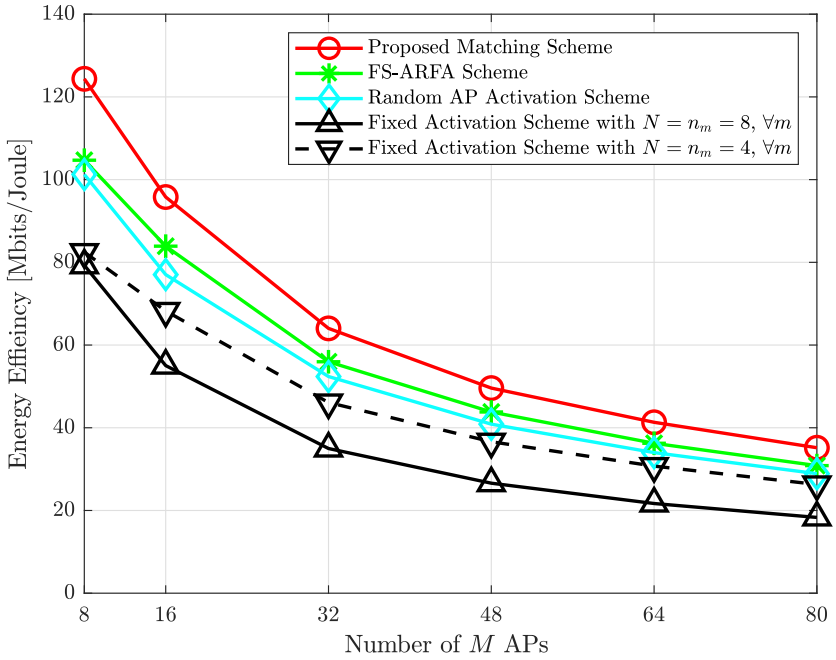

Figure 4.4: The EE versus M APs with same simulation parameters as well as same comparable schemes as mentioned in Figure 4.2.

achievable rate at the expense of the EE.

On the other hand, Figure 4.6 shows the total power consumption increases when N_r increases. It is obvious that the proposed scheme has the lowest total power consumption. Then, the random AP activation scheme comes in the second place and then the FS-ARFA, the fixed activation with 50% and fully connected RF chains at each AP schemes, respectively. Therefore, it can be seen that the proposed scheme based on the Hungarian algorithm can overcome all mentioned schemes in this work. For example, when $N_r = 32$, the proposed scheme can attain 186.932 W, while the random AP activation scheme achieves 198.006 W. In addition, the FS-ARFA and the fixed activation RF chains when $N = n_m = 4$ and $N = 8$ schemes can achieve 204.168 W, 208.741 W and 361.739 W, respectively.

Figure 4.7 demonstrates the impact of K UEs on the EE when $M = 32$, $N = 8$, and $N_r = 64$. It is obvious that the EE increases as K increases. This is because the achievable rate in the uplink wireless systems cannot be affected by inter-user interference. Compared to the schemes in this work, the proposed matching technique provides much-enhanced EE at both low and high number of UEs, as anticipated. For example, when $K = 16$, the proposed scheme can attain 12.63%, 29.62%, 33.5%, and 67.32% EE improvement compared to the FS-ARFA scheme, the random AP activation, and the fixed 50% and full RF chains in active state schemes, respectively. It is obvious that the FS-ARFA scheme

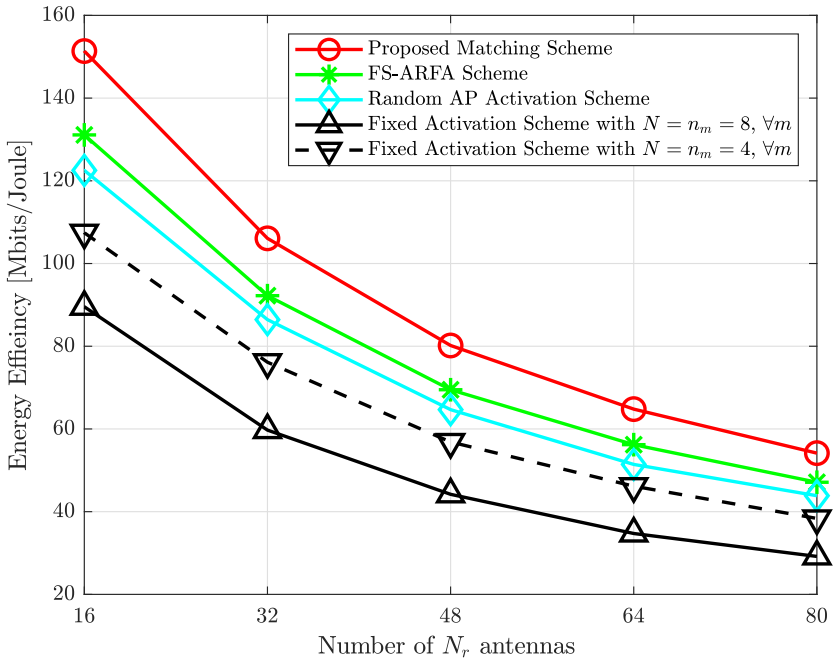

Figure 4.5: The EE versus N_r antennas with $K = 8$, $M = 32$ and $N = 8$.

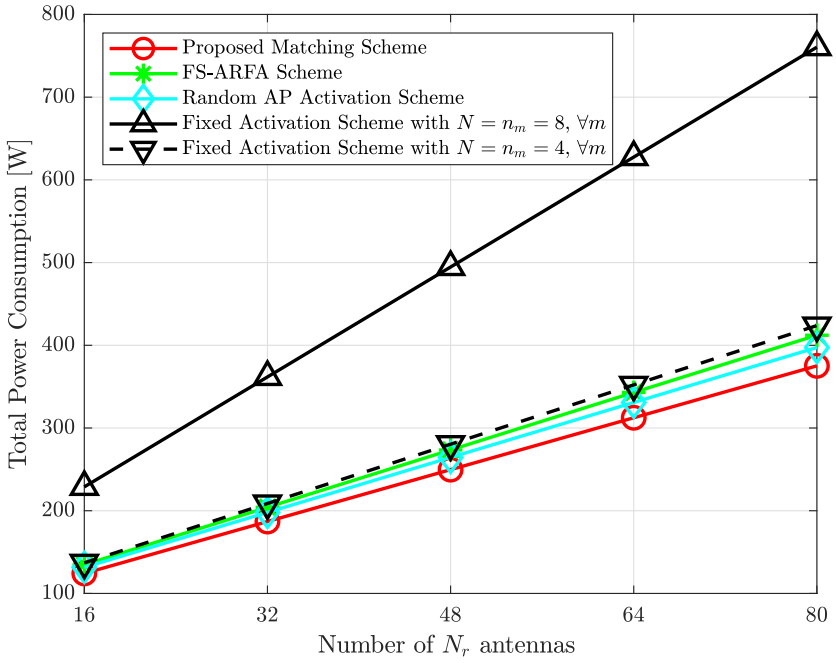

Figure 4.6: The power consumption versus N_r APs with $K = 8$, $M = 32$ and $N = 8$.

seeks to reduce the performance loss without taking into consideration the total power consumption, especially when the cell-free network has a large number of M APs, N_r antennas, and K UEs.

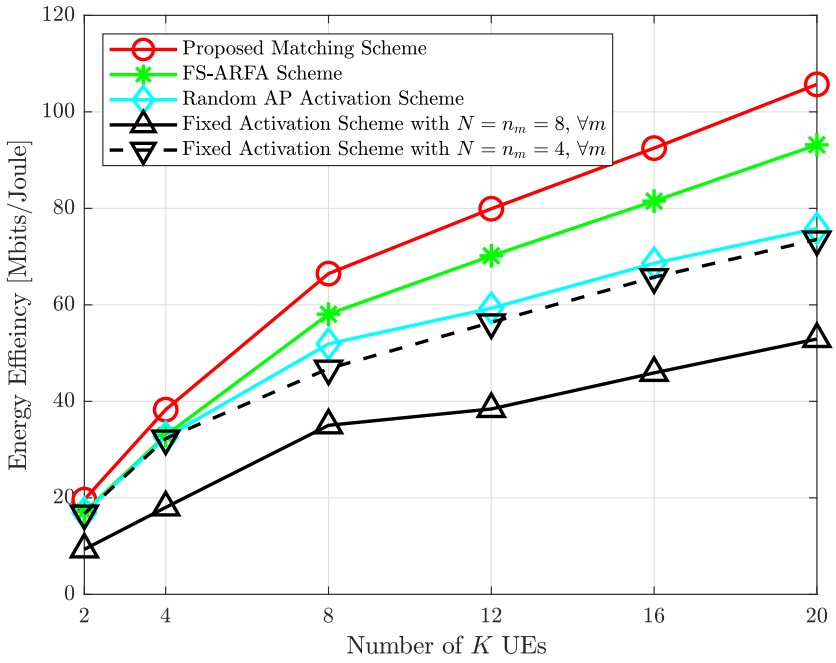

Figure 4.7: The EE versus K UEs with $N_r = 64$, $M = 32$ and $N = 8$.

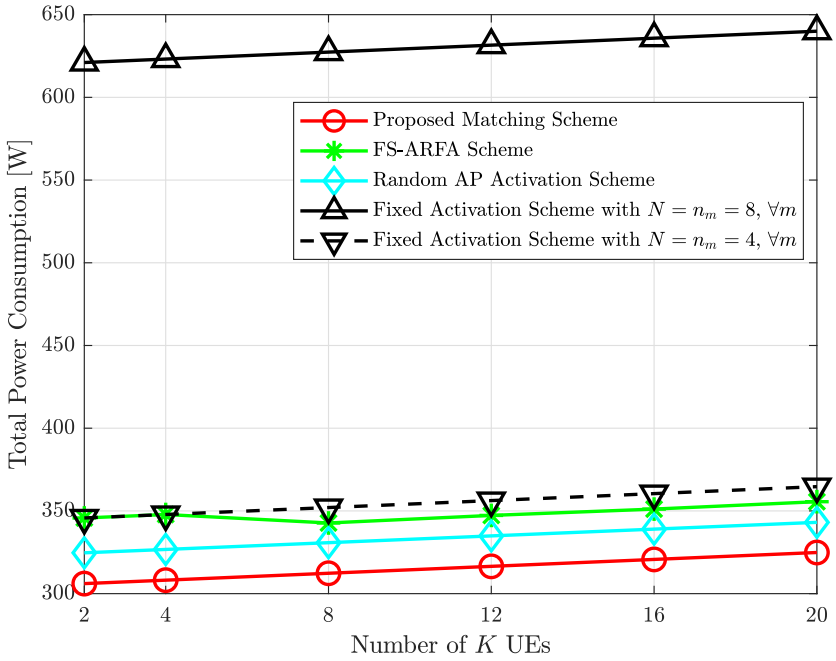

Figure 4.8: The power consumption versus K UEs with $N_r = 64$, $M = 32$ and $N = 8$.

Figure 4.8 reveals that clear gains in the total power consumption obtained by all mentioned schemes in this chapter. Figure 4.8 also demonstrates that when K increases, so should the total power consumption. For example, the proposed scheme can attain 320.681 W, while the random AP activation scheme achieves 338.996 W with $K = 16$, $N_r = 64$, $N = 8$, and $M = 32$. In addition, the proposed scheme attain lower total power consumption compared to the FS-ARFA, and fixed activation with $N = n_m = 4$ and $N = n_m = 8$ for all APs schemes by 9.0605%, 11.7%, and 65.89%, respectively.

4.6 Summary

In this chapter, we propose a low complexity matching scheme for RF chains activation for uplink cell-free mm-Wave massive MIMO systems. We considered a hybrid beamforming scheme in which all analog and digital combiners for all APs are executed at the CPU based on the received CSI from all APs. Then, we formulated an assignment problem to match APs and the activated RF chains to maximize the total EE. Also, we utilized the Hungarian algorithm to solve the formulated problem to achieve the optimal analog combiner based on matching the sets of RF chains to APs to maximize the total achievable. We also investigated the power consumption of our proposed scheme and compared the findings to state-of-the-art methods of RF chain activation. Our proposed matching technique has a significantly lower computational complexity, yielding a higher total EE.

Based on the obtained results in this chapter, the next chapter will propose matching theory in order to mitigate the pilot contamination issue since the previous two chapter focused on the EE, SE and power consumption when τ_p is larger than K UEs. Therefore, the next chapter will answer the following question: can we exploit the advantages of matching theory to be applied in pilot assignment and pilot power control in order to mitigate the pilot contamination issue when τ_p is smaller than K UEs?

Chapter 5

Mitigation Pilot Contamination Based on Matching Theory for Uplink Cell-Free Massive MIMO Systems

This chapter proposes two novel schemes based on the matching theory to mitigate the pilot contamination effect in the uplink cell-free massive MIMO systems while maintaining low computational complexity. The first scheme integrates matching theory and the genetic algorithm (GA) for pilot assignment, while the second is to utilize the Hungarian method for pilot control design. Furthermore, the work in this chapter has been submitted for publication in [141].

5.1 Introduction

The process of channel estimation is considered to be one of the most essential operations in the cell-free massive MIMO systems, as it directly influences the computations of precoding and detection vectors which are utilized for the uplink and downlink data transmission [16,17]. Regarding the TDD communication protocol, recent studies have developed pilot-based channel estimate algorithms in which UEs communicate τ-length pilot sequences to APs. The channel coherence time and the number of UEs are related to each other in the channel estimation process [12]. Furthermore, the pilot sequences assigned to UEs might be orthogonal or non-orthogonal, for instance, orthogonal pilot sequences can be allocated when there is a high τ_c coherence interval and a limited number of UEs. However, when τ_c is minimal, it is preferable to utilize non-orthogonal pilot sequences to reduce the resources required for channel estimation [17]. Therefore, the in-

terference between the transmitted pilot signal from the desired UE and other transmitted pilot signals from other UEs at each AP leads to the degradation of the estimated channel accuracy, impacting system performance. The term for this issue is called pilot contamination. Accordingly, pilot assignment techniques and power control design approach can be used to mitigate the pilot contamination effect on the system performance [10, 12, 17, 131]. Regarding the pilot power control design, during the training phase, if all pilot signals are transmitted at full power, a UE with a weak channel might be highly contaminated by UEs with strong channels. As a result, the total system performance deteriorates.

This chapter aims to mitigate the pilot contamination effect on the performance of the cell-free massive MIMO systems by proposing two schemes based on matching theory for the pilot assignment and the pilot power control design.

The contributions of this work are as follows

- The iterative Hungarian method is proposed to solve the formulated assignment optimization problem in order to obtain better-selected pilot sequences. The reason for doing that is to reduce the complexity of the GA by using the selected pilot sequences as input (*termed populations*) instead of putting τ^K possible combinations of the pilot sequences in the conventional GA, where τ is the length of the uplink training, and K denotes the number of UEs in the coverage area. Based on this, it can be guaranteed that the GA has lower computational complexity.

- We also propose a lower complexity pilot power control design for the uplink cell-free massive MIMO systems based on matching theory. It has been formulated a minimum-weighted assignment optimization problem and utilize the Hungarian method as well in order to obtain the optimal assignment between the pilot power control coefficients and the minimum channel estimation error for all UEs.

- Comprehensive simulation results are provided to demonstrate the performance of the proposed pilot assignment and pilot power control strategies under an extensive set of the cell-free massive MIMO scenarios. In particular, the number of APs, the number of antennas, the number of available pilot τ, and the number of UEs in the network have been analyzed in terms of the total uplink net throughput. In addition, the computational complexity analysis for the proposed schemes is studied in this work.

Section 5.2 provides the system model of this work, which includes uplink channel estimation, uplink data transmission and SE as a performance metric.

In section 5.3, the proposed schemes for both pilot assignment and pilot power control based on matching theory are provided. The complexity analysis of the proposed schemes to mitigate the pilot contamination is presented in section 5.5. Simulation results show the benefits of using matching theory to solve the issue of pilot contamination in the uplink cell-free massive MIMO systems against the state-of-the-art schemes in section 5.4. Section 5.6 presents the summary of this chapter.

5.2 System Model

In this chapter, the uplink cell-free massive MIMO systems is considered where the communication between M APs and K single-antenna UEs, randomly distributed in the coverage area, is coordinated by a CPU. Each AP is equipped with N_r receive antennas. Also, each AP has the option of being activated or deactivated in order to reduce the requirements for backhaul connection. The sets $\delta^{\mathrm{A}} = \{m_1^{\mathrm{A}}, ..., m_{M_{\mathrm{Activate}}}^{\mathrm{A}}\}$ and $\delta^{\mathrm{D}} = \{m_1^{\mathrm{D}}, ..., m_{M_{\mathrm{Deactivate}}}^{\mathrm{D}}\}$ denote the sets of activated and deactivated APs, respectively, such that $|\delta^A| + |\delta^D| = M$. The AP activation can be done by utilizing the largest-large-scale-fading scheme [131]. In addition, it is assumed that each UE in the network is served by a subset of δ^{A}. TDD is utilized in this work to process the transmission from K UEs to M APs.

Furthermore, by leveraging the estimated channels at M APs, the transmitted signals from K UEs in the coverage area can be decoded. Let $g_{k,m} \in \mathbb{C}^{N_r \times 1}$ denote the channel coefficient vector between k_{th} UE and m_{th} AP and it is expressed as

$$g_{k,m} = \sqrt{\beta_{k,m}} h_{k,m}, \tag{5.1}$$

where $\beta_{k,m}$ represents the large scale fading and $h_{k,m} \in \mathbb{C}^{N_r \times 1}$ denotes the small scale fading vector. Each UE and AP is likely to have a various set of scatters due to the random distribution of APs and UEs over a wide service area. Thus, $\{h_{k,m}\}$, $k = 1, ..., K$ and $m = 1, ..., M$, are assumed to be independent identically distributed (i.i.d.) $\mathcal{CN}(0, 1)$ random variables (RVs). It is also assumed that all APs are connected to the CPU via fronthaul links to serve all K UEs at the same time.

5.2.1 Uplink Channel Estimation

The parameter τ_c denotes the length of coherence interval (in symbols), which is larger than the length of the uplink training phase τ (in symbols). The pilot sequence for k_{th} UE is given by $\sqrt{\tau \eta_k} \phi_k \in \mathbb{C}^{\tau \times 1}$ where $||\phi_k||^2 = 1$ and η_k is the

power control coefficient for k_{th} UE, where $0 < \eta_k \leq 1$. Then, m_{th} AP receives the $\tau \times 1$ pilot vector from all UEs to be used for the channel estimation and this vector is expressed as

$$Y_{p,m} = \sqrt{\tau \rho_p} \sum_{k=1}^{K} g_{k,m} \eta_k^{\frac{1}{2}} \phi_k^H + \mathbf{N}_{p,m}, \tag{5.2}$$

where ρ_p denotes the normalized SNR of each pilot symbol (normalized by the noise power), where the noise power is $-174 \frac{\text{dBm}}{\text{Hz}} + 10 \log_{10}(B) + \text{Noise Figure}$, and B is the system bandwidth. $\mathbf{N}_{p,m}$ gives the matrix of additive noise at m_{th} AP with size $N_r \times \tau$. Also, all entire elements of $\mathbf{N}_{p,m}$ are assumed to be i.i.d. $\mathcal{CN}(0,1)$ RVs. The MMSE technique is utilized to estimate the channel $g_{k,m}$ between k_{th} UE and m_{th} AP after performing projection the received pilot signal $Y_{p,m}$ onto ϕ_k:

$$\begin{aligned} \hat{y}_{p,k,m} &= \phi_k^H Y_{p,m} \\ &= \sqrt{\tau \rho_p} g_{k,m} \eta_k^{\frac{1}{2}} + \sqrt{\tau \rho_p} \sum_{k' \neq k}^{K} g_{m,k'} \eta_{k'}^{\frac{1}{2}} \phi_k^H \phi_{k'} + \phi_k^H \mathbf{N}_{p,m}. \end{aligned} \tag{5.3}$$

Thus, the MMSE estimates of the channel between k_{th} UE and m_{th} AP is given as [10, 17]

$$\hat{g}_{k,m} = c_{k,m} (\sqrt{\tau \rho_p} g_{k,m} \eta_k^{\frac{1}{2}} + \sqrt{\tau \rho_p} \sum_{k' \neq k}^{K} g_{m,k'} \eta_{k'}^{\frac{1}{2}} \phi_k^H \phi_{k'} + \phi_k^H \mathbf{N}_{p,m}), \tag{5.4}$$

where $c_{k,m} = \frac{\sqrt{\tau \rho_p} \beta_{k,m} \eta_k^{\frac{1}{2}}}{\tau \rho_p \sum_{k'=1}^{K} \beta_{k',m} \eta_{k'} |\phi_k^H \phi_{k'}|^2 + 1}$. In addition, each AP in the coverage area individually estimates the channel and there is no cooperation among APs on the channel estimation process [10].

5.2.2 Uplink Data Transmission

The transmitted signal from k_{th} UE is denoted by $x_k = \sqrt{\eta_k} s_k$, where s_k, that satisfies $\mathbb{E}\{|s_k|^2\} = 1$, represents k_{th} UE transmitted symbol. The received signal from all UEs in the cell-free network to m_{th} AP is given by

$$y_{u,m} = \sqrt{\rho_u} \sum_{k=1}^{K} g_{k,m} x_k + n_{u,m}, \tag{5.5}$$

where $n_{u,m} \in \mathbb{C}^{N_r \times 1}$ presents the noise at m_{th} AP where its elements are assumed to be i.i.d. $\mathcal{CN}(0,1)$ RVs and ρ_u is the uplink normalized SNR data transmission (also normalized by the noise power, as mentioned in the previous section).

In order to detect the transmitted symbol from k_{th} UE, the AP sends the product of its $y_{u,m}$ received signal, from K UEs using the obtained estimated channel $\hat{g}_{k,m}$, to the CPU via the fronthaul link [17]. Thus, the CPU receives

$$r_{u,k} = \sum_{m \in \delta^{\text{A}}} \sum_{n=1}^{N_r} [\hat{g}_{k,m}]_n^* \, [y_{u,m}]_n \, . \tag{5.6}$$

5.2.3 Spectral Efficiency

Analysis techniques that are similar to those used in [10, 17], are utilized in this subsection to obtain the derivation of the uplink SE. Therefore, the main function of the CPU in the cell-free MIMO network is to detect the desired signal x_k from $r_{u,k}$. In addition, similar assumption is considered in this chapter to perform the detection of x_k, the statistical knowledge of the channel that is only used by the CPU. Thus, the received signal at the CPU from k_{th} UE as shown in (5.6) is decomposed as follows

$$r_{u,k} = \text{DS}_k \cdot x_k + \text{BU}_k \cdot x_k + \sum_{k' \neq k}^{K} \text{UI}_{kk'} \cdot x_k + \text{N}_k, \tag{5.7}$$

where

$$\text{DS}_k \triangleq \sqrt{\rho_u} \, \mathbb{E}\Big\{ \sum_{m \in \delta^{\text{A}}} \sum_{n=1}^{N_r} [\hat{g}_{mk}]_n^* [g_{mk}]_n \Big\},$$

$$\text{BU}_k \triangleq \sqrt{\rho_u} \sum_{m \in \delta^{\text{A}}} \sum_{n=1}^{N_r} [\hat{g}_{mk}]_n^* [g_{mk}]_n - \text{DS}_k,$$

$$\text{UI}_{kk'} \triangleq \sqrt{\rho_u} \sum_{m \in \delta^{\text{A}}} \sum_{n=1}^{N_r} [\hat{g}_{mk}]_n^* [g_{mk'}]_n,$$

and

$$\text{N}_k \triangleq \sum_{m \in \delta^{\text{A}}} \sum_{n=1}^{N_r} [\hat{g}_{mk}]_n^* [n_{u,m}]_n,$$

present the desired signal, the beamforming gain uncertainty, and the interference caused by k'_{th} UE. Thus, the uplink SE is obtained by considering the second, third and fourth term as an effective noise as well as using the worst case Gaussian

noise argument [10, 17, 131, 142], as follows

$$\mathrm{SE} = \frac{\tau_c - \tau}{\tau_c} \sum_{k=1}^{K} \log_2(1 + \mathrm{SINR}_k), \tag{5.8}$$

where SINR_k denotes signal-to-interference-plus-noise ratio which is written as

$$\mathrm{SINR}_k = \frac{\left|\mathrm{DS}_k\right|^2}{\mathbb{E}\left\{\left|\mathrm{BU}_k\right|^2\right\} + \mathbb{E}\left\{\left|\mathrm{UI}_{kk'}\right|^2\right\} + \mathbb{E}\left\{\left|\mathrm{N}_k\right|^2\right\}}. \tag{5.9}$$

Finally, the closed form expression of (5.9) can be obtained by following equations as

$$\mathrm{DS}_k = N_r\sqrt{\rho_u \eta_k} \sum_{m \in \delta^{\mathrm{A}}} \sqrt{\tau\rho_p}\beta_{k,m} c_{k,m}, \tag{5.10}$$

$$\mathbb{E}\{|\mathrm{BU}_k|^2\} = N_r \rho_u \eta_k \sum_{m \in \delta^{\mathrm{A}}} \sqrt{\tau\rho_p}\beta_{k,m}^2 c_{k,m}, \tag{5.11}$$

and

$$\begin{aligned}\mathbb{E}\{|\mathrm{UI}_{kk'}|^2\} =& N_r^2 \rho_u \eta_{k'} |\phi_k^H \phi_{k'}|^2 \Big(\sum_{m \in \delta^{\mathrm{A}}} \sqrt{\tau\rho_p}\beta_{k,m} c_{k,m} \frac{\beta_{m,k'}}{\beta_{k,m}}\Big)^2 \\ &+ N_r \rho_u \eta_{k'} \sum_{m \in \delta^{\mathrm{A}}} \sqrt{\tau\rho_p}\beta_{k,m}\beta_{m,k'} c_{k,m}.\end{aligned} \tag{5.12}$$

Thus, (5.10), (5.11) and (5.12) are used to obtain (5.9).

5.3 Mitigating Pilot Contamination Methodology

When numerous UEs communicate with the same AP, the pilot contamination phenomenon occurs when the UEs utilize the same pilot sequence. As a consequence, these UEs are assigned the same pilot sequence, resulting in a reduction in channel estimate accuracy. As a result, the effect of pilot contamination is addressed in this chapter by proposing two schemes of the pilot assignment and the pilot power control.

5.3.1 Pilot Assignment Scheme

The pilot set Δ_ϕ includes $\{1, 2, ..., \tau\}$ orthogonal pilot sequences and is given as

$$\Delta_\phi = \{\phi_1, \phi_2, ..., \phi_\tau\}. \tag{5.13}$$

K pilot sequences are randomly selected from Δ_ϕ and then these selected pilot sequences are assigned to K UEs. Therefore, the main aim of this stage in this chapter is to maximize the uplink SE by finding the optimal assignment between the pilot sequences to K UEs in order to alleviate the effect of the pilot contamination phenomenon. Thus, the optimization problem is formulated as

$$\max_{\mathcal{J}_l} \quad \left(\frac{\tau_c - \tau}{\tau_c} \sum_{k=1}^{K} \log_2(1 + \mathrm{SINR}_k) \right), \tag{5.14}$$

where $\mathcal{J}_l$ gives all possible cases of the pilot assignment in which $\mathcal{J}_l = \{\phi_l^1, \phi_l^2, ..., \phi_l^K\}$ and $l = \{1, 2, ..., \tau^K\}$. Thus, ϕ_l^k is selected from Δ_ϕ and then assigned to k_{th} UE. The optimization problem in 5.14 is NP-hard [143]. The exhaustive searching technique can solve this problem [97], but this scheme suffers from huge computational complexity, especially when there is a large number of UEs in the coverage area. Therefore, we propose a novel pilot assignment scheme based on an iterative Hungarian strategy and the GA by solving the pilot assignment optimization problem in (5.14) for the uplink cell-free massive MIMO systems. Moreover, the iterative Hungarian scheme is utilized to obtain the best populations of the GA instead of using τ^K populations as an input. Then, the GA is used to find the optimal pilot sequence for each UE in the coverage area.

The iterative Hungarian technique

It is assumed that there are $\mathcal{J}_l$ possible cases of pilot assignment when $l = 1, 2, ..., K$ rather than $l = 1, 2, ..., \tau^K$. Then, $\mathcal{J}_l$ is randomly generated and the SE for each UE is calculated based on the entire elements of $\mathcal{J}_l$ in order to produce the reward matrix as shown in the example of one iteration in Table 1.

Table 1: An Example of The Reward Matrix Between $\mathcal{J}_l$ and K UEs for $K = l = 4$.

	UE_1	UE_2	UE_3	UE_4
$\mathcal{J}_1$	$\mathrm{SE}_{1,1}(\boldsymbol{\phi_1^1})$	$\mathrm{SE}_{1,2}(\boldsymbol{\phi_1^2})$	$\mathrm{SE}_{1,3}(\boldsymbol{\phi_1^3})$	$\mathrm{SE}_{1,4}(\boldsymbol{\phi_1^4})$
$\mathcal{J}_2$	$\mathrm{SE}_{2,1}(\boldsymbol{\phi_2^1})$	$\mathrm{SE}_{2,2}(\boldsymbol{\phi_2^2})$	$\mathrm{SE}_{2,3}(\boldsymbol{\phi_2^3})$	$\mathrm{SE}_{2,4}(\boldsymbol{\phi_2^4})$
$\mathcal{J}_3$	$\mathrm{SE}_{3,1}(\boldsymbol{\phi_3^1})$	$\mathrm{SE}_{3,2}(\boldsymbol{\phi_3^2})$	$\mathrm{SE}_{3,3}(\boldsymbol{\phi_3^3})$	$\mathrm{SE}_{3,4}(\boldsymbol{\phi_3^4})$
$\mathcal{J}_4$	$\mathrm{SE}_{4,1}(\boldsymbol{\phi_4^1})$	$\mathrm{SE}_{4,2}(\boldsymbol{\phi_4^2})$	$\mathrm{SE}_{4,3}(\boldsymbol{\phi_4^3})$	$\mathrm{SE}_{4,4}(\boldsymbol{\phi_4^4})$

Therefore, an assignment optimization problem is formulated as

$$\begin{aligned} \max_{\alpha_{l,k}\in[0,1]} \quad & \sum_{l=1}^{K}\sum_{k=1}^{K} \mathrm{SE}_{l,k}(\alpha_{l,k}), \\ \text{s.t.} \quad & \sum_{l=1}^{K} \alpha_{l,k} = 1, \ \forall k, \\ & \sum_{k=1}^{K} \alpha_{l,k} = 1, \text{for } \forall l, \end{aligned} \tag{5.15}$$

where $\mathrm{SE}_{l,k}$ is the k_{th} SE corresponding to l_{th} pilot sequence, and $\alpha_{l,k}$ indicates l_{th} pilot sequence (ϕ_l^k) is assigned to k_{th} UE. The constrains of the optimization problem are to ensure l_{th} pilot sequence is assigned to only one UE. Furthermore, problem (5.15) can be solved by applying the Hungarian method. This algorithm is iteratively performed K times in order to prepare the K possible populations for the GA in the following section. Algorithm 4 summarises the whole procedures of the proposed iterative Hungarian scheme. The first step is used to obtain τ orthogonal sequences based obtaining the right singular value decomposition. Then, it is required to initialize (ϵ) random number from the range $[1, \tau]$ and its corresponding orthogonal pilot sequence can be determined from the previous step. Once $\mathcal{J}_l = [\phi_l^1, \phi_l^2, ..., \phi_l^K]$ is obtained, it is required to compute its corresponding $[\mathrm{SE}_{l,1}(\phi_l^1), \mathrm{SE}_{l,2}(\phi_l^2), ..., \mathrm{SE}_{l,K}(\phi_l^K)]$ by using $\mathrm{SE}_{l,k}(\phi_l^k) = \frac{\tau_c-\tau}{\tau_c}\log_2(1+\mathrm{SINR}_{l,k})$. The reward matrix is generated as illustrated in Table 1 for each i_{th} iteration. Accordingly, the Hungarian method is used to solve the assignment optimization problem in (5.15). Moreover, as shown in Figure 5.1, the suggested algorithm's high-level diagram begins by assigning UE_k to $\mathcal{J}_l$ randomly. Then, the Hungarian algorithm starts by reducing each row in the input reward matrix, which consists of the computed $\mathrm{SE}_{l,k}$ with all $\mathcal{J}_l$, by subtracting the minimum item in each row from all other items in the same row, and then repeating the process for each column. Then, we look for the convenient $\mathcal{J}_l$ for each UE_k. If UE_k is already assigned to $\mathcal{J}_l$, it is better to be assigned with another $\mathcal{J}_l$, we prime the alternative before moving on to the next $\mathcal{J}_l$ candidate pilot sequences; however, if that is the only $\mathcal{J}_l$ pilot sequences for which UE_k is qualified, we would like to reassign any other UE_k to those $\mathcal{J}_l$, this step is known as a percolation process. We reassign UE_K to their $\mathcal{J}_K$ to guarantee the assignment can provide the maximum SE, which is the resolvability test. As a result, we can be confident that we make progress toward our goal of identifying the best assignment with each iteration in order to prepare $K \times K$ the best possible populations.

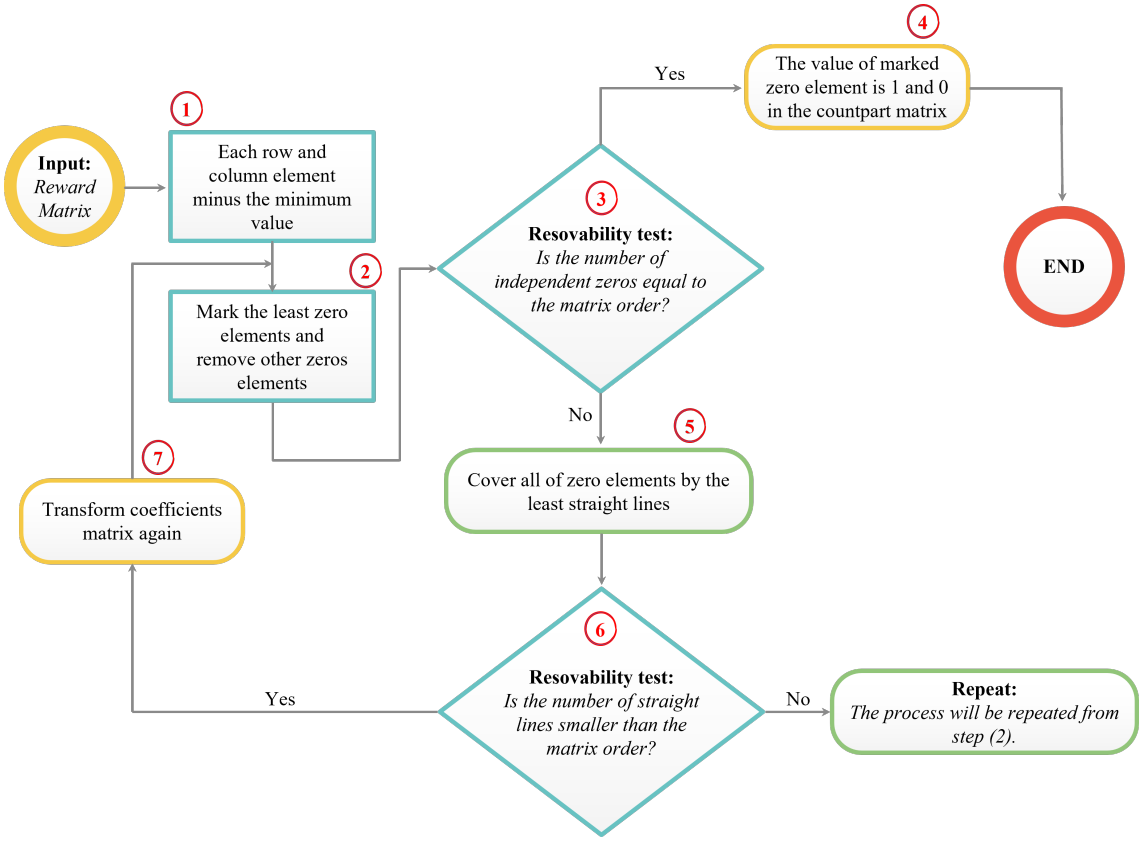

Figure 5.1: Flow chart of the Hungarian algorithm.

Algorithm 4: The proposed iterative Hungarian scheme [28] to solve (5.15)

Input: K, τ, τ_c

Result: The best possible combinations of pilot sequences $\mathcal{J}_l^\star$ where $l = 1, 2, ..., K$.

- Compute τ orthogonal sequences by obtaining right singular value decomposition.
- **for** $i = 1 : K$ **do**
  - **for** $l = 1 : K$ **do**
    - **for** $k = 1 : K$ **do**
      - Initialize random number ϵ, where $1 \leq \epsilon \leq \tau$, and compute its corresponding orthogonal pilot sequence (ϕ_l^k).
    - **end**
    - Compute $\mathcal{J}_l = [\phi_l^1, \phi_l^2, ..., \phi_l^K]$.
    - Compute $[\mathrm{SE}_{l,1}(\phi_l^1), \mathrm{SE}_{l,2}(\phi_l^2), ..., \mathrm{SE}_{l,K}(\phi_l^K)]$ by using $\mathrm{SE}_{l,k}(\phi_l^k) = \frac{\tau_c - \tau}{\tau_c} \log_2(1 + \mathrm{SINR}_{l,k})$.
  - **end**
  - Generate the reward matrix as illustrated in Table 1.
  - Apply the Hungarian algorithm [28] to obtain the maximum $\mathrm{SE}_{l,K}(\phi_l^k)$ as shown in Figure 5.1.
- **end**
- Obtain $[\mathcal{J}_{l=1}^\star, \mathcal{J}_{l=2}^\star, ..., \mathcal{J}_{l=K}^\star]$.

The proposed GA scheme

GA is an efficient stochastic method for solving optimal problems that is based on natural selection and natural genetics [144–146]. The GA technique is used to solve the optimization problem, and it contains population initialization, fitness value evaluation, and genetic operations including selection, crossover, and mutation to produce the next generation population. The GA operations are iteratively repeated until the best solution is achieved [146].

Algorithm 5 shows the main steps of the proposed GA to obtain the optimal pilot sequences to be assigned to K UEs in the uplink cell-free massive MIMO systems. The possible pilot sequences are obtained by using the iterative Hungarian algorithm, and these possible pilot sequences are considered as an input of the GA and termed as *Populations* which includes multiple chromosomes. Thus, *Populations* can be given as

$$Populations = [\mathcal{J}^{\star}_{l=1}, \mathcal{J}^{\star}_{l=2}, ..., \mathcal{J}^{\star}_{l=K}]. \tag{5.16}$$

Then, each chromosome is expressed as $\mathcal{J}^{\star}_{l=k} = [\phi^1_k, \phi^2_k, ..., \phi^K_k]$. The chromosome includes multiple genes. These genes are encoded to τ integer numbers, such that $\{1, 2, ..., \tau\}$. Therefore, this process is called *gene encoding*. After that, each chromosome has its fitness value which is the total SE for the uplink cell-free massive MIMO systems and this fitness value can be obtained by utilizing equation (5.8). This process called *fitness evaluation*. Inside each GA iteration, there are four main steps. **Step (1)** is the selection process. This process is to select parents to perform crossover process and these selected parents can be obtained by Roulette Wheel Selection technique. When ball is thrown in, each chromosome with higher fitness value has a chance to be selected. **Step (2)** is to obtain new offspring by using partially-matched crossover (PMX) crossover technique because it is not permissible to highly repeat genes on the new offspring [147]. **Step (3)** describes the mutation process in order to avoid local optimum [144, 147]. This process can be done by choosing random gene with the GA mutation probability and swapping the selected random gene by randomly choosing another gene from the range $[1, \tau]$. Then, the updated new offspring is evaluated by using equation (5.8) and the populations are updated by the new offspring after the crossover and mutation operations. All of the previous steps are repeated if $l < \Gamma$ iterations. Finally, K pilot sequences with the highest fitness value in the last population are obtained to be assigned to K UEs.

Algorithm 5: The proposed GA to obtain the optimal pilot sequences to be assigned to K UEs.

Input: $[\mathcal{J}^{\star}_{l=1}, \mathcal{J}^{\star}_{l=2}, ..., \mathcal{J}^{\star}_{l=K}]$, Γ iterations.

Result: K pilot sequences to be assigned to K UEs

- Compute fitness value for $[\mathcal{J}^{\star}_{1}, \mathcal{J}^{\star}_{2}, ..., \mathcal{J}^{\star}_{K}]$ based on equation (5.8)

for $l = 1 : \Gamma$ **do**

- **Step (1)**: Parents can be selected from all populations by using Roulette Wheel Selection technique.
- **Step (2)**: New offspring ← PMX approach of parents [147].
- **Step (3)**: Updated new offspring ← applying mutation process on the obtained new offspring from the previous step.
- **Step (4)**: Updated populations ← parents ∪ Updated new offspring.

end

5.3.2 Pilot Power Control Design

We propose a lower complexity pilot power control design for the uplink cell-free massive MIMO systems based on matching theory. It has been formulated as a minimum weighted assignment optimization problem in order to assign the pilot power control coefficients to the minimum channel estimation error for each UE. The formulated assignment problem is expressed as

$$\begin{aligned} \max_{\alpha_{i,k}\in[0,1]} \quad & \sum_{i=1}^{K}\sum_{k=1}^{K}\left(\sum_{m\in\delta^{\mathrm{A}}}(1-\sqrt{\tau\rho_p}\eta_{i,k}^{1/2}c_{k,m})\right)(\alpha_{i,k}), \\ \text{s.t.} \quad & \sum_{i=1}^{K}\alpha_{i,k}=1,\ \forall k, \\ & \sum_{k=1}^{K}\alpha_{i,k}=1, \text{for } \forall i. \end{aligned} \tag{5.17}$$

The previous formulated assignment problem in this work is related to the previous section by finding the optimal pilot power for each UE and this formulated problem does not involve some continuous variables η_k as [17], because it has been assumed that $\eta_{i,k}$ is a fixed random variable of the pilot power control coefficient, such that $0 \leq \eta_{i,k} \leq 1$. Therefore, the reward matrix of the proposed matching scheme in this section includes the estimated channel quality based on random values of all UEs pilot power coefficients. Figure 5.2 demonstrates the steps to obtain the optimal pilot power control coefficients for all UEs in the cell-free

network. Firstly, it is generated K random pilot power $\eta_{i,k}$ for each UE, where $i = 1, 2, ..., K$ that indicates the number of random pilot power. Secondly, each $\eta_{i,k}$ is substituted in $(\sum_{m\in\delta^A}(1-\sqrt{\tau\rho_p}\eta_{i,k}^{1/2}c_{k,m}))$ in order to obtain the estimated channel quality. Therefore, the reward matrix with size $K \times K$ is obtained based on the values of the estimated channel quality corresponding to the random pilot power for each UE. Finally, the Hungarian algorithm is utilized to find the minimum of the largest of all UE normalized mean-squared errors with optimal pilot control power for each UE.

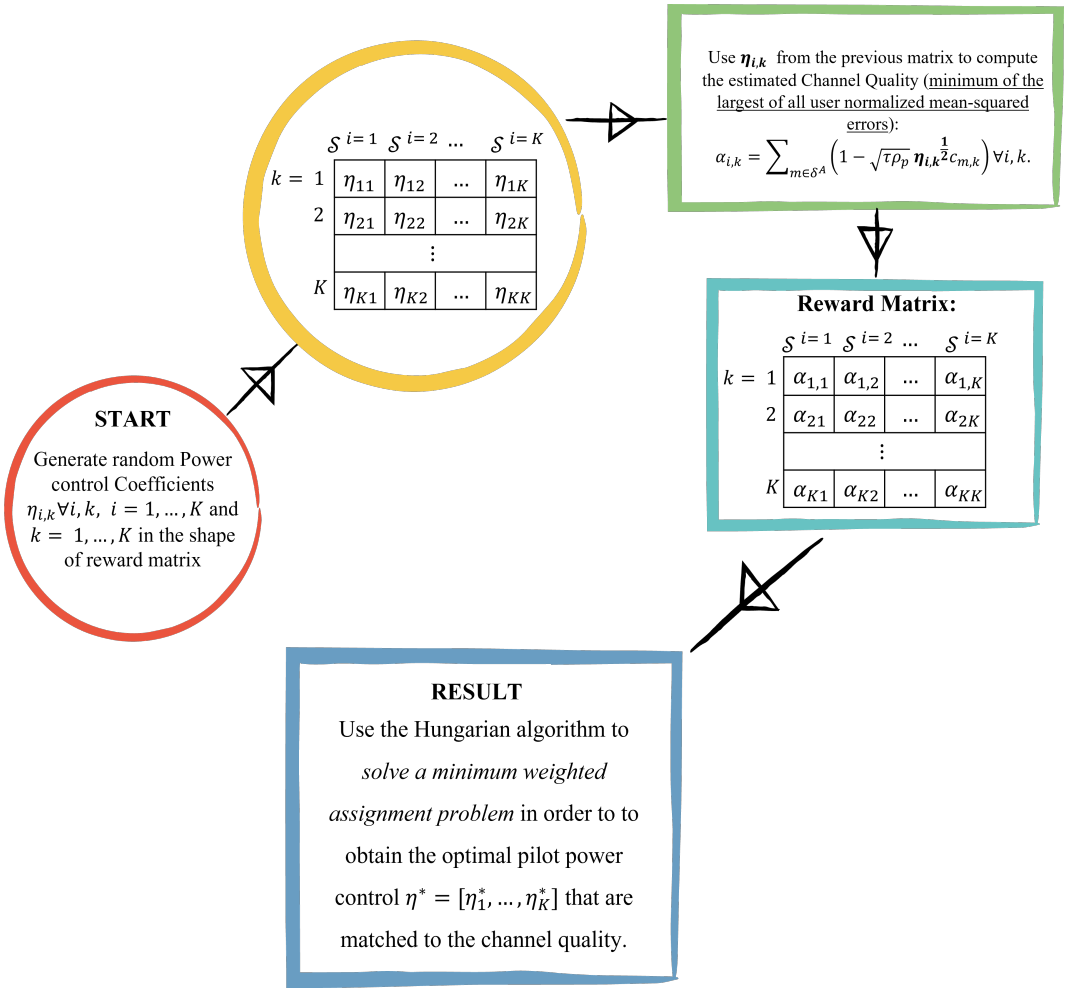

Figure 5.2: Steps of the proposed pilot power control design based on matching technique to enhance the uplink cell-free massive MIMO systems performance.

5.4 Simulation Results and Discussions

In this section, the performance of uplink cell-free massive MIMO systems is evaluated by taking into account the impact of the available pilots τ, the number of M APs, the number of K UEs, and the number of N_r antennas which are equipped for each AP in the cell-free network. The performance metric in this

chapter is the total uplink net throughput, by taking into account the channel estimation overhead, which is defined as $B \times \left(\frac{\tau_c - \tau}{\tau_c} \sum_{k=1}^{K} \log_2(1 + \mathrm{SINR}_k)\right)$. M APs and K UEs are randomly distributed in the square area $D \times D$ km^2, and the wrapped around technique is utilized to simulate a network in order to emulate the condition of being without boundaries. Table 2 includes all utilized simulation parameters in this chapter.

Table 2: Simulation parameters.

Parameter	**Value**
D	1000 m
Carrier frequency (f)	1.9 GHz
Bandwidth (B)	20 MHz
Coherence interval (τ_c)	200 samples
Pilot sequence transmit power (ρ_p)	100 mW
UE uplink transmit power (ρ_u)	100 mW
Noise Figure	9 dB

The large scale fading coefficients $\beta_{k,m}$ is expressed as

$$\beta_{k,m} = \mathrm{PL}_{k,m}(10\frac{\sigma_{sh}\chi_{k,m}}{10}), \tag{5.18}$$

where $\mathrm{PL}_{k,m}$ gives the pathloss, and $10^{\frac{\sigma_{sh}\chi_{k,m}}{10}}$ shows the shadow fading with standard deviation $\sigma_{sh}\chi_{k,m}$ and $\chi_{k,m} \sim \mathcal{CN}(0,1)$. Thus, three slope pathloss models are utilized in which the pathloss exponent is 3.5 when the distance between the k_{th} UE and m_{th} AP is denoted by $d_{k,m}$ and is larger than d_1, the pathloss exponent is 2 when $d_0 < \mathrm{d}_{k,m} \leq d_1$ and 0 when $d_{k,m} \leq d_0$, where $d_0 = 10$ m and $d_1 = 50$ m [10]. Therefore, the Hata-Cost pathloss models are given as [148]

$$\mathrm{PL}_{k,m}[\mathrm{dB}] = \begin{cases} -\mathrm{L} - 35\log_{10}(d_{k,m}), \text{ if } \mathrm{d}_{k,m} > d_1 \\ -\mathrm{L} - 15\log_{10}(d_1) - 20\log_{10}(d_{k,m}), \text{ if } d_0 < \mathrm{d}_{k,m} \leq d_1 \\ -\mathrm{L} - 15\log_{10}(d_1) - 20\log_{10}(\mathrm{d}_0), \text{ if } d_{k,m} \leq d_0 \end{cases} \tag{5.19}$$

where $\mathrm{L} = 46.3 + 33.9\log_{10}(f) - 13.82\log_{10}(h_{AP}) - (1.1\log_{10}(f) - 0.7)h_{UE} + (1.56\log_{10}(f) - 0.8$, where f denotes the carrier frequency in (GHz). $h_{AP} = 15$ m and $h_{UE} = 1.65$ m represents the antenna height of the m_{th} AP and the k_{th}

UE, respectively. Most earlier studies of the shadowing correlation model assumed that the shadowing coefficients are uncorrelated, however in actuality, the transmitter and receiver may be surrounded by similar obstacles. The shadowing coefficients are therefore correlated, which may have an impact on the system's performance. Therefore, the shadowing and correlation models are described in [[10], (54)-(55)]. All results are obtained by using Mont Carlo simulation whereby new APs and UEs locations are randomly located in each iteration. Finally, the parameters of the proposed scheme of the pilot assignment based on the integration between the Hungarian scheme and the GA have been set as $\Gamma = 200$, the mutation probability = 0.8, and the percentage of the crossover probability is 80%. The main reason behind proposing the integration between these two algorithms is to reduce the computational complexity compared to the conventional GA and achieve close to the optimal results based on the exhaustive searching method.

Figure 5.3 shows the cumulative distribution function (CDF) of the total uplink throughput for different pilot assignment schemes when $M = 40$, $K = 10$, $N_r = 1$, $\eta_k = 1$, and $\tau = 2$. The proposed scheme based on the integration between the Hungarian scheme and the GA is compared to the exhaustive search scheme in which all possible (τ^K) pilot sequences are evaluated and the pilot sequence that can provide the maximum total net throughput will be taken, the conventional GA [99], the greedy and random schemes [10]. It is obvious that the proposed scheme can achieve almost the same as the exhaustive search scheme. This is because the the proposed scheme utilizes the Hungarian method to provide the initial population for the GA in order to search for the nearby the optimal solution rather than using random initial population as the conventional GA does. In addition, the proposed scheme can overcome other schemes with respect to both $95\% -$ likely and median of the total uplink net throughput.

Figure 5.4 illustrates that the CDF of the total uplink net throughput with two cases of M APs, as $M = 100$ and $M = 200$, with $K = 40$, $N_r = 1$, $\eta_k = 1$, and $\tau = 5$. It can be seen that the proposed pilot assignment scheme can overcome other schemes in both cases of M. It is also noted that the total uplink net throughput increases as M increases. However, there are no improvements in the gaps of both $95\% -$ likely and median due to increasing the number of APs in the cell-free network. This is because τ plays a vital role in the system performance and it is less associated with K UEs. For example, when $M = 200$, the proposed scheme can achieve 48.654 (Mbits/Sec) $95\% -$ likely total uplink net throughput compared to 45.30 (Mbits/Sec), 42.001 (Mbits/Sec), 41.8 (Mbits/Sec) for the conventional GA, greedy scheme, and random scheme, respectively.

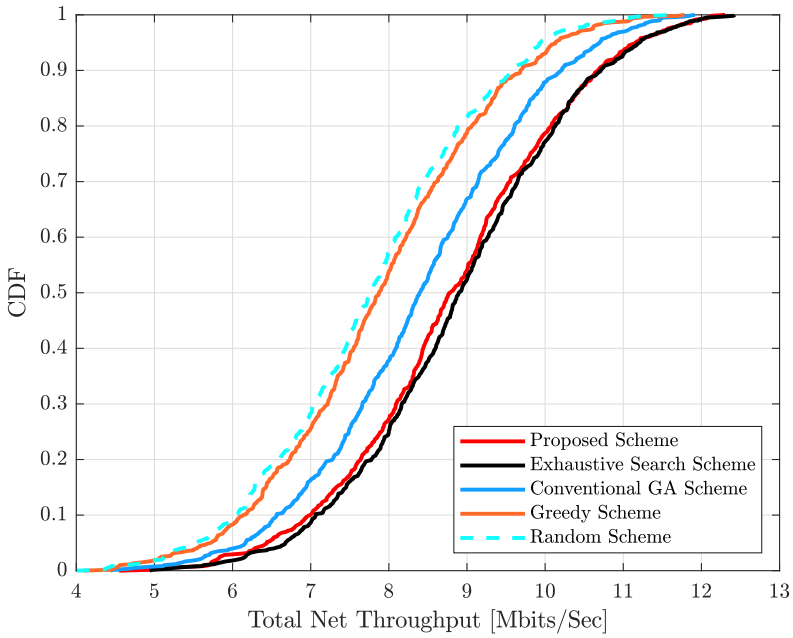

Figure 5.3: CDF of the total uplink net throughput for different pilot assignment schemes with $M = 40$, $K = 10$, $N_r = 1$, $\eta_k = 1$, and $\tau = 2$.

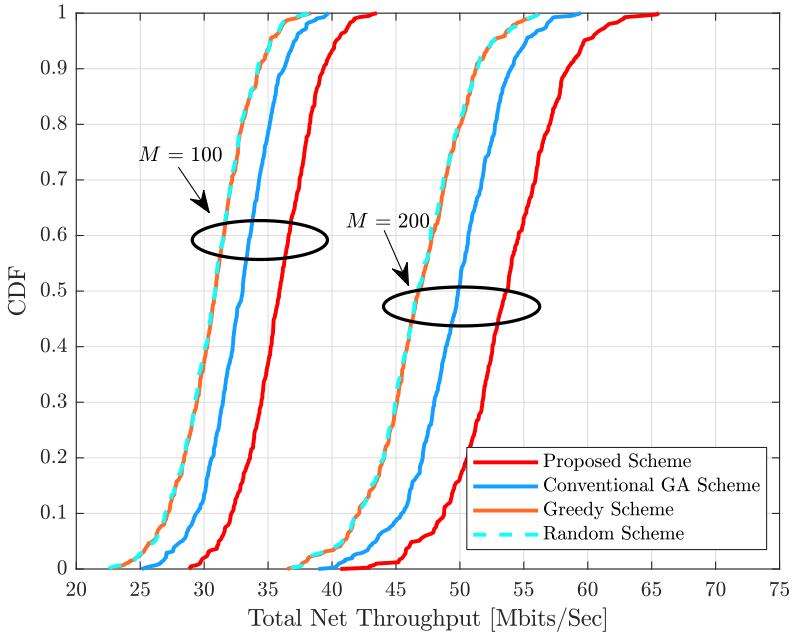

Figure 5.4: CDF of the total uplink net throughput for different pilot assignment schemes with $K = 40$, $N_r = 1$, $\eta_k = 1$, and $\tau = 5$.

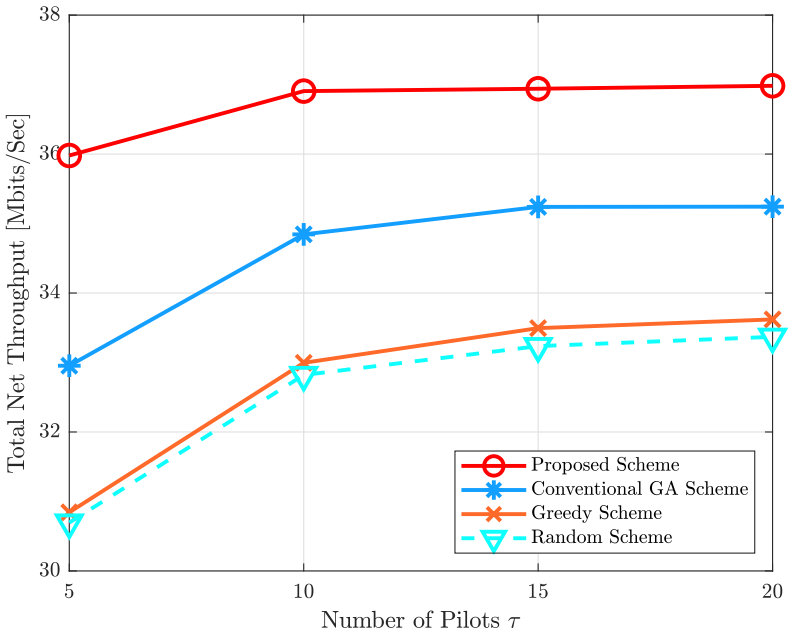

Figure 5.5: Total uplink net throughput versus various τ available pilots with $M = 100$, $K = 40$, $\eta_k = 1$, and $N_r = 1$.

Figure 5.5 demonstrates the total uplink net throughput versus various available pilots τ, when $M = 100$, $K = 40$, $\eta_k = 1$, and $N_r = 1$. It can be seen that the total uplink net throughput slowly increases as the number of available pilots τ increases because when τ becomes large, the time for uplink data transmission per coherence interval becomes small. On the other hand, when τ is small, the accuracy of the estimated channel decreases and this will affect on the system performance because the strong effect of the pilot contamination phenomenon. In addition, the gap between the proposed scheme and other schemes in this work increases when τ decreases. It is obvious that the proposed scheme of pilot assignment can mitigate the pilot contamination phenomenon in the uplink cell-free massive MIMO systems. For example, the total uplink net throughput of the cell-free massive MIMO network with $\tau = 10$ improves by 5.75%, 11.2%, and 12% comparing with the conventional GA, the greedy scheme, and the random scheme, respectively.

Figure 5.6 provides the total uplink net throughput of the proposed scheme for both pilot assignment, and the pilot power control design compared with the state-of-the-are schemes which are the pilot power control design using second-order Taylor approximation with greedy pilot assignment [17], and the greedy pilot assignment when all UEs in the cell-free network transmit their pilot signals with full pilot power [10]. It is obvious that the proposed scheme in this chapter offers around 5%, and 18% improvement in the total uplink net throughput com-

pared with the pilot power control design [17] and full pilot power transmission during the training phase in [10], respectively. In addition, it can be seen that small number of APs with small available pilots τ increase the pilot contamination effect and the proposed scheme can mitigate the effect of pilot contamination.

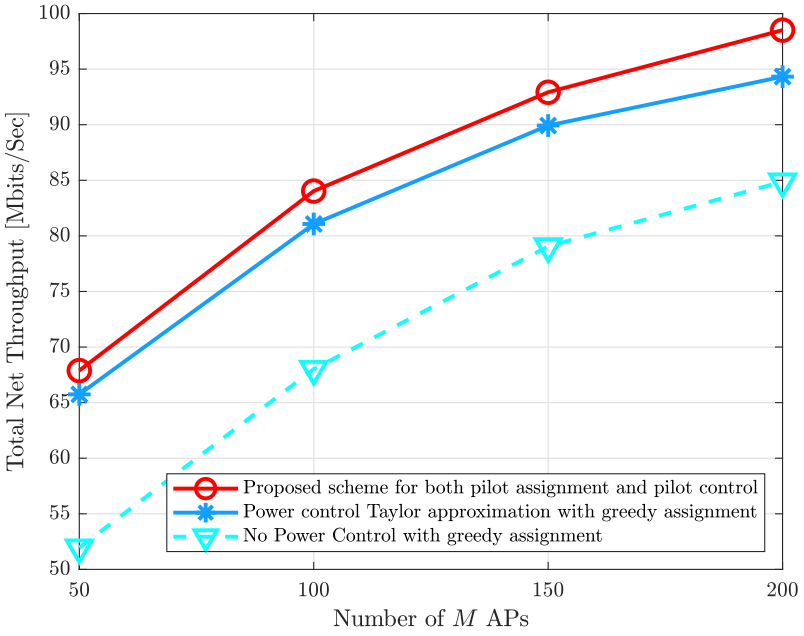

Figure 5.6: Total uplink net throughput for the proposed schemes of both pilot assignment as well as pilot power control compared to the state-of-the-art schemes versus various M APs with $K = 40$, $\tau = 5$, and $N_r = 16$.

Figure 5.7 shows the impact of the N_r antennas on the total uplink net throughput of the proposed schemes for both pilot assignment and power control compared to [10], and [17]. As expected, as the number of N_r increases, the uplink net throughput of all schemes increase. However, the proposed schemes in this chapter can offer around 3%, and 22% improvement compared to the mentioned schemes. This is because the greedy pilot assignment of other schemes cannot obtain the optimal pilot sequences for K UE, while the proposed pilot assignment can achieve near to the optimal results as mentioned previously.

Figure 5.8 indicates the total uplink net throughput with $K = \{20, 40, 60, 80\}$ with $N_r = 16$, $M = 100$, and $\tau = 5$. It is obvious that the uplink net throughput increases as K increases. This is because the inter-user interference cannot affect on the SE of the uplink systems. The proposed schemes in this chapter can overcome the mentioned schemes. For example, when $K = 60$, the proposed schemes to mitigate the pilot contamination can attain 112.464 [Mbits/Sec], the

pilot power control with greedy assignment achieves 106.254 [Mbits/Sec], and the greedy pilot assignment without pilot power control achieves 85.2676 [Mbits/Sec].

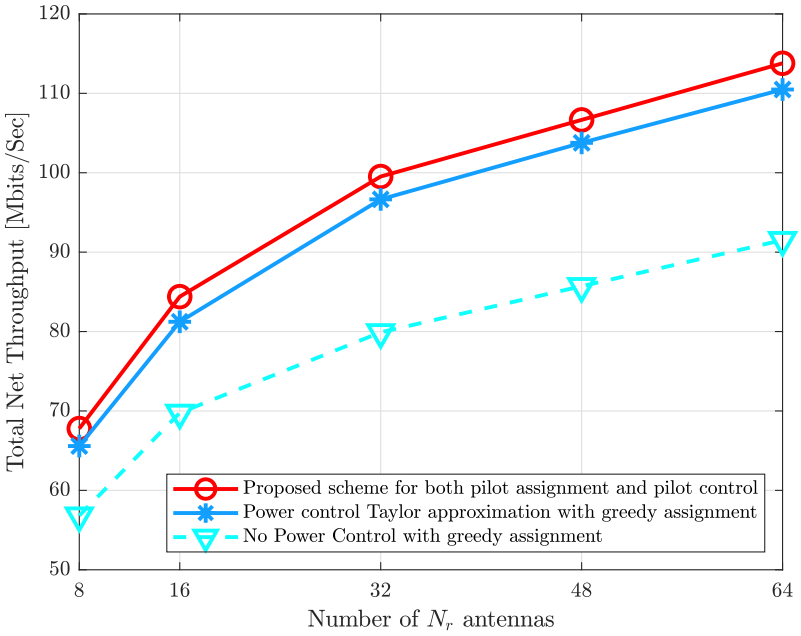

Figure 5.7: Total uplink net throughput for the proposed schemes of both pilot assignment as well as pilot power control compared to the state-of-the-art schemes versus various N_r receive antennas with $M = 100$, $K = 40$, and $\tau = 5$.

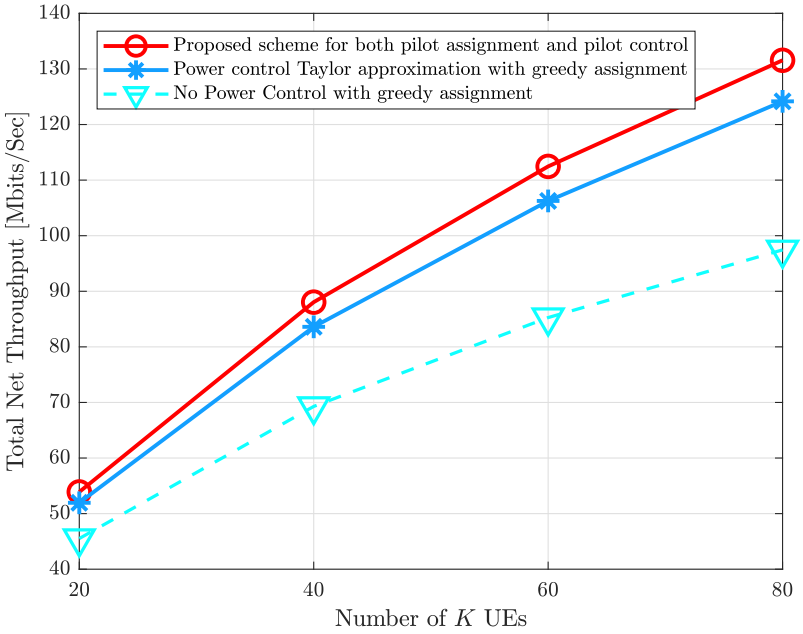

Figure 5.8: Total uplink net throughput for the proposed schemes of both pilot assignment as well as pilot power control compared to the state-of-the-art schemes versus various K UEs with $M = 100$, $N_r = 16$, and $\tau = 5$.

Figure 5.9 demonstrates the impact of several numbers of the available pilots τ on the system performance in terms of the total uplink net throughput. It can be seen that the proposed schemes for both pilot assignment as well as the pilot power control design can attain better performance compared to other schemes. In addition, it is obvious that taking into consideration both of pilot assignment and pilot power control coefficients can strongly enhance the system performance by mitigating the pilot contamination effect.

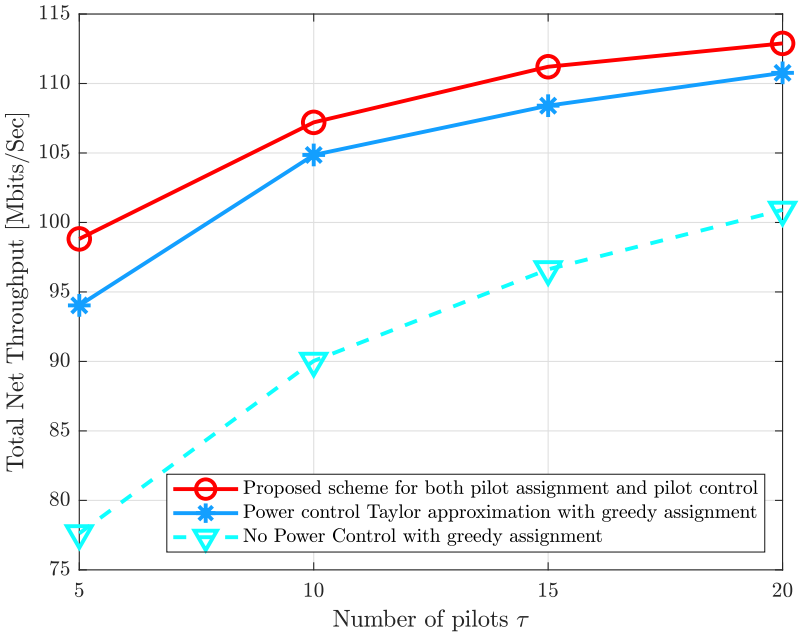

Figure 5.9: Total uplink net throughput for the proposed schemes of both pilot assignment as well as pilot power control compared to the state-of-the-art schemes versus various τ available pilots with $M = 100$, $N_r = 16$, and $K = 40$.

5.5 Complexity Analysis

The complexity analysis of the proposed scheme based on the integration between the Hungarian method and the GA is $\mathcal{O}(\Gamma \mathcal{P} K)$ [101], where $\mathcal{P}$ is the population size and it is equal to K, while the complexity analysis of the conventional GA differs from the proposed scheme by the population size, which is τ^K [99, 101]. In addition, the complexity analysis of the benchmark greedy scheme, the random scheme, and the exhaustive search scheme are $\mathcal{O}(KM)$, $\mathcal{O}(K)$, and $\mathcal{O}(\tau^K)$, respectively. On the other side, the CPU computational time in seconds is proposed to analyse the complexity of the proposed schemes for both pilot assignment and the pilot power control compared to the pilot power control based on using second-order Taylor approximation with greedy pilot assignment.

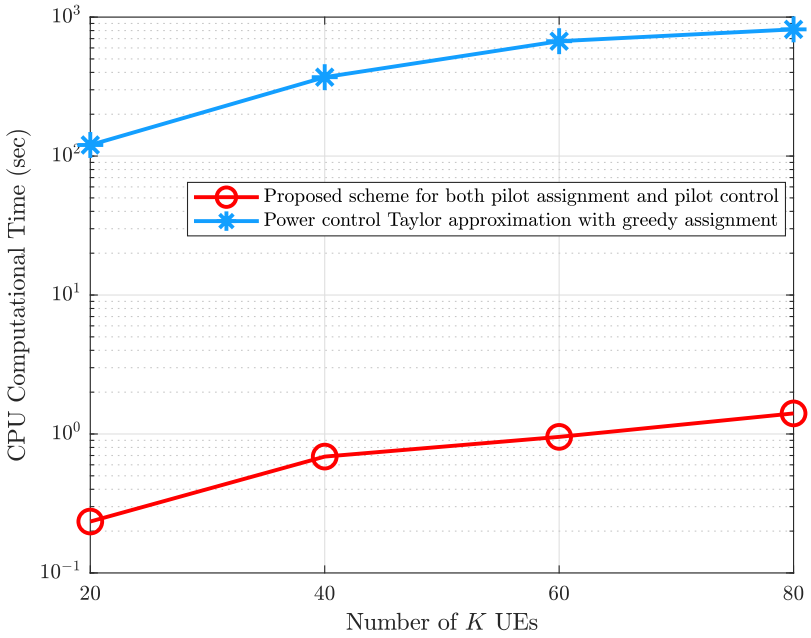

Figure 5.10: CPU computational time comparison of our proposed schemes of mitigation the pilot contamination against power control design using a Taylor approximation with greedy assignment scheme for increasing number of K UEs.

5.6 Summary

In this chapter, it has been proposed two novel schemes based on the matching technique for mitigating the pilot contamination in the uplink cell-free massive MIMO systems. In the first scheme, we proposed integrating the Hungarian method and the GA to assign the pilot sequences to the K UEs in the coverage area. We formulated an assignment optimization problem to select the best possible pilot sequences to be an input for the GA to iteratively obtain the optimal pilot sequences that can maximize the uplink SE. In the second scheme to alleviate the pilot contamination effect, we proposed a novel pilot power control design based on a matching technique between random pilot power and its corresponding channel estimation accuracy for each UE. Therefore, we formulated a minimum-weighted assignment optimization problem and solved it using the Hungarian algorithm. We also investigated our proposed schemes' total uplink net throughput. We compared the findings to state-of-the-art strategies for pilot assignment schemes and pilot power control design by considering the impact of the number of M APs, K UEs, N_r antennas, and τ available pilots. Our proposed methodology has a significantly lower computational complexity with higher total uplink net throughput.

Chapter 6

Conclusions and Future Directions

The contributions of this thesis, concluding remarks and the future research directions are summarized in this chapter.

6.1 Summary of The Work

In this thesis, the first chapter introduced a generic description of the cell-free massive MIMO systems and an overview of the matching theory. This chapter includes the motivation of using the matching theory in different subjects in the uplink cell-free massive MIMO systems, such as pilot assignment, pilot power control, and optimal hybrid beamforming design to reduce the power consumption concerning antenna selection and RF chains activation.

Chapter 2 provided the literature review of all structures of massive MIMO systems, mm-Wave technology, the applied signal processing techniques in mm-Wave massive MIMO systems, and the cell-free massive MIMO systems, including the FDD and TDD communication methods, the channel estimation, the uplink data transmission and all related works of the hybrid beamforming design in the cell-free mm-Wave massive MIMO systems. Based on the analysis of this chapter, the following conclusions have been reached:

1. With high beamforming gains, the cell-free network can overcome path loss in mm-Wave communication by using large antenna arrays at the APs. A considerable amount of power is required, however, because conventional digital signal processing requires a dedicated RF chain and ADC for each antenna. This necessitates an optimal design of hybrid beamforming de-

sign, which is more energy-efficient. However, there are limited works in the literature focusing on the hybrid beamforming design to minimize the power consumption in the cell-free and small cells mm-Wave massive MIMO systems.

2. The antenna selection technique can be considered to solve the power consumption issue in the cell-free mm-Wave massive MIMO systems. However, there are two main drawbacks. Firstly, the high correlated channels in the mm-Wave communication technology will cause degradation in the system performance because switching off some antennas without taking into account some antennas at each AP can contribute more to the interference than the desired power. Secondly, the main concept of cell-free massive MIMO systems is based on a large number of distributed APs in the coverage area. This has substantial computational complexity to select the optimal antennas at each AP using the exhaustive searching method.

3. It has been noted that the number of RF chains at each AP and the total number of APs in the cell-free network are proportional to the total power consumption. Therefore, RF chain activation is considered to be another solution to minimize the power consumption in the cell-free mm-Wave massive MIMO systems. However, an efficient and low complexity scheme is required to activate the set RF chains at each AP to maximize the EE while maintaining the total achievable rate from a significant loss due to switching off some RF chains.

4. Pilot assignment and pilot power control play a vital role in mitigating the pilot contamination issue in enhancing the accuracy of the channel estimation in the cell-free massive MIMO systems. In contrast, most of the current works focus on the pilot assignment technique by assuming the full power of each transmitted pilot without taking into account the optimal pilot power control; on the other hand, assuming pilot power control design but with a random pilot assignment technique that cannot guarantee much enhancement in the accuracy of the estimated channel. This is to avoid the substantial computational complexity required in the real-time implementation when large number of both APs and UEs exist in the coverage area.

In Chapter 3, the hybrid beamforming architecture with CPSs for uplink decentralized cell-free mm-Wave massive MIMO systems is proposed based on exploiting antenna selection to reduce power consumption. However, current antenna selection techniques are applied for conventional massive MIMO, not cell-free massive MIMO systems, as mentioned previously. Therefore, the substantial computational complexity of these techniques to optimally select antennas for cell-free massive MIMO networks is caused by numerous distributed APs in the service area and their large antennas. The architecture proposed in this chapter solved this issue by employing a low-complexity matching technique to obtain the selected of antennas to be activated, chosen based on channel magnitude and by switching off antennas that contribute more to interference power than to desired signal power for each RF chain at each AP, instead of assuming all RF chains at each AP have the same number of selected antennas. Therefore, an assignment optimization problem based on a bipartite graph has been formulated for the uplink cell-free mm-Wave massive MIMO system. Then, the Hungarian method was proposed to solve this problem due to its ability to solve this assignment problem in a polynomial time. Simulated results show that, despite several APs and antennas, the proposed matching approach is more energy-efficient and has lower computational complexity than state-of-the-art schemes.

Chapter 4 exploited the advantage of using matching theory due to its low computational complexity to activate or deactivate the RF chains in the signal combining design, mainly when there exist a large number of APs inside the coverage area under the assumption of using centralized cell-free mm-Wave massive MIMO systems. This chapter has formulated a maximum weighted assignment optimization problem to assign each AP to its set of active RF chains that can maximize the total EE of the cell-free massive MIMO network. Then, this chapter proposed a novel matching method based on the Hungarian algorithm to solve the formulated optimization problem and obtain the maximum total EE and studied the complexity analysis of the proposed scheme compared to the state-of-the-art techniques. Simulation results in this chapter revealed that the proposed matching scheme has a significantly lower computational complexity, yielding a higher total EE while achieving a higher total achievable rate compared to random APs activation and fixed activation scheme with 50% active RF chains at each AP.

Based on what was mentioned in Chapter 2, Chapter 5 focused on mitigating the pilot contamination phenomenon by proposing the matching theory in both pilot assignment and pilot power control to enhance the channel estimation accuracy. In Chapter 5, the iterative Hungarian scheme has been proposed to

solve the formulated assignment optimization problem to obtain better-selected pilot sequences. The reason for doing that is to reduce the complexity of the GA by using the selected pilot sequences as input (*termed populations*) instead of putting τ^K possible combinations of the pilot sequences in the conventional GA. Then, a lower complexity approach for pilot power control design for the uplink cell-free massive MIMO systems has been proposed based on matching theory by formulating a minimum weighted assignment optimization problem. It uses matching theory based on the Hungarian method to obtain the optimal matching between the pilot power control coefficients and the minimum channel estimation error for all UEs. Comprehensive simulation results are provided to demonstrate the performance of the proposed pilot assignment and pilot power control strategies under an extensive set of cell-free massive MIMO scenarios. In addition, the computational complexity analysis for the proposed schemes is studied in this chapter. Simulation results revealed that the proposed methodology to mitigate the pilot contamination issue has a significantly lower computational complexity with higher total uplink net throughput.

6.2 Future Directions

In this section, future research directions on how to use the proposed matching scheme in this thesis in different directions in wireless communication systems are discussed.

1. It would be interesting to incorporate low complexity RF chains activation based on the matching theory with low-resolution analog-to-digital converters (ADCs) due to their low hardware complexity [149, 150] in order to further reduce the power consumption.

2. It would be possible to utilize the proposed schemes based on the matching theory for mitigating the pilot contamination phenomenon, as mentioned in Chapter 5, in the cell-free mm-Wave massive MIMO systems, which can be also incorporated with the proposed matching scheme for antenna selection or RF chain activation to enhance the channel estimation accuracy and reduce the power consumption, respectively.

3. A developing paradigm for future communication networks, the Internet of Things (IoT), involves many machine-type devices sending short data packets to a base station (BS) regularly. Massive MIMO systems can provide high connectivity because of their high capacity, reliability, and

EE [151, 152]. The cell-free massive MIMO based on matching theory for both pilot assignment and pilot power control to enhance the channel estimation accuracy, antenna selection, and RF chain activation for reducing power consumption can now support IoT systems and outperform the IoT network supported by co-located massive MIMO systems by exploiting more excellent coverage provided by distributed APs having a large number of antennas.

4. In the cell-free massive MIMO systems, the AP Switch On/Off (ASO) strategy design is becoming more prominent due to the growing demand for green communications [89]. Based on the location and data traffic generated by the UEs, some APs are automatically turned on and off. Because numerous APs deployed in the network, the neighbouring APs of the UEs would likely cover the SE demand. ASO aims to increase the system's energy efficiency and reduce its carbon footprint by efficiently utilizing some, but not all, of the system's available APs to serve the dynamic traffic load demands. Therefore, the matching theory is a promising technique to be applied to ASO due to its ability to match each UE to a set of APs by exploiting the large-scale fading and making a tradeoff between computational complexity, EE and SE.

5. It would be interesting to investigate the flexibility of activating or deactivating the RF chains in the signal combining design in the cell-free mm-Wave massive MIMO systems by proposing the integration between matching theory and the GA because this can achieve near the optimal results in terms of the achievable rate compared to the exhaustive searching method. Furthermore, the early stage of the GA is to create the initial population randomly, referred to as the algorithm's first generation. $M!$ possible combinations of the initial population in the cell-free mm-Wave massive MIMO systems when the initial population size equals M APs, and each individual represents the active RF chains. The key challenge in creating a random population is rapidly and effectively determining the active RF chains at each AP from among these $M!$, especially when the cell-free network has many distributed APs. It would be interesting to propose an efficient matching approach based on the matching theory to acquire the required initial population instead of constructing $M!$ random populations and choosing the best initial population. Thus, M random active RF chains can be generated and formulated as an assignment optimization problem to assign each AP to the suitable active RF chains. This will enhance the

total achievable rate and lower computational complexity compared to the exhaustive search method.

6. UAVs have emerged as a viable option for providing backup connectivity in post-disaster scenarios due to the rising number of wireless networks being damaged or destroyed following natural disasters. In disaster zones, truck-mounted BSs can be used to provide network coverage to UEs based on the notion of delay-tolerant communications. However, the performance of UAVs in providing wireless coverage is known to be hampered by their battery life, which restricts their flight periods [144]. To reduce the difficulty of identifying the shortest path to obtain the minimum energy requirements for a single UAV to visit all the BSs and return a gateway to the core network, an integrated matching theory based on the integration between the Hungarian method and GA can be applied to reduce the complexity compared to the conventional GA. For example, it is assumed that the UAV needs to visit n BSs, and the distance square matrix with size $n \times n$ is created. Then, a minimum weighted assignment problem is formulated and solved by the Hungarian method. The Hungarian method's obtained result is considered an input of the GA to find the shortest distances that can achieve the minimum energy requirements quickly and effectively. This is because it is not practical to find the shortest path among a large number of BSs using the conventional GA.

Bibliography

[1] 5G-PPP. Key challenges for the 5g infrastructure ppp. [Online]. Available: https://5g-ppp.eu/

[2] J. Zhao, "A survey of intelligent reflecting surfaces (irss): Towards 6g wireless communication networks," 2019. [Online]. Available: https://arxiv.org/abs/1907.04789

[3] K. Tekbıyık, A. R. Ekti, G. K. Kurt, and A. Görçin, "Terahertz band communication systems: Challenges, novelties and standardization efforts," *Physical Communication*, vol. 35, p. 100700, 2019. [Online]. Available: https://www.sciencedirect.com/science/article/pii/S1874490718307766

[4] C. Pan, J. Yi, C. Yin, J. Yu, and X. Li, "Joint 3d uav placement and resource allocation in software-defined cellular networks with wireless backhaul," *IEEE Access*, vol. 7, pp. 104 279–104 293, 2019.

[5] M. Mozaffari, A. Taleb Zadeh Kasgari, W. Saad, M. Bennis, and M. Debbah, "Beyond 5g with uavs: Foundations of a 3d wireless cellular network," *IEEE Transactions on Wireless Communications*, vol. 18, no. 1, pp. 357–372, 2019.

[6] D. Maryopi, "Centralized cell-free massive mimo with low-resolution fronthaul," Ph.D. dissertation, University of York, 2020.

[7] T. L. Marzetta, "Noncooperative cellular wireless with unlimited numbers of base station antennas," *IEEE Transactions on Wireless Communications*, vol. 9, no. 11, pp. 3590–3600, 2010.

[8] F. Rusek, D. Persson, B. K. Lau, E. G. Larsson, T. L. Marzetta, O. Edfors, and F. Tufvesson, "Scaling up mimo: Opportunities and challenges with very large arrays," *IEEE Signal Processing Magazine*, vol. 30, no. 1, pp. 40–60, 2013.

[9] E. Nayebi, A. Ashikhmin, T. L. Marzetta, and H. Yang, "Cell-free massive mimo systems," in *2015 49th Asilomar Conference on Signals, Systems and Computers*, 2015, pp. 695–699.

[10] H. Q. Ngo, A. Ashikhmin, H. Yang, E. G. Larsson, and T. L. Marzetta, "Cell-free massive mimo versus small cells," *IEEE Transactions on Wireless Communications*, vol. 16, no. 3, pp. 1834–1850, 2017.

[11] Y. Zhao, "Power allocation in cell-free massive mimo: Using deep learning methods," Ph.D. dissertation, 2022.

[12] S. Elhoushy, M. Ibrahim, and W. Hamouda, "Cell-free massive mimo: A survey," *IEEE Communications Surveys Tutorials*, vol. 24, no. 1, pp. 492–523, 2022.

[13] I. Ahmed, H. Khammari, A. Shahid, A. Musa, K. S. Kim, E. De Poorter, and I. Moerman, "A survey on hybrid beamforming techniques in 5g: Architecture and system model perspectives," *IEEE Communications Surveys Tutorials*, vol. 20, no. 4, pp. 3060–3097, 2018.

[14] E. E. Bahingayi and K. Lee, "Hybrid combining based on constant phase shifters and active/inactive switches," *IEEE Transactions on Vehicular Technology*, vol. 69, no. 4, pp. 4058–4068, 2020.

[15] N. T. Nguyen, K. Lee, and H. Dai, "Hybrid beamforming and adaptive rf chain activation for uplink cell-free millimeter-wave massive mimo systems," *IEEE Transactions on Vehicular Technology*, pp. 1–1, 2022.

[16] O. Elijah, C. Y. Leow, T. A. Rahman, S. Nunoo, and S. Z. Iliya, "A comprehensive survey of pilot contamination in massive mimo—5g system," *IEEE Communications Surveys Tutorials*, vol. 18, no. 2, pp. 905–923, 2016.

[17] T. C. Mai, H. Q. Ngo, M. Egan, and T. Q. Duong, "Pilot power control for cell-free massive mimo," *IEEE Transactions on Vehicular Technology*, vol. 67, no. 11, pp. 11 264–11 268, 2018.

[18] Y. Gu, W. Saad, M. Bennis, M. Debbah, and Z. Han, "Matching theory for future wireless networks: fundamentals and applications," *IEEE Communications Magazine*, vol. 53, no. 5, pp. 52–59, 2015.

[19] S. Bayat, Y. Li, L. Song, and Z. Han, "Matching theory: Applications in wireless communications," *IEEE Signal Processing Magazine*, vol. 33, no. 6, pp. 103–122, 2016.

[20] M. A. Imran, A. Al Ayidh, L. Li, G. Zhao, and Q. H. Abbasi, *URLLC massive MIMO link operation design for wireless networked control system.* John Wiley sons Ltd, 2020.

[21] Z. Han, Y. Gu, and W. Saad, *Matching theory for wireless networks.* Springer, 2017.

[22] D. Gale and L. S. Shapley, "College admissions and the stability of marriage," *The American Mathematical Monthly*, vol. 69, no. 1, pp. 9–15, 1962. [Online]. Available: https://doi.org/10.1080/00029890.1962.11989827

[23] A. E. Roth and M. Sotomayor, "Chapter 16 two-sided matching," ser. Handbook of Game Theory with Economic Applications. Elsevier, 1992, vol. 1, pp. 485–541. [Online]. Available: https://www.sciencedirect.com/science/article/pii/S1574000505800190

[24] D. Manlove, *Algorithmics of matching under preferences.* World Scientific, 2013, vol. 2.

[25] P. Liu, R. Berry, and M. Honig, "A fluid analysis of a utility-based wireless scheduling policy," *IEEE Transactions on Information Theory*, vol. 52, no. 7, pp. 2872–2889, 2006.

[26] Z. Jiang, Y. Ge, and Y. Li, "Max-utility wireless resource management for best-effort traffic," *IEEE Transactions on Wireless Communications*, vol. 4, no. 1, pp. 100–111, 2005.

[27] K. Hamidouche, W. Saad, and M. Debbah, "Many-to-many matching games for proactive social-caching in wireless small cell networks," in *2014 12th International Symposium on Modeling and Optimization in Mobile, Ad Hoc, and Wireless Networks (WiOpt)*, 2014, pp. 569–574.

[28] J. Munkres, "Algorithms for the assignment and transportation problems," *Journal of the society for industrial and applied mathematics*, vol. 5, no. 1, pp. 32–38, 1957.

[29] S. Bayat, R. H. Louie, B. Vucetic, and Y. Li, "Dynamic decentralised algorithms for cognitive radio relay networks with multiple primary and secondary users utilising matching theory," *Transactions on Emerging Telecommunications Technologies*, vol. 24, no. 5, pp. 486–502, 2013. [Online]. Available: https://onlinelibrary.wiley.com/doi/abs/10.1002/ett.2663

[30] S. Bayat, R. H. Y. Louie, Z. Han, B. Vucetic, and Y. Li, "Distributed user association and femtocell allocation in heterogeneous wireless networks," *IEEE Transactions on Communications*, vol. 62, no. 8, pp. 3027–3043, 2014.

[31] ——, "Physical-layer security in distributed wireless networks using matching theory," *IEEE Transactions on Information Forensics and Security*, vol. 8, no. 5, pp. 717–732, 2013.

[32] E. A. Jorswieck, "Stable matchings for resource allocation in wireless networks," in *2011 17th International Conference on Digital Signal Processing (DSP)*, 2011, pp. 1–8.

[33] A. Schweizer, J. Siliquini, and T. Devadason, "On the performance of advanced stable matching algorithms in combined input output queued network switches," in *2007 Asia-Pacific Conference on Communications*, 2007, pp. 223–226.

[34] A. M. El-Hajj, Z. Dawy, and W. Saad, "A stable matching game for joint uplink/downlink resource allocation in ofdma wireless networks," in *2012 IEEE International Conference on Communications (ICC)*, 2012, pp. 5354–5359.

[35] R. Elliott, "A measure of fairness of service for scheduling algorithms in multiuser systems," in *IEEE CCECE2002. Canadian Conference on Electrical and Computer Engineering. Conference Proceedings (Cat. No.02CH37373)*, vol. 3, 2002, pp. 1583–1588 vol.3.

[36] E. Castañeda, A. Silva, A. Gameiro, and M. Kountouris, "An overview on resource allocation techniques for multi-user mimo systems," *IEEE Communications Surveys Tutorials*, vol. 19, no. 1, pp. 239–284, 2017.

[37] Z. Chen and E. Björnson, "Channel hardening and favorable propagation in cell-free massive mimo with stochastic geometry," *IEEE Transactions on Communications*, vol. 66, no. 11, pp. 5205–5219, 2018.

[38] M. A. Albreem, M. Juntti, and S. Shahabuddin, "Massive mimo detection techniques: A survey," *IEEE Communications Surveys Tutorials*, vol. 21, no. 4, pp. 3109–3132, 2019.

[39] H. Yang and T. L. Marzetta, "Performance of conjugate and zero-forcing beamforming in large-scale antenna systems," *IEEE Journal on Selected Areas in Communications*, vol. 31, no. 2, pp. 172–179, 2013.

[40] N. Fatema, G. Hua, Y. Xiang, D. Peng, and I. Natgunanathan, "Massive mimo linear precoding: A survey," *IEEE Systems Journal*, vol. 12, no. 4, pp. 3920–3931, 2018.

[41] D. Qiao, Y. Wu, and Y. Chen, "Massive mimo architecture for 5g networks: Co-located, or distributed?" in *2014 11th International Symposium on Wireless Communications Systems (ISWCS)*, 2014, pp. 192–197.

[42] J. Wu, Z. Zhang, Y. Hong, and Y. Wen, "Cloud radio access network (c-ran): a primer," *IEEE Network*, vol. 29, no. 1, pp. 35–41, 2015.

[43] S. Elhoshy, M. Ibrahim, M. Ashour, T. Elshabrawy, H. Hammad, and M. R. M. Rizk, "A dimensioning framework for indoor das lte networks," in *2016 International Conference on Selected Topics in Mobile Wireless Networking (MoWNeT)*, 2016, pp. 1–8.

[44] R. Irmer, H. Droste, P. Marsch, M. Grieger, G. Fettweis, S. Brueck, H.-P. Mayer, L. Thiele, and V. Jungnickel, "Coordinated multipoint: Concepts, performance, and field trial results," *IEEE Communications Magazine*, vol. 49, no. 2, pp. 102–111, 2011.

[45] Z. Liu and L. Dai, "A comparative study of downlink mimo cellular networks with co-located and distributed base-station antennas," *IEEE Transactions on Wireless Communications*, vol. 13, no. 11, pp. 6259–6274, 2014.

[46] J. Wang and L. Dai, "Asymptotic rate analysis of downlink multi-user systems with co-located and distributed antennas," *IEEE Transactions on Wireless Communications*, vol. 14, no. 6, pp. 3046–3058, 2015.

[47] C. K. Agubor, I. Akwukwuegbu, M. Olubiwe, C. O. Nosiri, A. Ehinomen, A. A. Olukunle, S. O. Okozi, L. Ezema, and B. C. Okeke, "A comprehensive review on the feasibility and challenges of millimeter wave in emerging 5g mobile communication," *Adv. Sci. Technol. Eng. Syst*, vol. 4, no. 3, pp. 138–144, 2019.

[48] ITU. Wrc-19 identifies additional frequency bands for 5g - itu hub. [Online]. Available: https://www.itu.int/hub/2020/01/wrc-19-identifies-additional-frequency-bands-for-5g/

[49] N. T. Nguyen and K. Lee, "Coverage and cell-edge sum-rate analysis of mmwave massive mimo systems with orp schemes and mmse receivers," *IEEE Transactions on Signal Processing*, vol. 66, no. 20, pp. 5349–5363, 2018.

[50] A. N. Uwaechia and N. M. Mahyuddin, "A comprehensive survey on millimeter wave communications for fifth-generation wireless networks: Feasibility and challenges," *IEEE Access*, vol. 8, pp. 62 367–62 414, 2020.

[51] M. Ibrahim, S. Elhoushy, and W. Hamouda, "Uplink performance of mmwave-fronthaul cell-free massive mimo systems," *IEEE Transactions on Vehicular Technology*, vol. 71, no. 2, pp. 1536–1548, 2022.

[52] I. A. Hemadeh, K. Satyanarayana, M. El-Hajjar, and L. Hanzo, "Millimeter-wave communications: Physical channel models, design considerations, antenna constructions, and link-budget," *IEEE Communications Surveys Tutorials*, vol. 20, no. 2, pp. 870–913, 2018.

[53] S. A. Busari, K. M. S. Huq, S. Mumtaz, L. Dai, and J. Rodriguez, "Millimeter-wave massive mimo communication for future wireless systems: A survey," *IEEE Communications Surveys Tutorials*, vol. 20, no. 2, pp. 836–869, 2018.

[54] A. L. Swindlehurst, E. Ayanoglu, P. Heydari, and F. Capolino, "Millimeter-wave massive mimo: the next wireless revolution?" *IEEE Communications Magazine*, vol. 52, no. 9, pp. 56–62, 2014.

[55] Z. Pi and F. Khan, "An introduction to millimeter-wave mobile broadband systems," *IEEE Communications Magazine*, vol. 49, no. 6, pp. 101–107, 2011.

[56] D. Tse and P. Viswanath, *Fundamentals of wireless communication*. Cambridge university press, 2005.

[57] T. Bai, A. Alkhateeb, and R. W. Heath, "Coverage and capacity of millimeter-wave cellular networks," *IEEE Communications Magazine*, vol. 52, no. 9, pp. 70–77, 2014.

[58] T. Bogale, X. Wang, and L. Le, "Chapter 9 - mmwave communication enabling techniques for 5g wireless systems: A link level perspective," in *mmWave Massive MIMO*, S. Mumtaz, J. Rodriguez, and L. Dai, Eds. Academic Press, 2017, pp. 195–225. [Online]. Available: https://www.sciencedirect.com/science/article/pii/B9780128044186000091

[59] L. Wei, R. Q. Hu, Y. Qian, and G. Wu, "Key elements to enable millimeter wave communications for 5g wireless systems," *IEEE Wireless Communications*, vol. 21, no. 6, pp. 136–143, 2014.

[60] S. Hur, T. Kim, D. J. Love, J. V. Krogmeier, T. A. Thomas, and A. Ghosh, "Millimeter wave beamforming for wireless backhaul and access in small cell networks," *IEEE Transactions on Communications*, vol. 61, no. 10, pp. 4391–4403, 2013.

[61] J. Wang, Z. Lan, C. woo Pyo, T. Baykas, C. sean Sum, M. Rahman, J. Gao, R. Funada, F. Kojima, H. Harada, and S. Kato, "Beam codebook based beamforming protocol for multi-gbps millimeter-wave wpan systems," *IEEE Journal on Selected Areas in Communications*, vol. 27, no. 8, pp. 1390–1399, 2009.

[62] A. Alkhateeb, J. Mo, N. Gonzalez-Prelcic, and R. W. Heath, "Mimo precoding and combining solutions for millimeter-wave systems," *IEEE Communications Magazine*, vol. 52, no. 12, pp. 122–131, 2014.

[63] L. Chen, Y. Yang, X. Chen, and W. Wang, "Multi-stage beamforming codebook for 60ghz wpan," in *2011 6th International ICST Conference on Communications and Networking in China (CHINACOM)*, 2011, pp. 361–365.

[64] Y. M. Tsang, A. S. Y. Poon, and S. Addepalli, "Coding the beams: Improving beamforming training in mmwave communication system," in *2011 IEEE Global Telecommunications Conference - GLOBECOM 2011*, 2011, pp. 1–6.

[65] S. Sun, T. S. Rappaport, R. W. Heath, A. Nix, and S. Rangan, "Mimo for millimeter-wave wireless communications: beamforming, spatial multiplexing, or both?" *IEEE Communications Magazine*, vol. 52, no. 12, pp. 110–121, 2014.

[66] S. Han, C.-l. I, Z. Xu, and C. Rowell, "Large-scale antenna systems with hybrid analog and digital beamforming for millimeter wave 5g," *IEEE Communications Magazine*, vol. 53, no. 1, pp. 186–194, 2015.

[67] T. E. Bogale, L. B. Le, A. Haghighat, and L. Vandendorpe, "On the number of rf chains and phase shifters, and scheduling design with hybrid analog–digital beamforming," *IEEE Transactions on Wireless Communications*, vol. 15, no. 5, pp. 3311–3326, 2016.

[68] S. Mumtaz, J. Rodriguez, and L. Dai, *MmWave massive MIMO: a paradigm for 5G*. Academic Press, 2016.

[69] X. Huang, Y. J. Guo, and J. D. Bunton, "A hybrid adaptive antenna array," *IEEE Transactions on Wireless Communications*, vol. 9, no. 5, pp. 1770–1779, 2010.

[70] Y. J. Guo, X. Huang, and V. Dyadyuk, "A hybrid adaptive antenna array for long-range mm-wave communications [antenna applications corner]," *IEEE Antennas and Propagation Magazine*, vol. 54, no. 2, pp. 271–282, 2012.

[71] A. F. Molisch, V. V. Ratnam, S. Han, Z. Li, S. L. H. Nguyen, L. Li, and K. Haneda, "Hybrid beamforming for massive mimo: A survey," *IEEE Communications Magazine*, vol. 55, no. 9, pp. 134–141, 2017.

[72] A. Adhikary, J. Nam, J.-Y. Ahn, and G. Caire, "Joint spatial division and multiplexing—the large-scale array regime," *IEEE Transactions on Information Theory*, vol. 59, no. 10, pp. 6441–6463, 2013.

[73] E. Nayebi, A. Ashikhmin, T. L. Marzetta, H. Yang, and B. D. Rao, "Precoding and power optimization in cell-free massive mimo systems," *IEEE Transactions on Wireless Communications*, vol. 16, no. 7, pp. 4445–4459, 2017.

[74] E. Björnson and L. Sanguinetti, "Making cell-free massive mimo competitive with mmse processing and centralized implementation," *IEEE Transactions on Wireless Communications*, vol. 19, no. 1, pp. 77–90, 2020.

[75] A. Papazafeiropoulos, P. Kourtessis, M. D. Renzo, S. Chatzinotas, and J. M. Senior, "Performance analysis of cell-free massive mimo systems: A stochastic geometry approach," *IEEE Transactions on Vehicular Technology*, vol. 69, no. 4, pp. 3523–3537, 2020.

[76] J. Zhang, S. Chen, Y. Lin, J. Zheng, B. Ai, and L. Hanzo, "Cell-free massive mimo: A new next-generation paradigm," *IEEE Access*, vol. 7, pp. 99 878–99 888, 2019.

[77] S. Elhoushy and W. Hamouda, "Performance of distributed massive mimo and small-cell systems under hardware and channel impairments," *IEEE Transactions on Vehicular Technology*, vol. 69, no. 8, pp. 8627–8642, 2020.

[78] ——, "Towards high data rates in dynamic environments using hybrid cell-free massive mimo/small-cell system," *IEEE Wireless Communications Letters*, vol. 10, no. 2, pp. 201–205, 2021.

[79] Y. Li and G. A. Aruma Baduge, "Noma-aided cell-free massive mimo systems," *IEEE Wireless Communications Letters*, vol. 7, no. 6, pp. 950–953, 2018.

[80] S. Kusaladharma, W. P. Zhu, W. Ajib, and G. Amarasuriya, "Achievable rate analysis of noma in cell-free massive mimo: A stochastic geometry approach," in *ICC 2019 - 2019 IEEE International Conference on Communications (ICC)*, 2019, pp. 1–6.

[81] M. Bashar, K. Cumanan, A. G. Burr, H. Q. Ngo, L. Hanzo, and P. Xiao, "Noma/oma mode selection-based cell-free massive mimo," in *ICC 2019 - 2019 IEEE International Conference on Communications (ICC)*, 2019, pp. 1–6.

[82] M. A. Arfaoui, M. D. Soltani, I. Tavakkolnia, A. Ghrayeb, M. Safari, C. M. Assi, and H. Haas, "Physical layer security for visible light communication systems: A survey," *IEEE Communications Surveys Tutorials*, vol. 22, no. 3, pp. 1887–1908, 2020.

[83] Y. Liu, X. Liu, X. Mu, T. Hou, J. Xu, M. Di Renzo, and N. Al-Dhahir, "Reconfigurable intelligent surfaces: Principles and opportunities," *IEEE Communications Surveys Tutorials*, vol. 23, no. 3, pp. 1546–1577, 2021.

[84] Z. H. Shaik, E. Björnson, and E. G. Larsson, "Cell-free massive mimo with radio stripes and sequential uplink processing," in *2020 IEEE International Conference on Communications Workshops (ICC Workshops)*, 2020, pp. 1–6.

[85] Y. Ma, Z. Yuan, G. Yu, and Y. Chen, "Efficient parallel schemes for cell-free massive mimo using radio stripes," 2020. [Online]. Available: https://arxiv.org/abs/2012.11076

[86] T. Zhou, K. Xu, X. Xia, W. Xie, and X. Yang, "Achievable rate maximization for aerial intelligent reflecting surface-aided cell-free massive mimo system," in *2020 IEEE 6th International Conference on Computer and Communications (ICCC)*, 2020, pp. 623–628.

[87] J. An and F. Zhao, "Trajectory optimization and power allocation algorithm in mbs-assisted cell-free massive mimo systems," *IEEE Access*, vol. 9, pp. 30 417–30 425, 2021.

[88] M. Giordani, M. Polese, M. Mezzavilla, S. Rangan, and M. Zorzi, "Toward 6g networks: Use cases and technologies," *IEEE Communications Magazine*, vol. 58, no. 3, pp. 55–61, 2020.

[89] S. Chen, J. Zhang, J. Zhang, E. Björnson, and B. Ai, "A survey on user-centric cell-free massive mimo systems," *Digital Communications and Networks*, 2021. [Online]. Available: https://www.sciencedirect.com/science/article/pii/S2352864821001024

[90] S. Kim and B. Shim, "Fdd-based cell-free massive mimo systems," in *2018 IEEE 19th International Workshop on Signal Processing Advances in Wireless Communications (SPAWC)*, 2018, pp. 1–5.

[91] A. Abdallah and M. M. Mansour, "Angle-based multipath estimation and beamforming for fdd cell-free massive mimo," in *2019 IEEE 20th International Workshop on Signal Processing Advances in Wireless Communications (SPAWC)*, 2019, pp. 1–5.

[92] S. Chen, S. Sun, Y. Wang, G. Xiao, and R. Tamrakar, "A comprehensive survey of tdd-based mobile communication systems from td-scdma 3g to td-lte(a) 4g and 5g directions," *China Communications*, vol. 12, no. 2, pp. 40–60, 2015.

[93] S. Buzzi and C. D'Andrea, "User-centric communications versus cell-free massive mimo for 5g cellular networks," in *WSA 2017; 21th International ITG Workshop on Smart Antennas*, 2017, pp. 1–6.

[94] S. Buzzi and A. Zappone, "Downlink power control in user-centric and cell-free massive mimo wireless networks," in *2017 IEEE 28th Annual International Symposium on Personal, Indoor, and Mobile Radio Communications (PIMRC)*, 2017, pp. 1–6.

[95] S. Buzzi, C. D'Andrea, A. Zappone, and C. D'Elia, "User-centric 5g cellular networks: Resource allocation and comparison with the cell-free massive mimo approach," *IEEE Transactions on Wireless Communications*, vol. 19, no. 2, pp. 1250–1264, 2020.

[96] S. Buzzi, C. D'Andrea, and C. D'Elia, "User-centric cell-free massive mimo with interference cancellation and local zf downlink precoding," in *2018 15th International Symposium on Wireless Communication Systems (ISWCS)*, 2018, pp. 1–5.

[97] H. Liu, J. Zhang, X. Zhang, A. Kurniawan, T. Juhana, and B. Ai, "Tabu-search-based pilot assignment for cell-free massive mimo systems," *IEEE Transactions on Vehicular Technology*, vol. 69, no. 2, pp. 2286–2290, 2020.

[98] S. Buzzi, C. D'Andrea, M. Fresia, Y.-P. Zhang, and S. Feng, "Pilot assignment in cell-free massive mimo based on the hungarian algorithm," *IEEE Wireless Communications Letters*, vol. 10, no. 1, pp. 34–37, 2021.

[99] X.-T. Dang, T. Lai-Thuc, A.-T. Nguyen, T. Vu-Huy, N. H. Anh Tran, and H.-D. Han, "A genetic algorithm based pilot assignment strategy for cell-free massive mimo system," in *2020 IEEE Eighth International Conference on Communications and Electronics (ICCE)*, 2021, pp. 93–98.

[100] H. Liu, J. Zhang, S. Jin, and B. Ai, "Graph coloring based pilot assignment for cell-free massive mimo systems," *IEEE Transactions on Vehicular Technology*, vol. 69, no. 8, pp. 9180–9184, 2020.

[101] C. Zhu, Y. Liang, T. Li, and F. Li, "Pilot assignment in cell-free massive mimo based on quantum bacterial foraging optimization," in *2021 13th International Conference on Wireless Communications and Signal Processing (WCSP)*, 2021, pp. 1–5.

[102] E. Björnson and L. Sanguinetti, "Cell-free versus cellular massive mimo: What processing is needed for cell-free to win?" in *2019 IEEE 20th International Workshop on Signal Processing Advances in Wireless Communications (SPAWC)*, 2019, pp. 1–5.

[103] ——, "Scalable cell-free massive mimo systems," *IEEE Transactions on Communications*, vol. 68, no. 7, pp. 4247–4261, 2020.

[104] G. Femenias and F. Riera-Palou, "Cell-free millimeter-wave massive mimo systems with limited fronthaul capacity," *IEEE Access*, vol. 7, pp. 44 596–44 612, 2019.

[105] J. Li, D.-W. Yue, and Y. Sun, "Performance analysis of millimeter wave massive mimo systems in centralized and distributed schemes," *IEEE Access*, vol. 6, pp. 75 482–75 494, 2018.

[106] N. T. Nguyen and K. Lee, "Unequally sub-connected architecture for hybrid beamforming in massive mimo systems," *IEEE Transactions on Wireless Communications*, vol. 19, no. 2, pp. 1127–1140, 2020.

[107] M. Alonzo and S. Buzzi, "Cell-free and user-centric massive mimo at millimeter wave frequencies," in *2017 IEEE 28th Annual International Symposium on Personal, Indoor, and Mobile Radio Communications (PIMRC)*, 2017, pp. 1–5.

[108] M. Alonzo, S. Buzzi, A. Zappone, and C. D'Elia, "Energy-efficient power control in cell-free and user-centric massive mimo at millimeter wave," *IEEE Transactions on Green Communications and Networking*, vol. 3, no. 3, pp. 651–663, 2019.

[109] A. Alkhateeb, Y.-H. Nam, J. Zhang, and R. W. Heath, "Massive mimo combining with switches," *IEEE Wireless Communications Letters*, vol. 5, no. 3, pp. 232–235, 2016.

[110] A. K. Sah and A. K. Chaturvedi, "Quasi-orthogonal combining for reducing rf chains in massive mimo systems," *IEEE Wireless Communications Letters*, vol. 6, no. 1, pp. 126–129, 2017.

[111] A. A. Ayidh, Y. Sambo, S. Ansari, and M. A. Imran, "Hybrid beamforming with fixed phase shifters for uplink cell-free millimetre-wave massive mimo systems," in *2021 Joint European Conference on Networks and Communications 6G Summit (EuCNC/6G Summit)*, 2021, pp. 19–24.

[112] T.-H. Tai, W.-H. Chung, and T.-S. Lee, "A low complexity antenna selection algorithm for energy efficiency in massive mimo systems," in *2015 IEEE International Conference on Data Science and Data Intensive Systems*, 2015, pp. 284–289.

[113] Z. Liu, W. Du, and D. Sun, "Energy and spectral efficiency tradeoff for massive mimo systems with transmit antenna selection," *IEEE Transactions on Vehicular Technology*, vol. 66, no. 5, pp. 4453–4457, 2017.

[114] X. Gao, L. Dai, and A. M. Sayeed, "Low rf-complexity technologies to enable millimeter-wave mimo with large antenna array for 5g wireless communications," *IEEE Communications Magazine*, vol. 56, no. 4, pp. 211–217, 2018.

[115] R. Méndez-Rial, C. Rusu, N. González-Prelcic, A. Alkhateeb, and R. W. Heath, "Hybrid mimo architectures for millimeter wave communications: Phase shifters or switches?" *IEEE Access*, vol. 4, pp. 247–267, 2016.

[116] Y. Xiong, S. Sun, L. Qin, N. Wei, L. Liu, and Z. Zhang, "Performance analysis on cell-free massive mimo with capacity-constrained fronthauls and

variable-resolution adcs," *IEEE Systems Journal*, vol. 16, no. 2, pp. 3296–3307, 2022.

[117] X. Song, T. Kühne, and G. Caire, "Fully-/partially-connected hybrid beamforming architectures for mmwave mu-mimo," *IEEE Transactions on Wireless Communications*, vol. 19, no. 3, pp. 1754–1769, 2020.

[118] G. M. Gadiel, N. T. Nguyen, and K. Lee, "Dynamic unequally subconnected hybrid beamforming architecture for massive mimo systems," *IEEE Transactions on Vehicular Technology*, vol. 70, no. 4, pp. 3469–3478, 2021.

[119] A. Al Ayidh, Y. Sambo, S. Olaosebikan, S. Ansari, and M. A. Imran, "Antenna selection based on matching theory for uplink cell-free millimetre wave massive multiple input multiple output systems," *Telecom*, vol. 3, no. 3, pp. 448–466, 2022. [Online]. Available: https://www.mdpi.com/2673-4001/3/3/24

[120] A. Alkhateeb, G. Leus, and R. W. Heath, "Limited feedback hybrid precoding for multi-user millimeter wave systems," *IEEE Transactions on Wireless Communications*, vol. 14, no. 11, pp. 6481–6494, 2015.

[121] O. E. Ayach, S. Rajagopal, S. Abu-Surra, Z. Pi, and R. W. Heath, "Spatially sparse precoding in millimeter wave mimo systems," *IEEE Transactions on Wireless Communications*, vol. 13, no. 3, pp. 1499–1513, 2014.

[122] A. Alkhateeb, O. El Ayach, G. Leus, and R. W. Heath, "Channel estimation and hybrid precoding for millimeter wave cellular systems," *IEEE Journal of Selected Topics in Signal Processing*, vol. 8, no. 5, pp. 831–846, 2014.

[123] C. D'Andrea, G. Interdonato, and S. Buzzi, "User-centric handover in mmwave cell-free massive mimo with user mobility," in *2021 29th European Signal Processing Conference (EUSIPCO)*, 2021, pp. 1–5.

[124] T. S. Rappaport, G. R. MacCartney, M. K. Samimi, and S. Sun, "Wideband millimeter-wave propagation measurements and channel models for future wireless communication system design," *IEEE Transactions on Communications*, vol. 63, no. 9, pp. 3029–3056, 2015.

[125] T. S. Rappaport, E. Ben-Dor, J. N. Murdock, and Y. Qiao, "38 ghz and 60 ghz angle-dependent propagation for cellular peer-to-peer wireless communications," in *2012 IEEE International Conference on Communications (ICC)*, 2012, pp. 4568–4573.

[126] T. L. Marzetta, *Fundamentals of massive MIMO*. Cambridge University Press, 2016.

[127] E. Björnson, J. Hoydis, and L. Sanguinetti, "Massive mimo networks: Spectral, energy, and hardware efficiency," *Found. Trends Signal Process.*, vol. 11, no. 3–4, p. 154–655, nov 2017. [Online]. Available: https://doi.org/10.1561/2000000093

[128] M. Li, W. Liu, X. Tian, Z. Wang, and Q. Liu, "Iterative hybrid precoder and combiner design for mmwave mimo-ofdm systems," *Wireless Networks*, vol. 25, no. 8, pp. 4829–4837, 2019.

[129] F. Sohrabi and W. Yu, "Hybrid digital and analog beamforming design for large-scale antenna arrays," *IEEE Journal of Selected Topics in Signal Processing*, vol. 10, no. 3, pp. 501–513, 2016.

[130] I. Estella Aguerri, A. Zaidi, G. Caire, and S. Shamai Shitz, "On the capacity of cloud radio access networks with oblivious relaying," *IEEE Transactions on Information Theory*, vol. 65, no. 7, pp. 4575–4596, 2019.

[131] H. Q. Ngo, L.-N. Tran, T. Q. Duong, M. Matthaiou, and E. G. Larsson, "On the total energy efficiency of cell-free massive mimo," *IEEE Transactions on Green Communications and Networking*, vol. 2, no. 1, pp. 25–39, 2018.

[132] L. D. Nguyen, T. Q. Duong, H. Q. Ngo, and K. Tourki, "Energy efficiency in cell-free massive mimo with zero-forcing precoding design," *IEEE Communications Letters*, vol. 21, no. 8, pp. 1871–1874, 2017.

[133] M. Bashar, K. Cumanan, A. G. Burr, H. Q. Ngo, E. G. Larsson, and P. Xiao, "Energy efficiency of the cell-free massive mimo uplink with optimal uniform quantization," *IEEE Transactions on Green Communications and Networking*, vol. 3, no. 4, pp. 971–987, 2019.

[134] J. García-Morales, G. Femenias, and F. Riera-Palou, "Energy-efficient access-point sleep-mode techniques for cell-free mmwave massive mimo networks with non-uniform spatial traffic density," *IEEE Access*, vol. 8, pp. 137 587–137 605, 2020.

[135] Y. Yu, P. G. M. Baltus, A. de Graauw, E. van der Heijden, C. S. Vaucher, and A. H. M. van Roermund, "A 60 ghz phase shifter integrated with lna and pa in 65 nm cmos for phased array systems," *IEEE Journal of Solid-State Circuits*, vol. 45, no. 9, pp. 1697–1709, 2010.

[136] G. H. Golub and C. F. Van Loan, *Matrix computations*. JHU press, 2013.

[137] D. Jungnickel and D. Jungnickel, *Graphs, networks and algorithms*. Springer, 2005, vol. 3.

[138] A. A. Ayidh, Y. Sambo, S. Ansari, and M. A. Imran, "Low-complexity rf chains activation based on hungarian algorithm for uplink cell-free millimetre-wave massive mimo systems," in *2022IEEE 31st Annual International Symposium on Personal, Indoor and Mobile Radio Communications*, vol. Accepted for publication, 2022.

[139] E. Björnson, L. Sanguinetti, J. Hoydis, and M. Debbah, "Optimal design of energy-efficient multi-user mimo systems: Is massive mimo the answer?" *IEEE Transactions on Wireless Communications*, vol. 14, no. 6, pp. 3059–3075, 2015.

[140] G. Femenias, N. Lassoued, and F. Riera-Palou, "Access point switch on/off strategies for green cell-free massive mimo networking," *IEEE Access*, vol. 8, pp. 21 788–21 803, 2020.

[141] A. Al Ayidh, Y. Sambo, and M. A. Imran, "Mitigation pilot contamination based on matching technique for uplink cell-free massive mimo systems," *Submitted for publication to Scientific Reports*, 2022.

[142] B. Hassibi and B. Hochwald, "How much training is needed in multiple-antenna wireless links?" *IEEE Transactions on Information Theory*, vol. 49, no. 4, pp. 951–963, 2003.

[143] W. Zeng, Y. He, B. Li, and S. Wang, "Pilot assignment for cell free massive mimo systems using a weighted graphic framework," *IEEE Transactions on Vehicular Technology*, vol. 70, no. 6, pp. 6190–6194, 2021.

[144] Y. A. Sambo, P. V. Klaine, J. P. B. Nadas, and M. A. Imran, "Energy minimization uav trajectory design for delay-tolerant emergency communication," in *2019 IEEE International Conference on Communications Workshops (ICC Workshops)*, 2019, pp. 1–6.

[145] P. Guo and Y. Han, "Chaotic genetic algorithm for structural optimization with discrete variables," *Journal of Liaoning Technical University*, vol. 26, no. 1, pp. 68–70, 2007.

[146] L. Najjar, "Pilot allocation by genetic algorithms for sparse channel estimation in ofdm systems," in *21st European Signal Processing Conference (EUSIPCO 2013)*, 2013, pp. 1–5.

[147] S. Sivanandam and S. Deepa, "Genetic algorithms," in *Introduction to genetic algorithms*. Springer, 2008, pp. 15–37.

[148] A. Tang, J. Sun, and K. Gong, "Mobile propagation loss with a low base station antenna for nlos street microcells in urban area," in *IEEE VTS 53rd Vehicular Technology Conference, Spring 2001. Proceedings (Cat. No.01CH37202)*, vol. 1, 2001, pp. 333–336 vol.1.

[149] J. Zhang, E. Björnson, M. Matthaiou, D. W. K. Ng, H. Yang, and D. J. Love, "Prospective multiple antenna technologies for beyond 5g," *IEEE Journal on Selected Areas in Communications*, vol. 38, no. 8, pp. 1637–1660, 2020.

[150] J. Zhang, L. Dai, X. Li, Y. Liu, and L. Hanzo, "On low-resolution adcs in practical 5g millimeter-wave massive mimo systems," *IEEE Communications Magazine*, vol. 56, no. 7, pp. 205–211, 2018.

[151] L. Liu, E. G. Larsson, W. Yu, P. Popovski, C. Stefanovic, and E. de Carvalho, "Sparse signal processing for grant-free massive connectivity: A future paradigm for random access protocols in the internet of things," *IEEE Signal Processing Magazine*, vol. 35, no. 5, pp. 88–99, 2018.

[152] L. Liu and W. Yu, "Massive connectivity with massive mimo—part i: Device activity detection and channel estimation," *IEEE Transactions on Signal Processing*, vol. 66, no. 11, pp. 2933–2946, 2018.